



UNIVERSITAT DE
BARCELONA

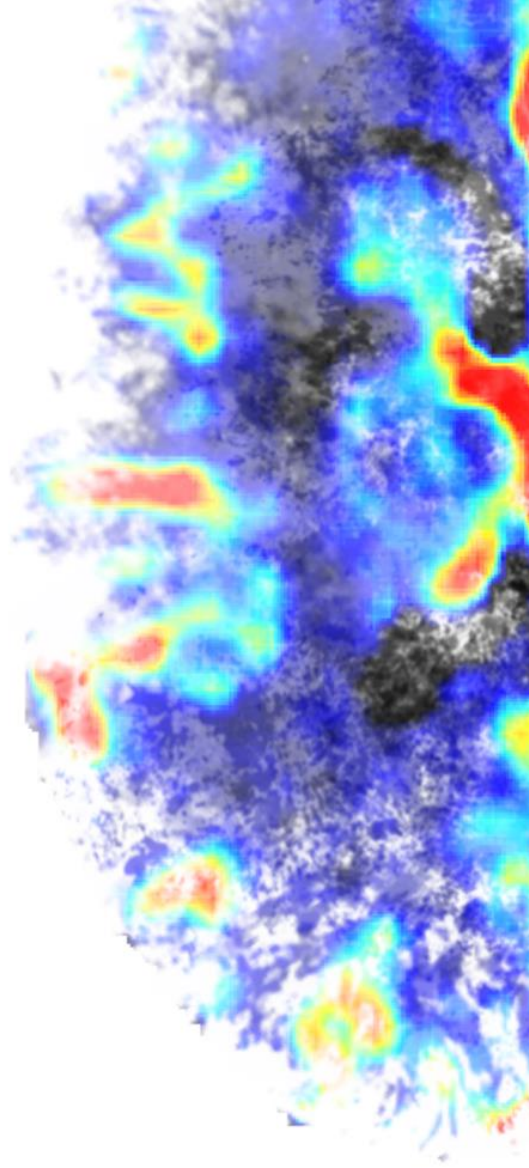
Advanced neuroimaging techniques in acute ischemic stroke: tissue viability, blood-brain-barrier status and clinical outcome prediction

Carlos Laredo Gregorio

ADVERTIMENT. La consulta d'aquesta tesi queda condicionada a l'acceptació de les següents condicions d'ús: La difusió d'aquesta tesi per mitjà del servei TDX (www.tdx.cat) i a través del Dipòsit Digital de la UB (diposit.ub.edu) ha estat autoritzada pels titulars dels drets de propietat intel·lectual únicament per a usos privats emmarcats en activitats d'investigació i docència. No s'autoritza la seva reproducció amb finalitats de lucre ni la seva difusió i posada a disposició des d'un lloc aliè al servei TDX ni al Dipòsit Digital de la UB. No s'autoritza la presentació del seu contingut en una finestra o marc aliè a TDX o al Dipòsit Digital de la UB (framing). Aquesta reserva de drets afecta tant al resum de presentació de la tesi com als seus continguts. En la utilització o cita de parts de la tesi és obligat indicar el nom de la persona autora.

ADVERTENCIA. La consulta de esta tesis queda condicionada a la aceptación de las siguientes condiciones de uso: La difusión de esta tesis por medio del servicio TDR (www.tdx.cat) y a través del Repositorio Digital de la UB (diposit.ub.edu) ha sido autorizada por los titulares de los derechos de propiedad intelectual únicamente para usos privados enmarcados en actividades de investigación y docencia. No se autoriza su reproducción con finalidades de lucro ni su difusión y puesta a disposición desde un sitio ajeno al servicio TDR o al Repositorio Digital de la UB. No se autoriza la presentación de su contenido en una ventana o marco ajeno a TDR o al Repositorio Digital de la UB (framing). Esta reserva de derechos afecta tanto al resumen de presentación de la tesis como a sus contenidos. En la utilización o cita de partes de la tesis es obligado indicar el nombre de la persona autora.

WARNING. On having consulted this thesis you're accepting the following use conditions: Spreading this thesis by the TDX (www.tdx.cat) service and by the UB Digital Repository (diposit.ub.edu) has been authorized by the titular of the intellectual property rights only for private uses placed in investigation and teaching activities. Reproduction with lucrative aims is not authorized nor its spreading and availability from a site foreign to the TDX service or to the UB Digital Repository. Introducing its content in a window or frame foreign to the TDX service or to the UB Digital Repository is not authorized (framing). Those rights affect to the presentation summary of the thesis as well as to its contents. In the using or citation of parts of the thesis it's obliged to indicate the name of the author.



```

[...
% ICBV: Matriz (imagen) del mapa
% VDel: Header del mapa VDel = s
% mapa Mean VMean = spm_vol(pathMean);
% = spm_vol(pathCBV); % DCT: Matriz
% de (det(VCBP.mat)); VolM(i) = Vol(i)/
% os(ICBVi,VCBV); % DETECTAMOS EMB
% mediante spm % guarda mapas:funcio
% = ICBVi; ICBV = ICBVi; IDela = IDela
% fpecial('gaussian'); % Aplicamos el
% h); IDela(i,:)= imfilter(IDela(i
% CBP; 'ICBV','IDela','Mean','DCT
% IONA DE PENUMBRA if exist(pathbajos,
% ita ruido bajos IBajos = spm_read_vol
% num2cell(num0), 'UniformOutput', false
% kcell = 1:size(splitlecos(indicte),1)
% zeros(size(IDela,1),size(IDela,2)); am
% sobran for kcell = 1:size(splitlecos
% to(kkall)) = zeros(size(IDela,1)
% loadVes; if exist('hafeact', 'var')
% = ((MaskPenDela+MaskBloodVes)=2).*B
% tir de Mascara de Delay [generaRO
% spm_read_vol(VMaskD); disp('DEBERE
% liquidoNO = DCT > 0; % DEFINIMOS M
% CBP try stricBP = ['CRP = ' CRP(i) ' CB
% old MaskCorCBP = (LiquidoNO>0 & Mask
% A CORE-PENUMBRA % Creamos el mapa
% PenucBP=100)=0; clear('MaskCorCBP', 'M
% Vol(i); %MAPAPENUMBRA
% MaskCorePenucBP') if exist(pathMask ru
% imagen de la mascara quita ruido bajo
% numbra CBP if thrCorCBP(k) == 30 %
% %; % mapas (VCBP,MAPAPENUMBRA, Nombre);
% %); statsCBP size = size(statsCBP); if
% volPenucBP(i,k) = statsCBP(120,1)/Area
% CBP(i,k)*100; % Ratio Potencial Recup
% % flagobr % DEFINIMOS EL CORE CON EL
% CBV = ['CRP = ' CRP(i) ' CBV = ' num2st
% = (LiquidoNO>0 & MaskBloodVes>0
% ICBV(i)*normalCBV(i)/100)); MaskNucleoCB
% MaskPenumbra + MaskNucleoCBV; MaskCor
% %pro_barCMHarr;funcion in-house' Po
% size); clear('MaskCorePenucBP') if exis
% %OUT; % Imagen de la mascara quita r
% % penumbra CBV if thrCorCBV(l) == 2.5
% % mapas (VCBP,MAPAPENUMBRA, Nombre);
% %); statsCBV size = size(statsCBV); if
% volPenucBV(i,l) = statsCBV(120,1)/Area
% lCBV(i,l)*100; % Ratio Potencial Recup
% % flagobr % DEFINIMOS EL CORE CON EL
% % try stricBPabs = ['CRP = ' CRP(i) ' CBPa
% %threshold MaskCorCBPabs = (LiquidoNO
% %MAPA CORE-PENUMBRA % Creamos el mapa
% % (MaskCorePenucBPabs=100)=0; clear('Mas
% %); Vol = Vol(i); %MAPAPENUMBRA
% %MaskCorePenucBPabs') if exist(pathMask ru
% % imagen de la mascara quita ruido baj
% % penumbra CBPabs if thrCorCBPabs(m)
% % = % guarda mapas (VCBP,MAPAPENUMBRA, Nombre);
% %; % Area, 'SubarrayID'); statsCBPabs
% %; % VolM(i); else volCorCBPabs(i,m)
% % CBPabs(i,m)+volPenucBPabs(i,m); PRR_CB
% % failm = [failm; (CRP(i)) (thrCorCBPabs
% % flagobva', 'var') = 1 for sel:thrCBVabs
% % (n)); disp(stricBPabs) % Seleccionam
% % = 0 & ICBV <= (thrCorCBVabs(n)); Mask
% % MaskCorePenucCBVabs = MaskPenumbra + Mas
% % %POSTPROCESADO DE LA MASCARA [postpro_B
% % PenucCBVabs,MaskDela7,Vol,thrCorMinclus'
% % do bajos VDRO = spm_vol(pathMask ru
% % %CBVabs.--DRO; end % Guardamos m
% % %PenucCBVabs_num2str(thrCorCBV
% % CORE % PENUMBRA
% % size(statsCBVabs)
[...

```

ADVANCED NEUROIMAGING TECHNIQUES IN ACUTE ISCHEMIC STROKE

TISSUE VIABILITY, BLOOD-BRAIN BARRIER STATUS
AND CLINICAL OUTCOME PREDICTION

CARLOS LAREDO GREGORIO



UNIVERSITAT DE
BARCELONA

Advanced neuroimaging techniques in acute
ischemic stroke: tissue viability, blood-brain barrier
status and clinical outcome prediction

Doctoral student

Carlos Laredo Gregorio

Affiliation

Institut d'Investigacions Biomèdiques August Pi i Sunyer (IDIBAPS)

Directors

Ángel Chamorro Sánchez

Sergio Amaro Delgado

Doctoral thesis submitted for the degree of Doctor of Philosophy
Medicine and Translational Research
Clinical and experimental neuroscience

Universitat de Barcelona

Barcelona

May 2021

Informe dels directors de la tesi

El Dr. *Ángel Chamorro Sánchez*, Doctor en Medicina y Cirurgia per la *Universitat de Barcelona*, Consultor Sènior del Servei de Neurologia de l'*Hospital Clínic de Barcelona* y Professor Titular de Neurologia de la *Universitat de Barcelona*, i el Dr. *Sergio Amaro Delgado*, Doctor en Medicina per la *Universitat de Barcelona*, Consultor del Servei de Neurologia de l'*Hospital Clínic de Barcelona* i Investigador de l'*Institut d'Investigacions Biomèdiques August Pi i Sunyer (IDIBAPS)*.

CERTIFIQUEN:

Que la memòria titulada “*Advanced neuroimaging techniques in acute ischemic stroke: tissue viability, blood-brain barrier status and clinical outcome prediction*”, presentada per Carlos Laredo Gregorio per optar al grau de *Doctor en Medicina i Recerca Translacional* per la *Universitat de Barcelona* s’ha realitzat sota la seva direcció i compleix tots els requisits necessaris per ser defensada davant el tribunal corresponent.

Dr. *Ángel Chamorro Sánchez*

Dr. *Sergio Amaro Delgado*

*Para Jacinto
y Esperanza*

AGRAÏMENTS

Gràcies al Dr. Ángel Chamorro, director d'aquesta Tesi. Gràcies a la seva direcció durant aquests anys he arribat fins aquí. Saber veure l'arbre alhora que tot el bosc és una facultat que no tothom té. Gràcies per creure en mi, i creure que la meva feina dins del grup era important. Gràcies per la teva forma de ser i treballar, ha sigut molt fàcil arribar fins aquí al teu costat.

Gràcies al Dr. Sergi Amaro, codirector d'aquesta Tesi. Gràcies per tota la feina que ha culminat no només en aquesta tesi, sinó en tots els resultats que hem anat obtenint durant aquests anys. Gràcies per la teva atenció al detall i per ajudar-me a conduir tot el treball que s'ha hagut de fer. "Què faria el Sergi?" serà una pregunta que no deixaré de fer-me quan hagi d'enfrontar-me als problemes futurs.

Gràcies al Dr. Raúl Tudela, gràcies a ell va començar tota aquesta aventura i em va fer de pont entre la Física i la Medicina. La seva ajuda ha sigut invaluable i totalment necessària per dur a terme aquesta Tesi.

Gràcies als companys del grup de Malalties Cerebrovasculars, sense ells aquest treball no s'hauria pogut dur a terme. Gràcies Arturo Renú per la teva disponibilitat i feina il·limitada (el *Brownie* tampoc no faria pas res sense l'*Snoopy*). Gràcies Xabier Urra per tot el teu coneixement i els consells que m'has donat. Gràcies Laura Llull per ser com ets i ajudar-me sempre que ho he necessitat. Gràcies Salvatore Rudilloso per la teva feina desmesurada. Gràcies Maty Vargas per totes les vegades que t'he molestat. Gràcies Víctor Obach per ser dels primers que vas veure que el grup necessitava un Físic. Gràcies a l'Eli Gonzalez per estar-hi en els moments més extenuants. Gràcies a tots, sempre heu tingut un somriure per mi i m'heu fet sentir com a casa.

Gràcies als companys del Laboratori d'Imatge de l'IDIBAPS. Gràcies al Carles Falcón, que em va ajudar a aterrar. Moltes gràcies Eloy, que has estat amb mi des del primer moment. Gràcies Anna Calvo pel teu suport tècnic quan encara ho havia d'aprendre tot, i gràcies després per tota la resta. Gràcies Íñigo Gabilondo, Elena Hernández Martínez de la Piscina, Sara Llufrí i Elena Fraga, pels cafès enriquidors. Gràcies a la Núria Bargalló per fer-me sentir com al meu laboratori. Gràcies a la Carmen Montejo, per ser-hi en els moments més difícils. Gràcies als *ceketes*: Jose Pariente, Àngels

Calvet i Saül Pascual, les persones més *producentes* que he conegut mai. Gràcies als amics del CEK, els que encara hi són i els que no (segueixen vius, només han canviat de feina): Mireia Masias, Magí Andorrà, Sara Andrés, Eli Solana, Emma Muñoz, Núria Moya, Bet López, Irene Pulido, Salut Albà, Sara Lahoz, Adriana y Lydia Fortea, Dani Ilzarbe, Anna Planas, Carles Justícia, Lupe Soria, César Garrido, Gisela Sugranyes, Silvia Alemany, Miquel Bioque, Brisa Sole, Esther Jiménez, Aleix Solanes, Antón Albajes, Quim Radua.

Gràcies als companys de l'Hospital, del Clínic de Barcelona i d'altres. Gràcies a la Dra. Laura Oleaga, sempre disposada a resoldre qualsevol problema. Gràcies al Dr. Luis San Román, Dr. Jordi Blasco, Drs. Napoleón Macías y Antonio López, per fer-me sentir a casa. Gràcies a la Dra. María Hernández, per acompanyar-me en la part professional i la personal. Gràcies a l'Alejandro Rodríguez, a l'Almudena Sánchez i a la Mònica Serrano, a l'Aurora Semerano, Mikel Vicente, Paco Purroy, Marco Mancosu, per fer que la feina fos més fàcil o, almenys, més divertida.

Gràcies als amics de Santa Coloma i als amics de Física. Gràcies a la colla per compartir els bons moments. Part del que sóc ho sóc gràcies a vosaltres.

Gràcies a la meva família, la millor que ningú hagi pogut tenir mai. A la meva àvia Encarna, que s'encarrega que tot vagi bé. A mon avi Pepe, a mons avis Jacinto i Dolores. A mons tiets Encarna i Tomàs, Pepe, Juanita i Antonio, Juanito i Marta, Francisco. A mons cosins: Laura, Illan, Eric, Dani i Paula. A la Dolors i el Josep, a l'Alex i al Javi, Karen i MaÀngels. A la Marina, l'Oliver i l'Elliot.

Gràcies a la Cris. Ella m'ajuda a fer les coses com cal i m'ajuda a estar tranquil quan sembla impossible. Ella que hi és de veritat en els moments bons i els dolents. Ella em fa feliç quan és més difícil. T'estimo.

Gràcies als meus pares, Jacinto i Esperanza. Mai hagués pensat que no hi serieu tots dos per veure'm llegir la tesi. Aquesta tesi és vostra, de la mateixa manera que totes les coses bones que he fet a la vida. Vosaltres m'ho heu donat tot i m'heu fet ser qui sóc. Gràcies, us estimo molt.

CONTENTS

Abbreviations	3
Presentation	5
Abstract	9
1. Introduction	13
1.1 Acute Ischemic Stroke	15
1.2 Neuroimaging in Acute Ischemic Stroke	19
1.3 CTP definition of tissue fate	24
1.4 CTP prediction of infarct core and clinical outcome	25
1.5 Perfusion parameters, glucose levels and hemorrhagic transformation	26
2. Hypothesis	29
3. Objectives	33
4. Results	37
4.1 Study 1: The accuracy of ischemic core perfusion thresholds varies according to time to recanalization in stroke patients treated with mechanical thrombectomy: A comprehensive whole-brain computed tomography perfusion study	39
4.2 Study 2: Variables influencing the association between CT perfusion predicted infarct core and clinical outcome in acute stroke	59

4.3 Study 3: Brain hemorrhage after endovascular reperfusion therapy of ischemic stroke: a threshold-finding whole-brain perfusion CT study	77
4.4 Study 4: Elevated glucose is associated with hemorrhagic transformation after mechanical thrombectomy in acute ischemic stroke patients with severe pretreatment hypoperfusion	93
5. Discussion	111
6. Conclusion	119
7. Bibliography	123

ABBREVIATIONS

AAI: Advanced Analysis of Interaction
AIF: Arterial Input Function
AIS: Acute Ischemic Stroke
ASPECTS: Alberta Stroke Program Early Computed Tomography Score
BBB: Blood-Brain Barrier
CBF: Cerebral Blood Flow
CBV: Cerebral Blood Volume
CMRO₂: Cerebral Metabolic Rate of Oxygen
CNS: Central Nervous System
CPP: Cerebral Perfusion Pressure
CT: Computed Tomography
CTP: Computed Tomography Perfusion
DWI: Diffusion Weighted Image
DT: Delay Time
ET: Endovascular Treatment
FLAIR: Fluid-Attenuated Inversion Recovery
HI: Hemorrhagic Infarction
HT: Hemorrhagic Transformation
IRF: Impulse Residue Function
MRI: Magnetic Resonance Imaging
mRS: Modified Rankin Scale
MT: Mechanical Thrombectomy
MTT: Mean Transit Time
NIHSS: National Institutes of Health Stroke Scale
OEF: Oxygen Extraction Fraction
PH: Parenchymal Hematoma
RCT: Randomized Clinical Trial
rtPA: Recombinant Tissue Plasminogen Activator
Tmax: Time to Maximum
TTP: Time to Peak
VLCBF: Very Low Cerebral Blood Flow
VLCBV: Very Low Cerebral Blood Volume

PRESENTATION

This Doctoral Thesis is presented as a compendium of articles that correspond to the same thematic unit: the value of advanced neuroimaging techniques to assess tissue viability, blood-brain barrier status and clinical and radiological outcome prediction. This thesis consists of two main objectives and four original scientific articles.

The first objective of the thesis is to evaluate the association between Computed Tomography Perfusion-derived information and clinical and radiological outcome of acute ischemic stroke patients depending on baseline clinical and radiological variables. The first objective is addressed in articles 1 and 2:

Article 1: **Laredo C**, Renú A, Tudela R, Lopez-Rueda A, Urra X, Llull L, Macías NG, Rudilosso S, Obach V, Amaro S, Chamorro Á. *The accuracy of ischemic core perfusion thresholds varies according to time to recanalization in stroke patients treated with mechanical thrombectomy: A comprehensive whole-brain computed tomography perfusion study.* J Cereb Blood Flow Metab. 2020 May;40(5):966-977. JCR Impact Factor 2019: 5.787. JCR Ranking in the category “Neurosciences”: 38/272 (Q1).

Article 2: **Laredo C**, Solanes A, Renú A, Rudilosso S, Llull L, López-Rueda A, Macías NG, Rodríguez A, Urra X, Obach V, Pariente JC, Chamorro A, Radua J, Amaro S. *Variables influencing the association between CT perfusion predicted infarct core and clinical outcome in acute stroke.* The second article has been sent for publication but it is still unpublished.

The second objective of the thesis is to evaluate the prognostic significance of Blood-Brain Barrier disruption measured in Computed Tomography Perfusion and its relationship with the risk of hemorrhagic transformation. The second objective is addressed in articles 3 and 4:

Article 3: Renú A*, **Laredo C***, Tudela R, Urra X, Lopez-Rueda A, Llull L, Oleaga L, Amaro S, Chamorro Á. *Brain hemorrhage after endovascular reperfusion therapy of ischemic stroke: a threshold-finding whole-brain perfusion CT study.* J Cereb Blood Flow Metab. 2017 Jan;37(1):153-165. JCR Impact Factor 2017: 6.045. JCR Ranking in the category “Neurosciences”: 29/261 (Q1).

Article 4: **Laredo C**, Renú A, Llull L, Tudela R, López-Rueda A, Urra X, Macías NG, Rudilosso S, Obach V, Amaro S, Chamorro Á. *Elevated glucose is associated with hemorrhagic transformation after mechanical thrombectomy in acute ischemic stroke patients with severe pretreatment hypoperfusion*. Sci Rep. 2020 Jun 29;10(1):10588. JCR Impact Factor 2019: 3.998. JCR Ranking in the category “Multidisciplinary Sciences”: 17/71 (Q1).

ABSTRACT

Imaging has a central role in prognostication and treatment decision making in acute ischemic stroke (AIS). Computed Tomography Perfusion (CTP) and Magnetic Resonance Imaging (MRI) are used to assess tissue viability and permeability of the Blood-Brain Barrier (BBB), but their sensibility and specificity are limited. This thesis aims to enhance the role of neuroimaging to understand the pathophysiology of AIS and assist a better prognostication of clinical outcomes. The main objectives of this thesis are: 1/ to evaluate the association between CTP-derived information and clinical and radiological outcome of AIS patients depending on baseline clinical and radiological variables and 2/ to evaluate the prognostic significance of BBB disruption measured in CTP and its relationship with the risk of hemorrhagic transformation (HT).

The first objective was addressed in two studies. In the first study, we evaluated the accuracy of CTP-derived ischemic core for the prediction of final infarct volume on MRI according to the time delay to recanalization. In the second study, we assessed the variables that interacted between CTP-derived ischemic core volumes and clinical outcomes and we then constructed a prediction tool based on those variables.

The second objective was addressed in two additional studies. In one study, we sought to identify the optimal CTP-derived parameters for the prediction of parenchymal hemorrhage after endovascular treatment and how these predictors could be affected by the duration of brain ischemia. In the other study, we analyzed the potential synergistic effects between glucose, blood perfusion parameters and brain hemorrhagic risk in patients treated with mechanical thrombectomy.

Overall these studies reinforced the strengths and limitations of CTP for predicting relevant clinical and radiological outcomes in AIS.

RESUM

El diagnòstic per imatge té un paper fonamental en el pronòstic i la presa de decisions en el tractament de l'ictus isquèmic agut. La Tomografia Computaritzada de Perfusió (TCP) i la Ressonància Magnètica (RM) s'utilitzen per avaluar la viabilitat del teixit cerebral i la permeabilitat de la barrera hematoencefàlica (BHE), però la seva sensibilitat i especificitat són limitades. Aquesta tesi doctoral pretén millorar el paper de la neuroimatge en el coneixement de la fisiopatologia de l'ictus i ajudar a aconseguir una millor predicció del pronòstic clínic i radiològic dels pacients. Els principals objectius de la tesi són: 1/ avaluar l'associació entre la informació derivada de la TCP i el pronòstic clínic i radiològic dels pacients amb ictus isquèmic agut en funció de les variables clíniques i radiològiques basals y 2/ avaluar la importància pronòstica de l'alteració de la BHE mesurada en la TCP i la seva relació amb el risc de transformació hemorràgica.

El primer objectiu es va abordar en dos estudis. En el primer estudi, es va avaluar la precisió de la definició del nucli de l'infart a la TCP per a la predicció del volum final d'infart mesurat a la RM en funció del temps de l'inici de símptomes fins a la recanalització. En el segon estudi, es van avaluar les variables que interactuaven en l'associació entre el volum de nucli de l'infart definit a la TCP i el pronòstic clínic i, a continuació, es va crear una eina de predicció basada en aquestes variables.

El segon objectiu es va abordar en dos estudis addicionals. En el primer estudi, es van identificar els paràmetres òptims definits a la TCP per a la predicció de l'hemorràgia parenquimatosa després de l'administració del tractament endovascular i com aquests predictors es podien veure afectats per la duració de la isquèmia. En el segon estudi, es van analitzar els possibles efectes sinèrgics entre la glucosa, els paràmetres de perfusió sanguínia i el risc hemorràgic en pacients tractats amb trombectomia mecànica.

En general, aquests estudis reforcen les fortaleeses i limitacions de la TCP per la predicció del pronòstic clínic i radiològic a l'ictus isquèmic agut.

1 · INTRODUCTION



1.1 Acute Ischemic Stroke

Acute ischemic stroke (AIS) occurs as the result of a sudden reduction of blood flow to the territory of a major brain artery. This reduction in flow is, in most cases, caused by the occlusion of a cerebral artery, which may be produced by numerous different causes. The duration, location and severity of the ischemia will be the main determinants of the clinical and brain tissue consequences of ischemic stroke [1-5]. AIS represents the first cause of permanent disability in adult people, the second most frequent cause of death for people older than 60 years and the second most common cause of dementia. Overall cost of stroke care accounts for approximately 3% to 7% of the total health-care expenditure in high-income countries [6, 7].

In the setting of AIS, the changes in cerebral blood flow (CBF) induce adjustments in cerebral hemodynamics. The arterial occlusion generates a decrease in cerebral perfusion pressure (CPP) that triggers the activation of systemic compensatory mechanisms to avoid this situation. These mechanisms include cardiovascular response, collateral perfusion recruitment and cerebral autoregulation. In a first stage, collateral flow is recruited to maintain CBF. The cerebral collateral circulation is the auxiliary vascular network that maintains CBF when the principal channels fail. The collateral networks in the brain include the posterior and anterior communicating arteries of the circle of Willis (primary collaterals, intracranial) and the ophthalmic artery and leptomeningeal vessels (secondary collaterals, extracranial). Both the primary and secondary collaterals can provide CBF to regions affected by an artery occlusion in AIS [8]. In a second stage, if collateral circulation is not recruited or is insufficient, CBF continues to fall thus increasing the action of the cerebral autoregulation response. Control of CBF under conditions of normal CPP is partly mediated by cerebral autoregulation and is determined by the caliber of the resistance vessels, primarily arterioles but also larger intracranial and extracranial arteries, which dilate and constrict in response to a variety of stimuli. The metabolic factor controlling CBF in the normal resting brain is cerebral oxygen metabolism. Vasodilation and vasoconstriction maintain the balance between oxygen delivery [$\text{CBF} \times \text{arterial oxygen content (CaO}_2\text{)}$] and oxygen metabolism. With both

hypoxemia and anemia, CBF increases in proportion to the reduction in CaO_2 to maintain oxygen delivery. In order to maintain the cerebral metabolic rate of oxygen (CMRO_2) constant, cerebral autoregulation dilates arteries to increase the oxygen extraction fraction (OEF) [9, 10].

Brain tissue has a relatively high consumption of oxygen and glucose, when the compensatory mechanisms are not sufficient to balance the reduction of blood flow, CBF continues to fall and the oxygen supply is then interrupted and metabolic demands unfulfilled thus leading to neuronal electrical activity arrest and to the impairment of the energy state necessary to maintain ion homeostasis [1, 10, 11]. If blood flow is not restored within minutes, a multifactorial cascade process (known as the ischemic cascade) starts, including major pathogenic mechanisms: excitotoxicity, inflammation [12, 13], oxidative-nitrosative stress [14], apoptosis and their complex bidirectional or multidirectional relationships [15]. The loss of energy reserves results in the imbalance of ion homeostasis and the release of excitotoxic neurotransmitters to the extracellular space, like glutamate. Glutamate binds to N-Methyl-D-aspartate promoting an influx of Ca^{2+} into the cell. The accumulation of Ca^{2+} initiates an activation of proteolytic enzymes that degrade essential membranes and proteins. At the same time, the overactivation of glutamate triggers an influx of Na^+ , Cl^- and water, with concomitant cell swelling and edema. The accumulation of Ca^{2+} , Na^+ and adenosine diphosphate causes the production of free radicals in the mitochondria and reactive oxygen/nitrogen species that damage lipids, proteins, nucleic acid and carbohydrates. Oxygen free-radicals also act as signaling molecules that trigger inflammation and apoptosis. Consequently, oxidative-nitrosative stress, excitotoxicity, energy failure and ionic imbalances are linked, and jointly and simultaneously contribute to ischemic cell death [1, 15, 16].

The metabolic, ionic and hemodynamic changes described above do not affect the ischemic territory homogeneously. In the center or core of the perfusion deficit permanent and anoxic depolarization develops, leading to irreversible neuronal loss. Between this lethally damaged core and the normal brain lies the penumbra, an area of constrained blood flow with partially preserved energy metabolism but electrically unexcitable but viable cells [11, 16]. These areas with residual perfusion present mild energy

failures but have an almost normal concentration of ATP due to a sufficient oxygen supply and low extracellular potassium accumulation. If no treatment is administered the penumbra can progress to infarction due to excitotoxicity or to secondary deleterious processes as spreading depolarization, inflammation, oxidative and nitrosative stress and apoptosis [1, 7, 11, 17].

Current therapies for AIS aim to rescue the hypoperfused but still viable ischemic penumbra by restoring the patency of the primary occluded artery (recanalization) and the downstream capillary blood flow (reperfusion) [18]. Recanalization of the occluded artery after stroke onset is associated with an increase in the odds of good functional outcome. However, 25% of patients do not reperfuse and about 50% of them do not achieve good clinical recovery despite complete recanalization, highlighting the fundamental role of adequate brain perfusion for the final ischemic tissue fate. [6]. Recanalization can be accomplished by medical or mechanical treatment, as follows.

Recombinant tissue plasminogen activator (rtPA) is considered the medical gold standard and is approved by the Food and Drug Administration to treat AIS. rtPA is a serine protease administered intravenously that activates plasminogen into plasmin, the latter dissolving and lysing the fibrin clot [19-21]. Early arterial recanalization is achieved in 50% of cases receiving rtPA and although it improves survival and clinical outcome [22], it is limited by its narrow therapeutic window (first 4.5 hours from stroke onset), contraindications (as coagulopathy, recent surgery, stroke in the previous 3 months or brain hemorrhage history), risk of post-treatment hemorrhagic transformation (HT) and limited efficacy when there is a proximal intracranial occlusion [22-26].

Mechanical thrombectomy (MT) has been established as standard treatment of AIS by seven recent randomized clinical trials (RCTs) that evaluated MT versus the best medical treatment [27-33]. An endovascular catheter is placed at the site of the blood clot and a mechanical thrombectomy device called stent retriever is released from the catheter, self-expands within the thrombus and removes it, restoring blood flow. There are also other types of thrombectomy devices like aspiration

catheters, which can be used combined with stent retrievers or alone, where the process involves clot fragmentation and aspiration through an electric pump providing negative pressure. In the meta-analysis of the data derived from RCTs, MT was proven to be superior to best medical treatment in improving stroke outcomes in selected patients with large vessel occlusions. However, less than half of the patients treated with MT achieved a good clinical outcome although 75% had full recanalization [34-36]. The rate of complete reperfusion was only of 38%, suggesting that the suboptimal efficacy of MT may be explained by a recanalization-reperfusion mismatch [6, 37]. In experimental models of brain ischemia/reperfusion, a number of mechanisms were found to play a role in the hampering of full reperfusion of the distal microcirculation despite full recanalization: distal micro-embolisms, blockage of perivascular space, capillary clogs or the effect of oxidative/nitrosative stress on the vasoconstriction and hypoperfusion of the microcirculation [38].

As mentioned before, in the context of acute brain ischemia and its treatment to achieve recanalization/reperfusion, a number of deleterious processes take place, including cellular bioenergetic failure, oxidative stress, excitotoxicity, hemostatic activation, microvascular injury, inflammation and blood brain barrier (BBB) dysfunction [16, 39, 40].

The BBB is the structure that separates the central nervous system (CNS) from the peripheral tissues [41] and it is formed by endothelial cells (with specialized tight junctions), pericytes, astrocytes, vascular smooth muscle cells, microglia and neurons. Interactions between these components are the main basis of the neurovascular unit concept, where each cell contributes to BBB structural and/or functional task. BBB regulates the movement of molecules, ions and cells between the blood and the CNS, regulating CNS homeostasis and protecting it from toxins, pathogens, injury, inflammation and disease. Despite restoration of blood flow, the ischemic cascade continues from hours to days. Although the use of reperfusion therapies has shown its substantial clinical benefits in selected patients, the use of these strategies can hypothetically result in the so called reperfusion injury and therefore increase the risk of hemorrhagic transformation (HT) due to BBB disruption.

HT is a relatively frequent complication of AIS and refers to a range of ischemia-related brain hemorrhagic transformations that can be divided into hemorrhagic infarction (HI) and parenchymal hematoma (PH) [42]. The presence of HT in the form of PH is associated with increased morbidity and mortality [43, 44]. In addition to toxicity secondary to thrombolytic drugs and direct procedural-related mechanical damage, one of the mechanisms involved in the appearance of HT is the severity and duration of brain ischemia.

1.2 Neuroimaging in Acute Ischemic Stroke

The brain accounts for approximately 2% of body weight and receives 16% of cardiac output. Healthy young adults have an average whole-brain CBF of approximately 46 mL/100 g/min, CMRO₂ of 3.0 mL/100 g/min (134 μmol/100 g/min), and cerebral metabolic rate of glucose of 25 μmol/100 g/min measured using the Kety-Schmidt technique. Under physiological conditions, brain CBF is paired to the metabolic demands and this balance is achieved through several structural and adaptive elements of the cerebral circulation including collateral flow and autoregulation [45, 46].

When an artery occlusion occurs, the intravascular pressure distal to the occlusion falls abruptly and a retrograde flow can appear through the anastomoses that characterize the collateral circulation. Retrograde compensation of blood flow by collateral circulation is a well-known phenomenon in major artery occlusions that affect the cerebral cortex, where flow direction can be bidirectional through leptomeningeal arteries and can compensate the areas of hypoperfused tissue distal to the occlusion. Collateral circulation can prevent or delay infarct growth and permanent neuronal damage in AIS, however, the functionality and extension of collateral circulation present an important variability between individuals, due to anatomic factors and others such as age, time of occlusion and atherosclerosis [47].

At the same time, cerebral autoregulation maintains relatively constant CBF by adjusting cerebral resistance and compensating for fluctuations in CPP. When a decrease of CPP occurs in AIS, intracranial vessels dilate to maintain CBF, increasing cerebral blood volume (CBV) and prolonging

blood mean transit time (MTT) to maximize OEF. As CPP continues to fall, vasodilation cannot compensate flow decline and CBF continues to drop. Despite this decrease in blood flow, metabolic activity in the brain is initially maintained by increasing the OEF from blood, but when this mechanism fails to meet the metabolic demands of the brain, cellular metabolism is impaired, and CMRO₂ starts to fall under physiologic values leading to the abovementioned cascade process [9, 10, 45, 46].

Imaging has a central role for the evaluation of tissue viability, vessel permeability and collateral circulation in AIS. Magnetic Resonance Imaging (MRI) and Computed Tomography Perfusion (CTP) are commonly used in clinical routine for the evaluation of brain hemodynamic status, estimation of ischemic core, outcome prediction, and treatment decision-making in the acute stroke setting [48-52].

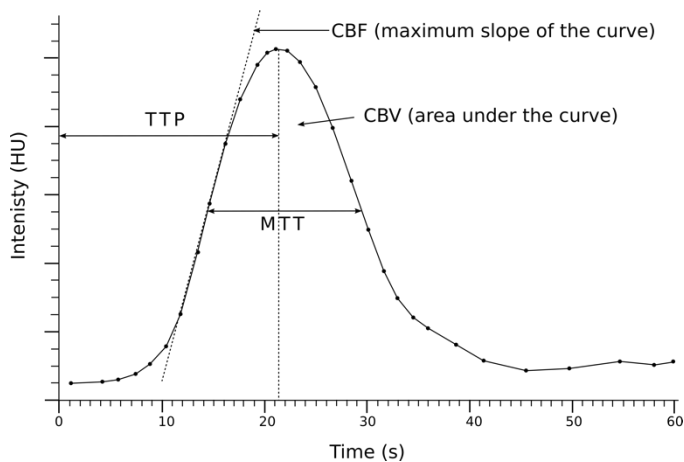


Figure 1. Time-Intensity curve of the CTP acquisition. Representation of a time-intensity curve in a certain pixel of the image. Time (in seconds) is represented in the x-axis and intensity (in Hounsfield Units) is represented in the y-axis. Each point in the graph represents the intensity of the pixel in each of the timepoints of the CTP acquisition. Cerebral Blood Flow (CBF), Cerebral Blood Volume (CBV), Mean Transit Time (MTT) and Time To Peak (TTP) are represented.

Diffusion-weighted imaging (DWI) provides information of the molecular motion of water. In healthy brain tissue, water molecules encounter several complex structures (like myelin along white matter tracts) that force diffusion directionality in the orientation of preferred motion. Diffusion of water drops following AIS reflecting the accumulation of water in the intracellular space, the presence of cytotoxic edema and the disruption of ion homeostasis. This diffusion decline translates in regions of high DWI signal in MRI. [10, 53].

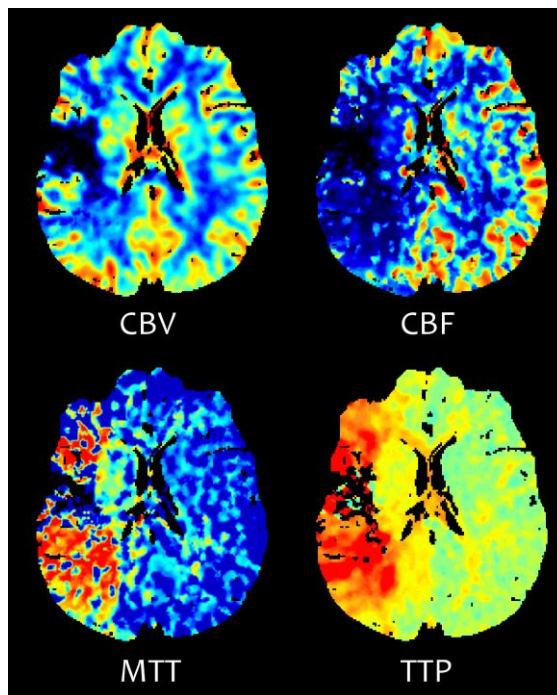


Figure 2. Perfusion Maps. Cerebral Blood Flow (CBF), Cerebral Blood Volume (CBV), Mean Transit Time (MTT) and Time To Peak (TTP) of an AIS patient from a 60s and 31 volumes CTP acquisition.

On the other hand, in the CTP technique, a series of CT images are acquired sequentially after the injection of a bolus of iodinated contrast agent. As the contrast agent goes from vessels to parenchyma, in each pixel of the image a time-intensity curve can be built, where the wash-in and wash-out of the iodinated contrast can be traced (Figure 1). Following acquisition, the pixel-wise analysis of the time-intensity curves with dedicated post-processing software allows the generation of parametric maps [54, 55]. These parametric maps, known as perfusion maps, represent different cerebral hemodynamic parameters, as follows [56-58] (Figure 2):

Cerebral Blood Volume (CBV)

Volume of blood in a unit of brain mass, including tissue and vessels, expressed in the unit mL/100g.

Cerebral Blood Flow (CBF)

Volume of blood flowing through a unit of brain mass per time unit, measured in mL/100g/min.

Mean Transit Time (MTT)

Average time required for blood passage through a volume unit of the parenchymal capillary network, measured in seconds.

Time to Peak (TTP)

Time between the injection and the maximum concentration of the contrast agent bolus at each voxel, measured in seconds.

Perfusion maps can be obtained by different postprocessing methods being the deconvolution analysis the most widely used. The deconvolution process intends to correct the time-intensity curves in each voxel for the shape of the arterial input function (AIF) (the time intensity curve acquired in a major artery) to obtain the tissue impulse residue function (IRF), which represents the (theoretical) tissue time-intensity curve resulting from an infinitely sharp bolus injection into the studied voxel:

$$C(t) = (CBF_t / k_H) \times AIF(t) \otimes R(t) \quad (\text{Eq. 1})$$

Where C is the concentration of the contrast agent in the voxel (measured), CBF is the (unknown) tissue blood flow, k_H is a correction constant taking into account different values of arterial and tissue hematocrit ($k_H = (1-H_a)/(1-H_t)$), AIF is the arterial input function in the artery leading to the ROI and $R(t)$ is the IRF. In other words, the concentration of the contrast agent measured in a voxel is the convolution of the arterial input function and the tissue IRF multiplied by the tissue blood flow.

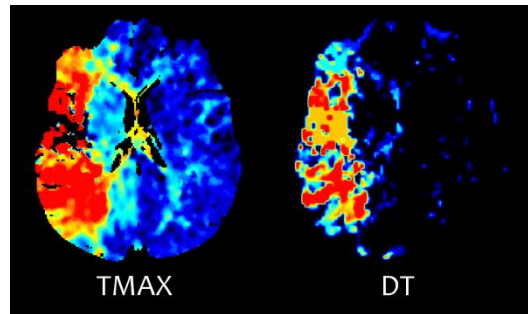


Figure 3. TMAX and DT Perfusion Maps. Time to Maximum (TMAX) and Delay Time (DT) Perfusion Maps of an AIS patient from a 60s and 31 volumes CTP acquisition.

With measured $C(t)$ and $AIF(t)$, an estimate of CBF and $R(t)$ can be obtained using a model-free deconvolution technique, such as the single value decomposition method. Perfusion maps can be calculated from this IRF: CBF as the peak height of the IRF curve, CBV from the area under the IRF curve and MTT as the ratio of CBV to CBF , according to the central volume principle. Time-to-Peak of the IRF curve will be the Time to Maximum (Tmax).

To compensate for arterial delay and dispersion effects that arise because the selected AIF in a major artery is taken to be the same as the AIF directly feeding the tissue, a vascular model involving an arterial transport function with a delay time and a relative dispersion was proposed [59]. The purpose of applying the transport function is to shift and broaden the AIF profile in an attempt to obtain a more realistic model of the physiology of acute stroke. With this methodology, CBF , CBV and MTT are calculated in the same way of a “simple” deconvolution with no delay correction, but Tmax map is replaced by a Delay Time (DT) map, which represents the time to peak of the delay and dispersion corrected IRF curve (Figure 3).

1.3 CTP definition of tissue fate

Pathophysiologically, ischemic core is defined as tissue that is irreversibly injured and will evolve to infarction even if reperfusion is achieved immediately, and penumbra as the tissue where blood flow levels are low but still sufficient to prevent irreversible cellular death but which is at risk of becoming infarct core if reperfusion does not occur [60]. CTP-derived definitions are probabilistic, representing the gathered information of one (or more) parametric values derived from a specific mathematical model. Although DWI has been established as the gold standard for the quantification of ischemic core due to its high sensitivity and reproducibility [49, 61], CTP imaging may provide similar ischemic core estimations as those derived from MRI [62-65] and is also used to assess the hemodynamic status of brain parenchyma and provide information of at-risk but still salvageable penumbra areas.

CTP provides information of tissue viability by reflecting changes in parenchymal autoregulatory mechanisms that follow AIS. The initial decreased CPP causes an increase in MTT and TTP. Vasodilation and collateral flow activation in an attempt to normalize CBF following arterial occlusion leads to an initial increase of CBV in the ischemic territory, but when compensatory mechanisms fail due to prolonged ischemia, CBF and CBV fall below tissue viability thresholds leading to infarct core areas [66]. On the other hand, increase in time-based maps as MTT and TTP but maintained and moderately reduced values in CBV and CBF respectively are indicative of penumbra areas. In order to obtain an automatic tool able to reduce interobserver variability and to improve the generalizability of tissue fate predictions, investigators have tried for years to establish predefined absolute or relative to normal tissue thresholds in perfusion maps to accurately define core and penumbra areas. The first studies used relative MTT ($>145\%$) and absolute CBV (<2 mL/100g) to define penumbra and core respectively [67]. However, more recent studies have moved to Tmax and DT maps (Tmax $>6s$, DT $>3s$) and relative CBF thresholds (30-45%) for the definition of penumbra and core respectively [62, 64].

The definition of core of the infarct has been used as selection criteria in the recently published DAWN and DEFUSE 3 MT trials that explored the

benefit of mechanical thrombectomy in the extended time window (beyond 6 hours from stroke onset) [32, 33]. The positive results of these trials lead to the inclusion of CTP evaluation in the American Heart Association guidelines [68] for treatment selection in patients beyond 6 hours of infarct evolution. However, a number of pitfalls related to the use of CTP predictions of tissue fate must be taken into account in the clinical setting. The main limitations for the extended use of CTP are the differences in acquisition parameters used in each scanner, the differences in software-specific optimal thresholds to define ischemic core, the variability of pre- and post-processing platforms [49, 65, 69-71] and the fact that perfusion maps are an “static picture” of the hemodynamic status of the brain at the moment of the acquisition.

1.4 CTP prediction of infarct core and clinical outcome

Although theoretical definitions of infarct core and penumbra are relatively well validated in certain stroke populations, universally accepted imaged-based definitions of tissue fate are still lacking. Even so, in general, greater volumes of CTP predicted infarct core have been found to be moderately associated with larger infarcts on follow-up imaging [62-65] and with worse clinical outcomes [72]. The variable association between predicted infarct core and clinical or radiological outcome metrics may be due to the fact that clinical and hemodynamic status in AIS patients is multifactorial, making challenging the task of knowing the relative importance of every single variable, including imaged-based definitions.

In the case of CTP imaging, a current concern is that several clinical, radiological and acute treatment variables may affect the predictive capacity of the CTP parameters and thresholds to predict tissue fate [49, 65, 69, 70, 71, 73, 74] and clinical outcome [75-77]. Among them, the impact of achieving an early and complete reperfusion on the capacity of a single CTP threshold to obtain a reliable prediction of final infarct volume or clinical outcomes is still uncertain [69, 78-86]. Moreover, other pretreatment and treatment-related variables have been shown to modify the relationship between predicted infarct core and clinical outcome metrics including age [87, 88], baseline NIHSS [60], time to reperfusion [88, 89], degree of reperfusion achieved [88, 90], collateral status [91],

baseline ASPECTS [92], hyperglycemia [93] or presence of white matter lesions [88, 94, 95].

1.5 Perfusion parameters, glucose levels and hemorrhagic transformation

As mentioned above, one of the mechanisms involved in the appearance of HT is the initial severity of brain ischemia, which can be reliably quantified using MRI or CTP, by measuring CBF, CBV and time-based measures such as TTP, TMAX or DT. MRI-based clinical studies of patients with AIS treated or not with thrombolysis have shown that very severe reductions of CBV (termed as Very Low CBV, VLCBV) are strongly associated with the risk of PH [96-98], particularly when delayed reperfusion occurs after thrombolysis [97]. Using CTP, the risk of HT has been related to a myriad of perfusion measures such as low relative CBV values [99], low relative CBF [100], longer relative MTT or Tmax [100, 101], higher permeability values [102] and severe hypoperfusion detected in TTP maps [103]. Specifically, in patients receiving endovascular reperfusion therapies, reduced pretreatment CBV or CBF values measured with CTP have been associated with poor clinical outcomes [104], including the risk of development of intracranial hemorrhage [105, 106]. However, the best CTP parameters and thresholds for the prediction of PH and their relationship with the occurrence and timing of reperfusion have not been sufficiently addressed in this patient population. The identification and validation of these biomarkers may be relevant for risk stratification of acute stroke patients receiving multimodal reperfusion therapies and for the evaluation of neuroprotective therapies in the setting of clinical trials.

As mentioned before, the potential mechanisms contributing to exacerbated neurovascular injury and poor outcomes after the onset of brain ischemia are multifactorial and include augmented oxidative and nitrosative stress, tissue acidosis, mitochondrial dysfunction, thromboinflammation and impairment of cerebral perfusion, among others [107, 108]. Consequently, severe hypoperfusion might not be a sufficient risk factor for the occurrence of HT and additional concurrent susceptibility conditions might be needed, such as elevated glucose levels. Higher blood glucose levels have been associated with a higher risk of HT after

reperfusion therapies as well as with significant reductions on the benefits of MT [109-111].

In preclinical models of brain ischemia, the interaction between hyperglycemia and reduced CBV or CBF during ischemia and at reperfusion is controversial and this issue has not been explored previously in humans [112-119]. Most studies found increased extent and severity of ischemia and greater neurological deficits in hyperglycemic animals [112, 113, 115-119]. However, when studying the interaction between hyperglycemia and blood perfusion measures, some authors found global reductions in blood flow or volume [112, 113], while other found only regional [115, 116, 118] or no differences between these measures [119]. Furthermore, the mechanisms by which glucose load affects post-ischemic cerebral perfusion remains unknown. The possible explanations for global or regional variations of CBF and CBV due to hyperglycemia found in the literature range from systemic changes induced by glucose, such as increased cerebrovascular resistance [115, 116] to endothelial cell injury [112], increased plasma hyperosmolality and blood hyperviscosity, decreased cerebral metabolic rate [113] or possible associations with downregulation of endogenous tissue plasminogen activator [114]. Arguably, the identification of a synergistic effect between hyperglycemia and severe hypoperfusion prior to reperfusion might be useful for the identification of subgroup of patients more prone to hemorrhagic complications after mechanical thrombectomy.

Overall, CTP allow the quantification of the severity of brain ischemia for the prediction of final infarct volume, clinical outcome and risk of HT. However, the information derived from CTP imaging is inaccurate and its sensibility and specificity may be influenced by a number of baseline clinical, radiological and procedure-related variables.

- 2.1 CTP estimation of infarct core is able to predict final infarct volume with an acceptable accuracy in AIS patients. However, an early and complete recanalization of the occluded vessel through endovascular treatment may impact significantly on the reliability of this prediction. We hypothesize that the optimal perfusion thresholds used for the definition of ischemic core will be modified according to the time from stroke onset to complete recanalization.
- 2.2 Infarct core estimated using CTP may not be reliable to predict accurately clinical outcome in AIS patients as it is dependent of clinical and radiological baseline variables. An advanced analysis of interaction between CTP-predicted infarct core and relevant clinical and radiological baseline variables will allow the identification of a selected subgroup of AIS patients in whom CTP-derived infarct core will be more accurate for predicting clinical outcome.
- 2.3 CTP allows the quantification of the severity of brain ischemia, one of the pathophysiological mechanisms involved in the appearance of HT in AIS patients treated with reperfusion therapies. We hypothesize that very severe reductions of CTP-derived perfusion parameters will be able to accurately predict the risk of HT in AIS patients receiving endovascular therapy.
- 2.4 Elevated glucose levels at stroke onset are associated with a higher risk of hemorrhagic complications after reperfusion therapies as well as with significant reductions on the benefits of MT. However, whether this association is influenced by the severity of hypoperfusion is unknown. We hypothesize that severely reduced CBV or CBF will boost the toxicity of increased blood glucose levels further increasing the risk of HT after endovascular treatment.



3. OBJECTIVES



- 3.1 To evaluate the impact of time from symptom onset to complete reperfusion on the accuracy of CTP maps for predicting final infarct volume and clinical outcome in AIS patients treated with MT.
- 3.2 To identify the pretreatment and treatment-related variables that influence the association between CTP-derived ischemic core and clinical outcome and to generate an integrative prediction tool in AIS patients.
- 3.3 To evaluate the best CTP parameters and the impact of time from stroke onset to treatment for the prediction of HT in AIS patients treated with MT.
- 3.4 To evaluate whether blood glucose levels modify the association between severe hypoperfusion measured with CTP and post-treatment HT in AIS patients treated with MT.




4. RESULTS



Study 1

The accuracy of ischemic core perfusion thresholds varies according to time to recanalization in stroke patients treated with mechanical thrombectomy: A comprehensive whole-brain computed tomography perfusion study.

The accuracy of ischemic core perfusion thresholds varies according to time to recanalization in stroke patients treated with mechanical thrombectomy: A comprehensive whole-brain computed tomography perfusion study

Carlos Laredo¹ , Arturo Renú¹, Raúl Tudela², Antonio Lopez-Rueda³, Xabier Urra¹, Laura Llull¹, Napoleón G Macías³, Salvatore Rudilosso¹, Víctor Obach¹, Sergio Amaro¹ and Ángel Chamorro¹

Abstract

Computed tomography perfusion (CTP) allows the estimation of pretreatment ischemic core after acute ischemic stroke. However, CTP-derived ischemic core may overestimate final infarct volume. We aimed to evaluate the accuracy of CTP-derived ischemic core for the prediction of final infarct volume according to time from stroke onset to recanalization in 104 patients achieving complete recanalization after mechanical thrombectomy who had a pretreatment CTP and a 24-h follow-up MRI-DWI. A range of CTP thresholds was explored in perfusion maps at constant increments for ischemic core calculation. Time to recanalization modified significantly the association between ischemic core and DWI lesion in a non-linear fashion (p -interaction = 0.018). Patients with recanalization before 4.5 h had significantly lower intraclass correlation coefficient (ICC) values between CTP-predicted ischemic core and DWI lesion ($n = 54$; best threshold relative cerebral blood flow (rCBF) < 25%, ICC = 0.673, 95% CI = 0.495–0.797) than those with later recanalization ($n = 50$; best threshold rCBF < 30%, ICC = 0.887, 95% CI = 0.811–0.935, $p = 0.013$), as well as poorer spatial lesion agreement. The significance of the associations between CTP-derived ischemic core and clinical outcome at 90 days was lost in patients recanalized before 4.5 h. CTP-derived ischemic core must be interpreted with caution given its dependency on time to recanalization, primarily in patients with higher chances of early recanalization.

Keywords

Computed tomography perfusion, ischemic core, ischemic stroke, recanalization, thrombectomy

Received 4 March 2019; Revised 15 April 2019; Accepted 15 May 2019

Introduction

Imaging has a central role for the evaluation of tissue viability, vessel permeability and collateral circulation in acute ischemic stroke.^{1,2} Diffusion-weighted imaging (DWI) on magnetic resonance imaging (MRI) has been established as the gold standard for the quantification of ischemic core, due to its high sensitivity and reproducibility.^{2,3} Computed tomography perfusion (CTP) imaging is also used to assess the hemodynamic state of brain parenchyma and may provide similar ischemic

¹Comprehensive Stroke Center, Department of Neuroscience, Hospital Clinic, University of Barcelona and August Pi i Sunyer Biomedical Research Institute (IDIBAPS), Barcelona, Spain

²CIBER de Bioingeniería, Biomateriales y Nanomedicina, Group of Biomedical Imaging of the University of Barcelona, Barcelona, Spain

³Radiology Department, Hospital Clinic, Barcelona, Spain

Corresponding author:

Sergio Amaro, Hospital Clinic, Villarroel 170, Barcelona 08036, Spain.
 Email: samaro@clinic.cat

core estimations as those derived from MRI.⁴⁻⁷ However, the main limitation for the extended use of CTP is the imprecision of the optimal perfusion parameters used for the quantification of ischemic core, in part due to its poor signal-to-noise ratio and to the variability of pre- and post-processing platforms.^{2,7-10}

Current data support the use of relative cerebral blood flow (CBF) with a threshold of 30% as the most accurate CTP estimator of ischemic core.^{4,6} However, a current concern is that several clinical, radiological and acute treatment variables may affect the predictive capacity of the CTP parameters and thresholds.^{2,7-12} Specifically, the impact of achieving an early and complete reperfusion on the capacity of a single CTP threshold to obtain a reliable prediction of final infarct volume or clinical outcomes is still uncertain.^{8,13-21}

Under the hypothesis that early reperfusion may impair the predictive capacity of CTP, we aimed to explore the impact of the timing of complete reperfusion on the accuracy of CTP for predicting final infarct volume and clinical outcomes through a comprehensive analysis of perfusion parameters and thresholds.

Material and methods

Subjects

Patients were part of a prospectively collected clinical registry of acute stroke patients treated with reperfusion therapies between March 2010 and December 2017 in a referral comprehensive stroke center. The specific selection criteria for this analysis were: 1/ availability of a pretreatment whole-brain CTP scan, 2/ the presence of a proximal intracranial arterial occlusion in the terminal internal carotid artery or the M1 segment of the middle cerebral artery without tandem occlusions, 3/ complete reperfusion after mechanical thrombectomy (MT), and 4/ availability of a follow-up MRI imaging performed within the first 24–72 h after stroke onset. According to these criteria, a total of 104 consecutive patients were retrospectively analyzed, as shown in the flowchart (Supplementary Figure 1). Ethics approval was acquired from the local Clinical Research Ethics Committee from Hospital Clinic of Barcelona under the requirements of Spanish legislation in the field of biomedical research, the protection of personal data (15/1999) and the standards of Good Clinical Practice, as well as with the Helsinki Declaration of 1975/1983. Patient consent was not required due to the retrospective nature of the study design and the lack of patient interaction. We adhered to the STARD (Standards for Reporting of Diagnostic Accuracy) guidelines (<http://www.stard-statement.org/>).

Demographics, clinical course, baseline neurological status (monitored with the National Institutes of Health Stroke Scale score, NIHSS),²² stroke subtype (according to the Trial of Org 10172 in Acute Stroke Treatment criteria, TOAST),²³ functional outcome (scored with the modified Rankin Scale score, mRS) at 90 days, and reperfusion-therapy modality (primary or rescue MT) were prospectively recorded on all patients. In this cohort of patients, reperfusion therapies were administered following contemporary guideline recommendations. MT was performed within 8 h in eligible patients with proximal arterial occlusion on CT angiography. The presence of a CTP-defined infarct core volume higher than 70 mL, an ASPECTS score lower than 6 or the absence of mismatch in patients with symptoms lasting >4.5 h from stroke onset type-redundant were considered as exclusion criteria for receiving MT. The mismatch profile was defined as the presence of a hypoperfusion lesion that was equal or higher than 120% of the infarct core. In patients treated with rescue MT after systemic thrombolysis, rtPA infusion was interrupted prematurely according to endovascular suite availability at the time of groin puncture.

CT perfusion imaging

Patients were scanned using a SIEMENS Somatom Definition Flash 128-section dual-source multidetector scanner (Siemens Healthineers, Erlangen, Germany), with a 98 mm z-coverage and 26 time points acquired each 1.5 s (total acquisition time, 39 s). Fifty milliliters of nonionic iodinated contrast were administered intravenously at 5 mL/s by using a power injector, followed by a saline flush of 20 mL at an injection rate of 2 mL/s. The imaging protocol included a baseline multimodal whole-brain CT scan, which included a plain CT (140 Kv, 127 mAs, FoV 225 mm, matrix 512 × 512, slice thickness 5 mm), a CT angiography (120 Kv, 663 mAs, FoV 261 mm, matrix 512 × 512, slice thickness 0.6 mm), and a CT perfusion (80 kV peak, 250 mAs, 1.5-s rotation, FoV 18 mm, matrix 512 × 512, and 49 2-mm thickness slices). CTP maps were then calculated by commercial software MISTar (Apollo Medical Imaging Technology, Melbourne, Australia) using a model-free singular value decomposition (SVD) algorithm with a delay and dispersion correction. The software automatically performs motion correction and selects an arterial input function (AIF) from an unaffected artery (usually the anterior cerebral artery) and a venous output function (VOF) from a large draining vein (the sagittal sinus). The software generates CBF, CBV, MTT and delay time (DT) maps. Of note, the delay corrected deconvolution method produces DT maps rather than the more extensively used Tmax

maps. An image processing pipeline using in-house fully automated software running in Matlab (v.2017b, Mathworks, Natick, MA) was developed in order to implement a comprehensive analysis of the perfusion maps. An absolute threshold of 3s was selected on the DT map to obtain the hypoperfused tissue (perfusion lesion). Inside this area, a range of relative and absolute thresholds was explored in the CBF and CBV maps at constant increments, as shown in Table 1. The relative thresholds were calculated as a percentage of mean perfusion values from the entire unaffected/contralateral hemisphere.

Angiographic assessment

The occlusion was graded on dynamic subtraction angiography (DSA) according to the modified thrombolysis in cerebral infarction (mTICI) classification (Grade 0: no perfusion; Grade 1: minimal flow past the occlusion but no perfusion; Grade 2a: partial reperfusion of less than half of the entire vascular territory; Grade 2b: partial reperfusion of more than half of the entire vascular territory; Grade 3: complete reperfusion without any flow defects). Recanalization was defined as complete if a grade 3 was obtained at the end of the MT. The mTICI score was graded by the interventionist team at the end of the procedure.

MRI imaging

The follow-up MRI was performed within a median (IQR) 38 h (20–64 h) from treatment and included diffusion-weighted images (DWI, parameters: Repetition time (TR)/echo time (TE) 10,800/89 ms, matrix 192×192 , field of view (FoV) 240 mm, slice thickness 3 mm, directions x,y,z, b-values: 0 and 1000 mm^2/s^2) and gradient echo T2*-weighted (GRE: TR/TE 764/26 ms; matrix 384×512 ; FoV 240 mm; slice thickness 5 mm) sequences. DWI lesion was delineated using AMIRA software by means of a semi-automated thresholding method to identify regions of interest with high DWI signal intensity (selection of pixels exceeding the DWI signal intensity of the mean values in the contralateral hemisphere by more than three standard deviations), as shown in Supplementary Figure 2.²⁴ In order to assure the comparability between pretreatment ischemic core CTP predictions and final DWI lesion, each CTP map was co-registered to the corresponding follow-up DWI using a rigid co-registration protocol (6-degrees of freedom) implemented with statistical parametric mapping (SPM12, Functional Imaging Laboratory, University College London, London, UK), as summarized in Supplementary Figure 2. CTP and DWI lesion overlap and spatial agreement were assessed using the Dice similarity coefficient that was calculated using the

Table 1. Range of thresholds explored in CT perfusion maps.

CTP map	Parameter	Range of explored thresholds	Increments
CBF	aCBF	0 to 36 mL/100 g/min	2 mL/100 g/min
	rCBF	0 to 100%	5%
CBV	aCBV	0 to 2.0 mL/100 g	0.1 mL/100 g
	rCBV	0 to 100%	5%

Imaging Processing Toolbox (MATLAB v.2017b, Mathworks, Natick, MA).

Statistical analysis

Continuous variables were reported as mean and standard deviation (SD) or as median and interquartile range (IQR) and were compared with the Student t or Mann–Whitney tests. Categorical variables were reported as proportions and compared with the χ^2 and Fisher exact test. To assess the correlation between CTP-predicted ischemic core and final DWI lesion volume on MRI, we conducted simple linear regression and intra-class correlation coefficient (ICC) and its 95% confidence intervals (95% CI). We used the ICC (two-way mixed model, absolute agreement for single measures) beyond other association tests to study the repeatability between the two repeated measurements of ischemic core, as the ICC estimation reflects both the degree of correlation and agreement between measurements of continuous data.²⁵ Reliability was considered to be good when the ICC was 0.80 or higher. To assess the consistency of the optimal parameter thresholds for predicting ischemic core found in the whole population, a sensitivity analysis including only those patients in whom tissue time attenuation curves (TACs) were not truncated at the end of the CTP acquisition was performed. For this subset analysis, truncated curves were defined as those in which the TACs did not have return of the venous outflow function to at least 50% of peak and not truncated curves as those who were effectively completed. To analyze the agreement and association between the predicted ischemic core and final DWI infarct volume, we also conducted difference plots (Bland–Altman plots), spatial agreement analyses through the use of the Dice similarity coefficient and Spearman correlation analyses. The best perfusion threshold at an individual level was defined as the one that achieved the lowest volume difference between final DWI lesion and CTP-defined ischemic core. To evaluate the relationship between the individual best threshold and time to recanalization, a set of regression models were used: linear, logarithmic, quadratic and cubic. A general linear model adjusted for the HERMES collaboration confounding variables (age,

Table 2. Demographics, baseline and procedure-related variables according to time to recanalization.

	mTICI3 < 4.5 h (n = 54)	mTICI3 ≥ 4.5 h (n = 50)	p
Age (years), median (IQR)	73 (64–78)	76 (64–82)	0.172
Prior mRS, median (IQR)	0 (0–1)	0 (0–1)	0.646
Females, n (%)	26 (48)	29 (58)	0.315
Smoking, n (%)	5 (9)	7 (14)	0.450
Hypertension, n (%)	24 (44)	31 (62)	0.073
Diabetes, n (%)	4 (7)	7 (14)	0.275
Dyslipidemia, n (%)	25 (46)	19 (38)	0.392
Atrial fibrillation, n (%)	17 (32)	21 (42)	0.266
Previous stroke, n (%)	5 (9)	4 (8)	0.819
Prior antithrombotic treatment, n (%)	23 (43)	25 (50)	0.449
Baseline SBP (mmHg), mean (SD)	138 (21)	143 (24)	0.237
Glucose (mg/dl), median (IQR)	115 (105–136)	119 (107–142)	0.711
Baseline NIHSS, median (IQR)	16 (10–20)	17 (8–19)	0.604
Pre-angio NIHSS, median (IQR)	18 (11–21)	17 (12–19)	0.207
Baseline ASPECTS, median (IQR)	9 (9–10)	9 (8–9)	0.135
Collateral score, median (IQR)	2 (2–3)	2 (1–3)	0.472
Time to CT perfusion (min), median (IQR)	81 (60–119)	269 (204–352)	<0.001
Time to MT onset (min), median (IQR)	156 (125–185)	348 (290–425)	<0.001
Duration of MT (min), median (IQR)	26 (15–40)	35 (16–45)	0.151
Time to mTICI 3 (min), median (IQR)	195 (155–225)	379 (318–477)	<0.001
TOAST classification			0.955
Atherothrombotic origin, n (%)	5 (9)	4 (8)	
Cardioembolic origin, n (%)	31 (58)	30 (60)	
Other etiologies, n (%)	18 (33)	16 (32)	
Ischemic core (mL), median (IQR)	23 (9–48)	12 (6–28)	0.055
Hypoperfused tissue (mL), median (IQR)	137 (103–168)	135 (67–165)	0.409

mTICI: modified thrombolysis in cerebral infarction; IQR: interquartile range; mRS: modified Rankin Scale; SBP: systolic blood pressure; NIHSS: National Institutes of Health Stroke Scale; ASPECTS: Alberta stroke program early CT score; CT: computed tomography; MT: mechanical thrombectomy; TOAST: trial of ORG 10172 in acute stroke treatment.

sex, baseline NIHSS, baseline ASPECTS, previous rTPA administration and occlusion site defined as Internal Carotid Artery, segments M1 or M2 of the Middle Cerebral Artery) was applied to assess the association between CTP-derived ischemic core and functional outcome at 90 days (ordinal mRS shift) with exploratory purposes.²⁶ For correlation and regression analysis, volume variables were transformed (cubic transformation) to meet normality criteria. The analysis was performed using SPSS Version 19.0 and R (v3.5.1), and the level of significance was established at a 0.05 level (2-sided).

Results

Baseline traits of the included population

Overall, 104 patients were included in the analysis from whom a total of 54 (52%) had complete recanalization

within the first 4.5 h and 50 (48%) after 4.5 h from symptom onset. Descriptive data on demographics and baseline variables according to time to recanalization are shown in Table 2. Of note, the baseline clinical and radiological traits were similar across time groups except for a trend towards higher CTP-predicted ischemic core volumes in the earlier recanalization group.

Best CTP definition of ischemic core in the whole population

According to the correlation coefficient analyses, the best pretreatment ischemic core perfusion definition for final DWI-lesion corresponded to the absolute CBF (aCBF) threshold of 6 mL/100 mg/min (ICC = 0.814, 95% CI = 0.758–0.890) and to the relative CBF (rCBF) threshold of 25% (ICC = 0.800, 95% CI = 0.743–0.881). Similar but slightly lower ICC values were obtained for the remainder perfusion

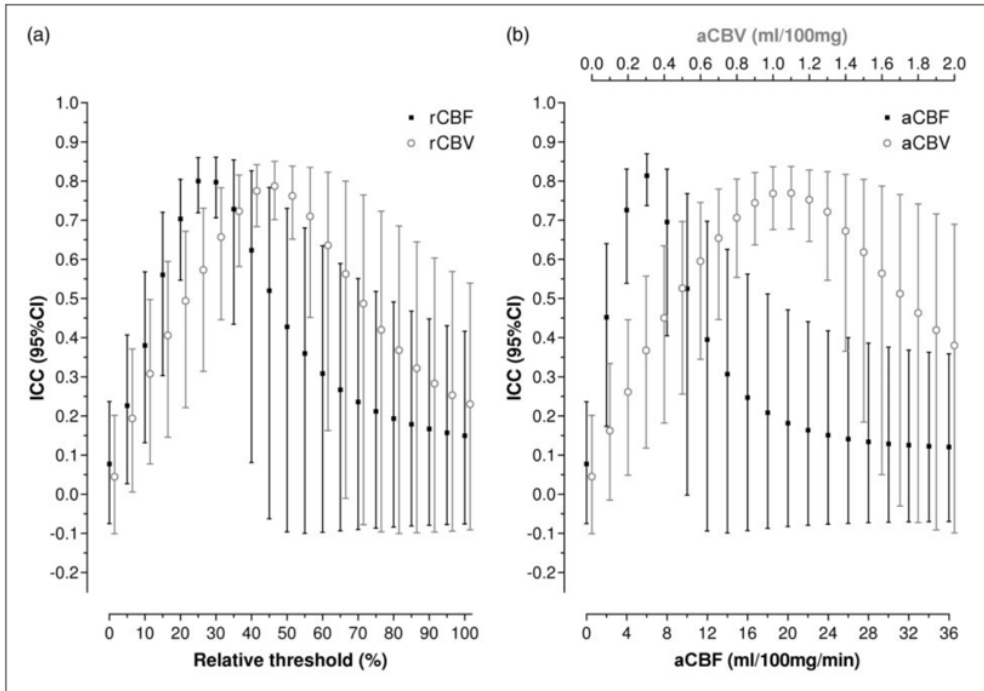


Figure 1. Intraclass correlation coefficient (ICC) and 95% confidence intervals (95%CI) between volume of ischemic core defined on CT perfusion and final infarct volume defined on DWI for the set of relative (a) and absolute (b) thresholds analyzed on cerebral blood flow (CBF) and cerebral blood volume (CBV) maps.

parameters ($rCBV < 45\%$, $ICC = 0.787$, $95\% \text{ CI} = 0.724\text{--}0.873$; and $aCBV < 1.1 \text{ mL}/100 \text{ g}$ $ICC = 0.769$, $95\% \text{ CI} = 0.701\text{--}0.861$) (Figure 1). Volumetric agreement was tested with the Bland–Altman plots, and total volumetric bias (average difference between DWI–CTP-predicted ischemic core) was -1.39 mL ($95\% \text{ limits of agreement: } -42.22\text{--}39.44$) for the ischemic core definition of $aCBF < 6 \text{ mL}/100 \text{ mg}/\text{min}$ and $+2.17 \text{ mL}$ ($95\% \text{ limits of agreement: } -36.34\text{--}40.68$) for the ischemic core definition of $rCBF < 25\%$ (Supplementary Figure 3).

Best CTP definition of ischemic core according to time from stroke onset to complete recanalization

A strong association was found between CTP lesion volume defined with each of the perfusion parameters and final DWI lesion. The strongest correlation was found for the $rCBF$ threshold of 25% (Spearman $\rho = 0.522$, $p < 0.001$). However, the time to complete recanalization modified significantly the association between the perfusion threshold and final DWI lesion ($p\text{-interaction} = 0.018$). The relationship between the best definition of CTP-predicted ischemic core for each patient (individual best threshold) and the time to recanalization was analyzed through the use of

curve estimation regression analysis that included linear, logarithmic, quadratic and cubic models. Overall, the best R-squared values were obtained in cubic regression models for all the perfusion parameters (Supplementary Table 1). Specifically, the highest R-squared values were 0.235 for $rCBF$, 0.178 for $rCBV$, 0.193 for $aCBF$ and 0.171 for $aCBV$. To determine a discrete time to recanalization cutoff point, we estimated the range of values where a plateau was reached in the cubic-fitted model for every perfusion parameter (Figure 2). Overall, the range of values fell between 240 and 420 min from symptom onset to recanalization. For practical purposes, a cutoff point of 4.5 h (270 min) was selected for further analyses.

In stratified analyses, patients with recanalization after 4.5 h had significantly higher ICC values ($n = 50$; best threshold $rCBF < 30\%$ $ICC = 0.887$, $95\% \text{ CI} = 0.811\text{--}0.935$) than those with earlier recanalization ($n = 54$; best threshold $rCBF < 25\%$ $ICC = 0.673$, $95\% \text{ CI} = 0.495\text{--}0.797$), $p = 0.013$ (Figure 3). According to Bland–Altman plots, CTP-predicted ischemic core was overestimated in the group of patients with earlier complete recanalization (average difference of -4.54 mL , $95\% \text{ limits of agreement: } -36.78\text{--}32.24$; $rCBF < 25\%$ threshold) in comparison with those with later recanalization (average difference

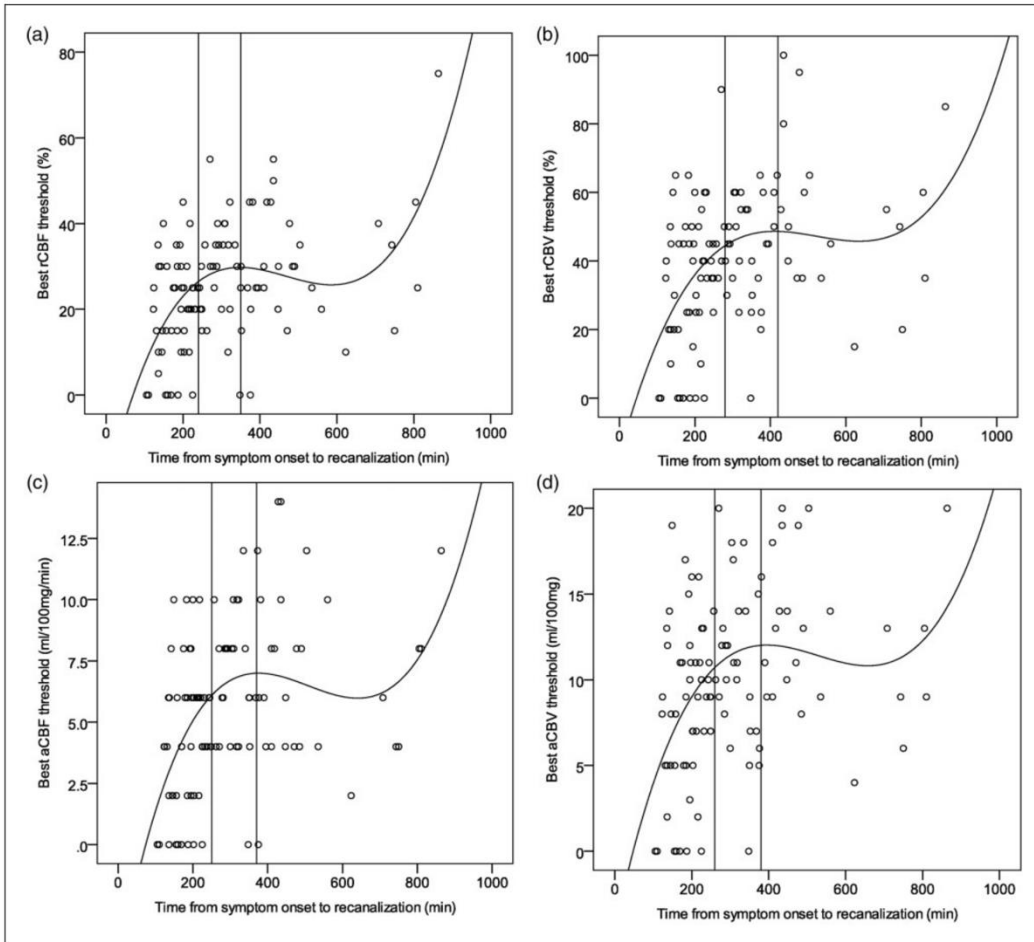


Figure 2. Individual best threshold (patient level) depending on the time from symptom onset to recanalization. The best fitting (highest r^2) was observed in cubic regression models and the plateau was reached for every threshold in the range between 240 and 420 min: rCBF (a, 240–350 min), rCBV (b, 280–420 min), aCBF (c, 250–370 min) and aCBV (d, 260–380 min).

of +2.30 mL, 95% limits of agreement: -36.14–40.74; rCBF < 30% threshold) (Supplementary Figure 3). As shown in Figure 4, the volumetric difference analysis between CTP predicted ischemic core and final DWI lesion resulted in a significant overestimation of final DWI lesion in most of the explored perfusion thresholds in the group of patients with full recanalization within the first 4.5 h in comparison with those with later recanalization. The correlation between CTP-predicted ischemic core and final DWI lesion was also poorer in patients who recanalized earlier [(Spearman $\rho = 0.446$ (95% confidence interval = 0.255–0.637); rCBF < 25% threshold)] in comparison with those with later recanalization [(Spearman $\rho = 0.679$ (95% confidence interval = 0.553–0.805); rCBF < 30% threshold)], $p = 0.049$. According to spatial agreement analyses, the Dice

similarity coefficient was significantly lower in the group of patients with earlier complete recanalization [median (IQR) 0.160 (0.118–0.202); rCBF < 25% threshold] in comparison with those with later recanalization [median (IQR) 0.228 (0.179–0.277); rCBF < 30% threshold], $p = 0.037$.

To assess the consistency of the optimal parameter thresholds for predicting ischemic core that were found in the whole population, a sensitivity analysis including only those patients with not truncated TACs at the end of the CTP acquisition was performed. A total of 92 (88%) patients had non-truncated curves, and 50 (54%) of them had recanalization within the first 4.5 h from stroke onset. In this subset of patients, those with recanalization after 4.5 h had significantly higher ICC values ($n = 42$; best threshold rCBF < 30% ICC = 0.892, 95% CI = 0.809–0.940) than those with

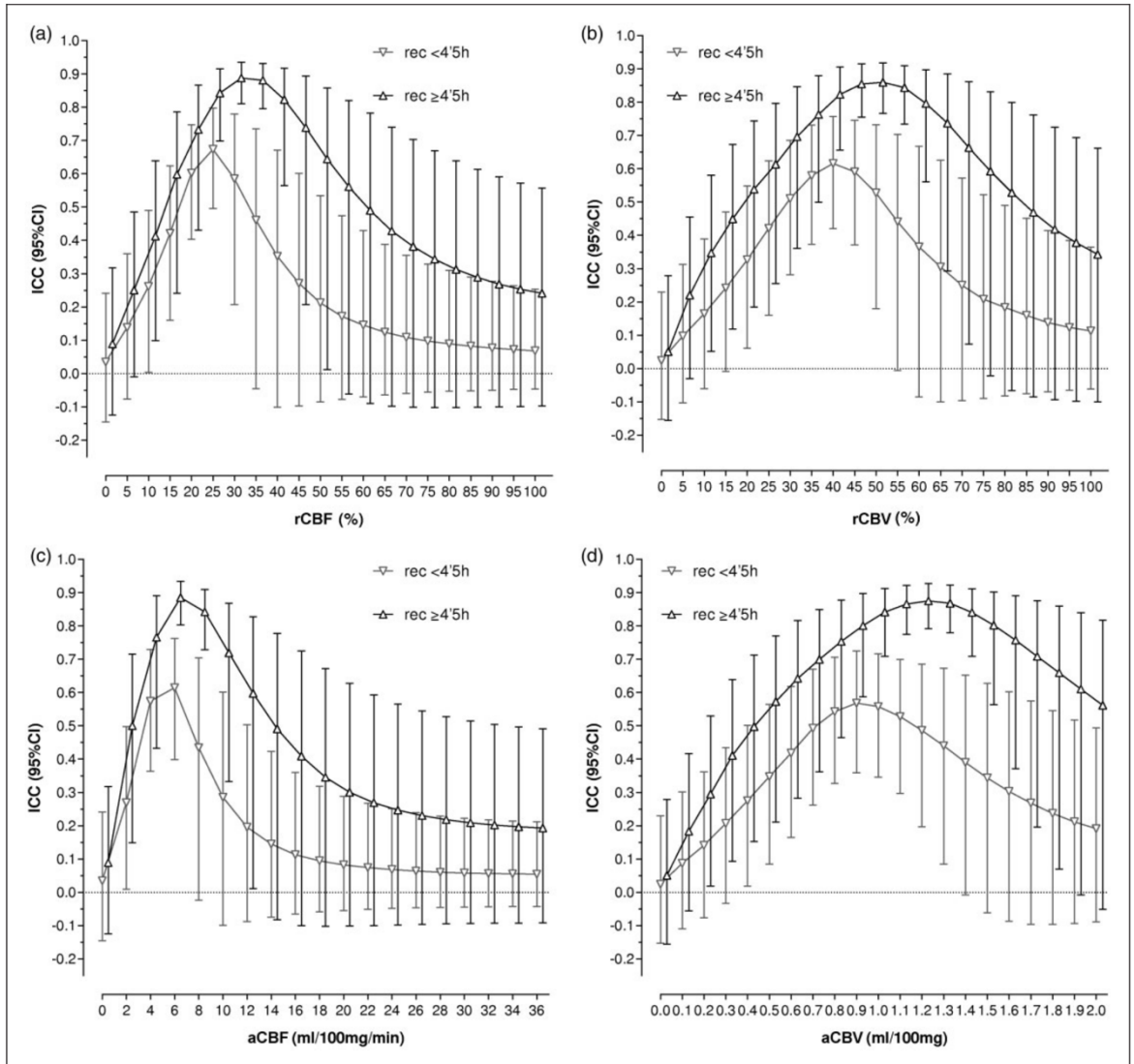


Figure 3. Intraclass correlation coefficient (ICC) and 95% confidence intervals (95% CI) between the volume of ischemic core defined on CT perfusion and final infarct volume defined on DWI depending on time from symptom onset to recanalization (complete recanalization before or after 4.5 h from symptom onset). Higher ICC values were found in patients with later recanalization for every analyzed threshold: rCBF (a), rCBV (b), aCBF (c) and aCBV (d).

earlier recanalization ($n=50$; best threshold $rCBF < 25\%$ $ICC=0.700$, $95\% CI=0.583-0.819$), $p=0.007$ (Supplementary Figure 4), as in the whole study sample.

CTP definition of ischemic core and functional outcome

In the whole cohort of patients, a subset of thresholds of relative and absolute perfusion parameters was found to be significantly associated with functional

outcome in exploratory analyses. These thresholds ranged from 30% to 40% of rCBF, 40% to 80% of rCBV and 1.2 to 2 mL/100 g of aCBV (Figure 5). However, the significance of these associations was influenced by the time from stroke onset to complete recanalization. In the subset of patients recanalized before 4.5 h of symptom onset, there were no significant associations between ischemic core and functional outcome, whereas some of these associations remained significant with wider confidence intervals in the subset of patients recanalized after 4.5 h (Figure 5).

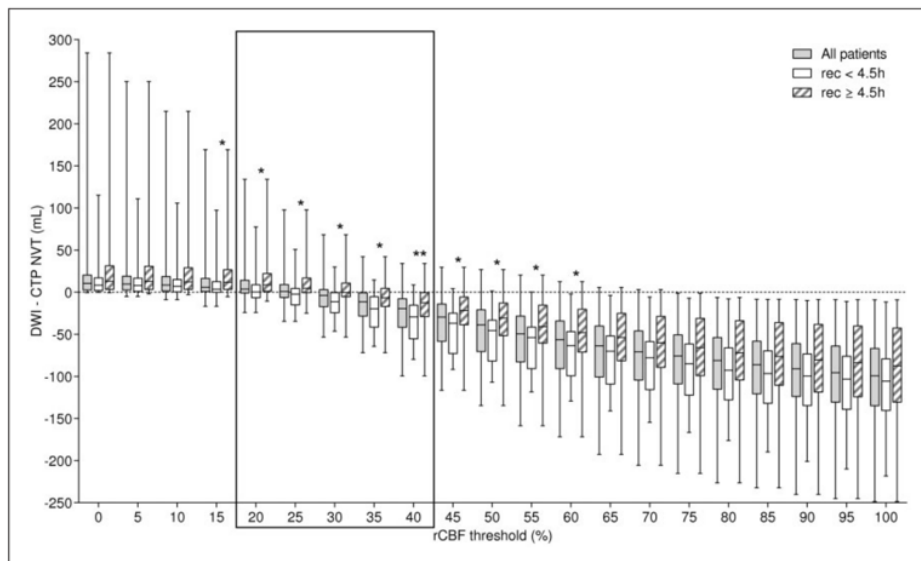


Figure 4. Volume difference between DWI final infarct and CTP ischemic core defined with a set of relative CBF thresholds. * $p < 0.01$ and ** $p < 0.005$ for the comparison of volume differences according to recanalization groups (<4.5 h vs. ≥ 4.5 h).

Discussion

In this study, we implemented a comprehensive approach to evaluate the accuracy of pretreatment CTP hemodynamic parameters and thresholds for the prediction of final infarct volume and long-term clinical outcome in a cohort of acute ischemic stroke patients successfully reperfused after MT. We demonstrated that the association between CTP-derived ischemic core predictions and final DWI lesion volume was significantly modified by time from stroke onset to recanalization in a non-linear fashion. Thus, the reliability of CTP-predicted ischemic core was good in patients with complete recanalization after 4.5 h from stroke onset, whereas it was only moderate in those who achieved earlier and complete recanalization. We also found associations between CTP-derived ischemic core and functional outcome regardless of time from stroke onset to complete recanalization, although these associations were lost in patients recanalized before 4.5 h from symptom onset. Altogether, these results highlighted the relevance of time to recanalization in the accuracy of pretreatment CTP imaging prediction of final infarct and long-term clinical outcome.

Previous studies have shown strong correlations between CTP-derived ischemic core volume estimation with both final infarct volume and clinical outcome.^{4–8,11–16,20,21,26–29} In agreement with these data, we found significant associations between CTP-derived ischemic core values, final infarct volume and clinical outcome at follow-up in the full cohort of patients who achieved a complete recanalization after MT. However,

a number of pretreatment variables, including baseline imaging features and acute reperfusion treatment modality have been extensively proved to modify the performance of CTP for final infarct prediction.^{7–12} Our results reinforce and expand previous observations supporting the dependency of optimal CTP thresholds on time to recanalization and the notion that CBF thresholds for tissue infarction may be more restrictive in patients with shorter time from stroke onset to reperfusion.^{8,13–19} Beyond the differences in CTP acquisition and post-processing protocols that were used in these studies, herein we included only a highly homogeneous stroke population consisting in patients that achieved full reperfusion at the end of MT thus minimizing the risk of infarct growth from the end of MT to follow-up MRI secondary to non-complete recanalization. Moreover, as a novel approach, we modeled the relationship between time to recanalization and CTP-DWI volumetric differences through curve estimation analyses across different perfusion parameters and thresholds and also explored their impact on long-term clinical outcome. Indeed, in contraposition with previous published data and according to ICC analyses,^{13,14,16} in patients with earlier recanalization, the reliability of CTP for the prediction of final infarct volume was only moderate; even using restrictive perfusion thresholds and ischemic core predicted values tended towards the overestimation of irreversible tissue injury. Reassuringly, Dice similarity coefficient and Spearman correlation analyses showed poorer spatial agreement and association between CTP-predicted ischemic core and final DWI lesion in patients with

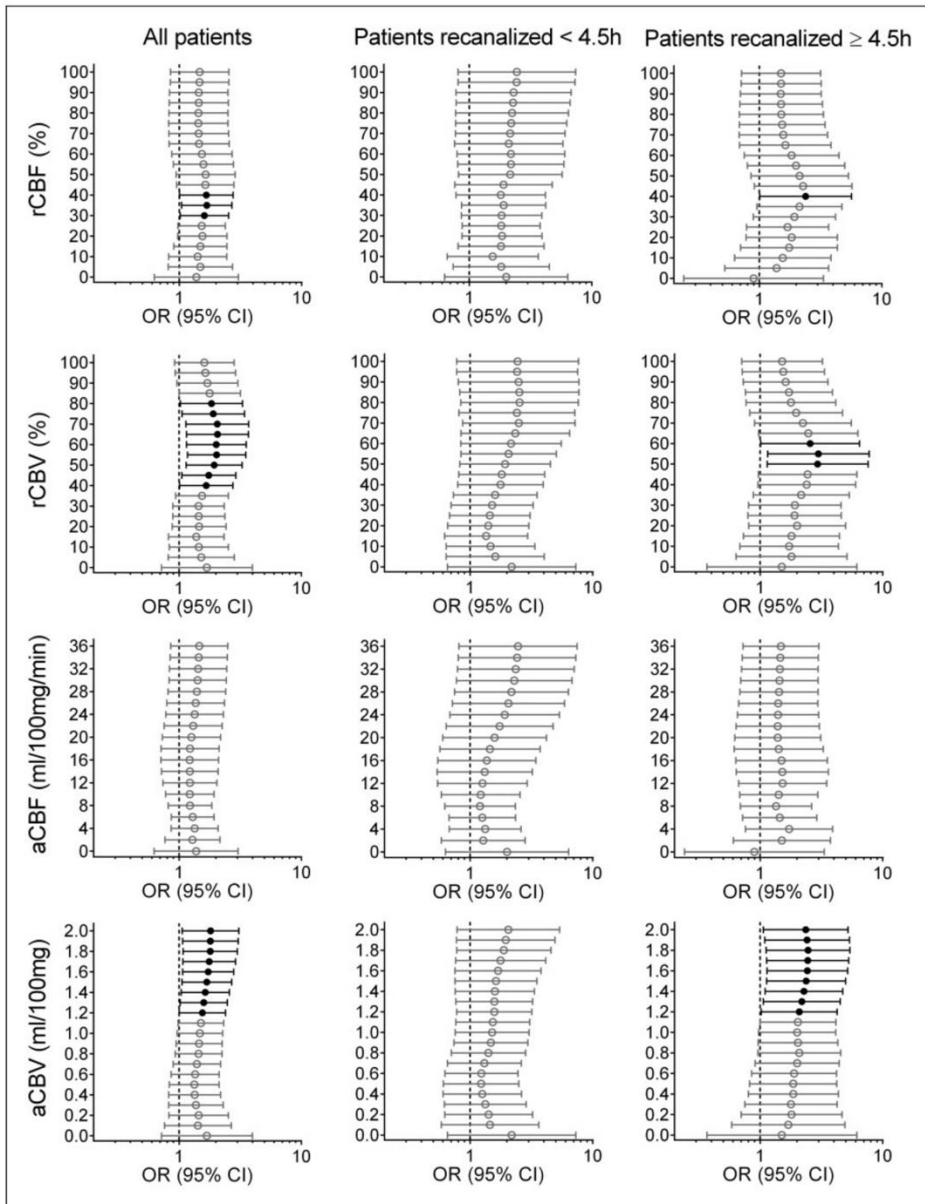


Figure 5. Odds ratios (OR) and 95% confidence intervals (95%CI) of the association between ischemic core defined with different absolute and relative thresholds and functional outcome. The significant associations are shown in bold ($p < 0.05$). A range of absolute and relative thresholds are significantly associated with functional outcome on the whole cohort of patients, fewer in the subset of patients recanalized after 4.5 h from symptom onset but no associations were found in those recanalized earlier.

earlier recanalization compared to those who recanalized later than 4.5 h. Moreover, the significance of the association of CTP-predicted ischemic core values with clinical outcome in multivariate models adjusted for the effect of confounders was lost in the subgroup of patients with earlier and complete recanalization regardless of the perfusion parameters and thresholds used for the prediction of infarct core. Overall, these

data support current guidelines arguing against the use of CTP-predicted ischemic core as selection criteria for MT in patients with short evolution from stroke onset to expected complete recanalization (e.g. if complete recanalization is expected within the first 4.5 h from stroke onset).³⁰

The main strength of the study was the comprehensive analysis of absolute and relative CTP parameters

and the exhaustive scanning of multiple different thresholds in whole-brain CTP acquisitions, a methodology that allowed obtaining perfusion measures of most of the affected brain tissue. Moreover, the imaging modality used for final infarct definition was CTP co-registered DWI in all the study population thus avoiding volumetric biases related to the use of different modalities (CT or MRI).^{31,32} In addition, patients were collected consecutively and managed following homogeneous therapeutic protocols according to contemporary clinical guidelines. Nonetheless, the study has several limitations. First, there should be acknowledged that the CTP methods used for the definition of ischemic core are a pragmatic approximation to a complex, dynamic and heterogeneous pathological process.³³ Furthermore, a number of additional variables beyond time to recanalization such as collateral status, age, pretreatment hyperglycemia or leukoaraiosis might hamper CTP-derived measures of ischemic core and penumbra.¹⁸ Further studies with larger numbers of patients to allow the comparison of CTP performance in subgroups of patients defined by more than one characteristic are warranted. Second, we analyzed the best perfusion parameters in two acquisitions that were not concurrent as pretreatment CTP-derived ischemic core estimates were compared with post-treatment DWI lesions. Although we restricted our analysis to patients who achieved a complete recanalization at the end of MT to minimize the odds of lesion change overtime between CTP acquisition and recanalization, individual imbalances in time from CTP acquisition to recanalization or post-recanalization lesion changes could have derived in some uncontrolled volume differences. Of note, CT perfusion acquisition parameters and post-processing platforms are an essential source of variability regarding the values obtained from perfusion maps and therefore our results may apply only to the protocol of acquisition and analysis that were employed in these series and may not be generalizable to other methodologies.^{7,9,11} Specifically, in this study CTP maps were calculated using a deconvolution algorithm with delay and dispersion correction and therefore the obtained results may not be applicable to delay-sensitive algorithms and software. Regarding the acquisition protocols, a limited acquisition time (<60s) may result in a delayed arrival of contrast agent with a consequent incomplete capture of the tissue TACs during acquisition. This delay may derive in truncation of tissue TACs that may preclude an accurate calculation of CTP parameters with a shift towards overestimation of perfusion deficits. Reassuringly, in this study, the consistency of the thresholds found in the whole population was confirmed in a sensitivity subgroup analysis that included only those patients without truncated typo-redundant TACs. In relation with the spatial agreement analysis, in this cohort of patients,

the Dice values were generally poor in agreement with previous reports. As previously described, the low values of the Dice coefficient might be related to limitations of co-registering different imaging modalities (pretreatment CTP and post-treatment DWI) that include non-isotropic data, different slice angulations and inherent distortions in DWI images.^{7,18} Finally, the analyses of the association between perfusion thresholds and clinical outcome were not corrected for multiple comparisons for their exploratory nature and might have been underpowered because of the limited size of the study.

In summary, this comprehensive threshold-finding study showed that time from symptom onset to recanalization modifies the association of CTP-derived ischemic core with final infarct DWI volumes and with long-term clinical outcome measures in patients who achieve complete recanalization after MT. We found accurate predictions of final infarct volume and long-term clinical outcome from CTP-derived ischemic core definitions, especially in those patients that achieved recanalization after 4.5h from symptom onset. Conversely, in the subset of patients who achieved complete and early recanalization within the first 4.5h from stroke onset, we did not find a single CTP typo-redundant parameter and threshold for the definition of pretreatment ischemic core accurate enough for the prediction of final infarct volume or long-term clinical outcome. Overall, these findings suggest that the reliability of CTP for the prediction of tissue fate or long-term clinical outcome must be interpreted with caution in the setting of acute stroke patients eligible for MT, primarily in those with short time of infarct evolution and with higher chances of early recanalization.

Funding

The author(s) disclosed receipt of the following financial support for the research, authorship, and/or publication of this article: We thank the support of the Spanish Ministry of Economy and Competitiveness for grant to AC (project PI15/00430 funded by Instituto de Salud Carlos III and co-funded by European Regional Development Fund ERDF). CL receives funding from Instituto de Salud Carlos III, with a Predoctoral Grant for Health Research (PFIS, FI16/00231). This work was partially developed at the building Centro Esther Koplowitz, Barcelona, CERCA Programme/Generalitat de Catalunya.

Declaration of conflicting interests

The author(s) declared no potential conflicts of interest with respect to the research, authorship, and/or publication of this article.

Authors' contributions


CL obtained the imaging data, implemented the post-processing of the perfusion maps, performed the statistical analysis

and wrote the first draft of the manuscript. AR, XU, LLI and SR obtained the clinical data. AR, RT, ALR and NGM supervised the neuroimage post-processing and analysis. AR, RT, XU, LLI, SR, VO, SA and AC revised the article critically for intellectual content. SA and AC designed the study, interpreted the data and wrote the final draft of the manuscript.

Supplementary material

Supplemental material for this article is available online.

ORCID iD

Carlos Laredo  <https://orcid.org/0000-0002-4626-6360>

References

- Warach SJ, Luby M, Albers GW, et al. Acute stroke imaging research roadmap III imaging selection and outcomes in acute stroke reperfusion clinical trials: consensus recommendations and further research priorities. *Stroke* 2016; 47: 1389–1398.
- Lev MH. Perfusion imaging of acute stroke: its role in current and future clinical practice. *Radiology* 2013; 266: 22–27.
- Schellinger PD, Bryan RN, Caplan LR, et al. Evidence-based guideline: the role of diffusion and perfusion MRI for the diagnosis of acute ischemic stroke: report of the Therapeutics and Technology Assessment Subcommittee of the American Academy of Neurology. *Neurology* 2010; 75: 177–85.
- Campbell BCV, Christensen SS, Levi CR, et al. Cerebral blood flow is the optimal CT perfusion parameter for assessing infarct core. *Stroke* 2011; 42: 3435–3440.
- Campbell BCV, Christensen SS, Levi CR, et al. Comparison of computed tomography perfusion and magnetic resonance imaging perfusion-diffusion mismatch in ischemic stroke. *Stroke* 2012; 43: 2648–53.
- Lin L, Bivard A, Krishnamurthy V, et al. Whole-brain CT perfusion to quantify acute ischemic penumbra and core 1. *0*. *Radiology* 2016; 279: 876–887.
- Cereda CW, Christensen S, Campbell BC, et al. A benchmarking tool to evaluate computer tomography perfusion infarct core predictions against a DWI standard. *J Cereb Blood Flow Metab* 2016; 36: 1780–1789.
- d'Esterre CD, Boesen ME, Ahn SH, et al. Time-dependent computed tomographic perfusion thresholds for patients with acute ischemic stroke. *Stroke* 2015; 46: 3390–3397.
- Schaefer PW, Souza L, Kamalian SS, et al. Limited reliability of computed tomographic perfusion acute infarct volume measurements compared with diffusion-weighted imaging in anterior circulation stroke. *Stroke* 2015; 46: 419–424.
- Christensen S and Lansberg MG. CT perfusion in acute stroke: practical guidance for implementation in clinical practice. *J Cereb Blood Flow Metab*. Epub ahead of print 22 October 2018.
- Kamalian S, Kamalian S, Maas MB, et al. CT cerebral blood flow maps optimally correlate with admission diffusion-weighted imaging in acute stroke but thresholds vary by postprocessing platform. *Stroke* 2011; 42: 1923–8.
- Chen C, Bivard A, Lin L, et al. Thresholds for infarction vary between gray matter and white matter in acute ischemic stroke: a CT perfusion study. *J Cereb Blood Flow Metab* 2019; 39: 536–546.
- Qiao Y, Zhu G, Patrie J, et al. Optimal perfusion computed tomographic thresholds for ischemic core and penumbra are not time dependent in the clinically relevant time window. *Stroke* 2014; 45: 1355–1362.
- Mui K, Yoo AJ, Verduzco L, et al. Cerebral blood flow thresholds for tissue infarction in patients with acute ischemic stroke treated with intra-arterial revascularization therapy depend on timing of reperfusion. *AJNR Am J Neuroradiol* 2011; 32: 846–851.
- Copen WA, Yoo AJ, Rost NS, et al. In patients with suspected acute stroke, CT perfusion-based cerebral blood flow maps cannot substitute for DWI in measuring the ischemic core. *PLoS One* 2017; 12: e0188891.
- Bivard A, Kleinig T, Miteff F, et al. Ischemic core thresholds change with time to reperfusion: a case control study. *Ann Neurol* 2017; 82: 995–1003.
- Martins N, Aires A, Mendez B, et al. Ghost infarct core and admission computed tomography perfusion: redefining the role of neuroimaging in acute ischemic stroke. *Interv Neurol* 2018; 7: 513–521.
- Hoving JW, Marquering HA, Majoie CBLM, et al. Volumetric and spatial accuracy of computed tomography perfusion estimated ischemic core volume in patients with acute ischemic stroke. *Stroke* 2018; 49: 2368–2375.
- Najm M, Al-Ajlan FS, Boesen ME, et al. Defining CT perfusion thresholds for infarction in the golden hour and with ultra-early reperfusion. *Can J Neurol Sci* 2018; 45: 339–342.
- Parsons MW, Pepper EM, Chan V, et al. Perfusion computed tomography: prediction of final infarct extent and stroke outcome. *Ann Neurol* 2005; 58: 672–679.
- Xie Y, Oppenheim C, Guillemin F, et al. Pretreatment lesion volume impacts clinical outcome and thrombectomy efficacy. *Ann Neurol* 2018; 83: 178–185.
- Institute of Neurological Disorders National and rt-PA Stroke Study Group. Tissue plasminogen activator for acute ischemic stroke. *N Engl J Med* 1995; 333: 1581–1588.
- Adams HP, Bendixen BH, Kappelle LJ, et al. Classification of subtype of acute ischemic stroke. Definitions for use in a multicenter clinical trial. TOAST. Trial of Org 10172 in Acute Stroke Treatment. *Stroke* 1993; 24: 35–41.
- Kakuda W, Lansberg MG, Thijs VN, et al. Optimal definition for PWI/DWI mismatch in acute ischemic stroke patients. *J Cereb Blood Flow Metab* 2008; 28: 887–891.
- Kottner J, Audige L, Brorson S, et al. Guidelines for reporting reliability and agreement studies (GRRAS) were proposed. *Int J Nurs Stud* 2011; 48: 661–671.

26. Saver JL, Goyal M, van der Lugt A, et al. Time to treatment with endovascular thrombectomy and outcomes from ischemic stroke: a meta-analysis. *JAMA* 2016; 316: 1279.
27. Haussen DC, Dehkharghani S, Rangaraju S, et al. Automated CT perfusion ischemic core volume and non-contrast CT ASPECTS (Alberta Stroke Program Early CT Score): correlation and clinical outcome prediction in large vessel stroke. *Stroke* 2016; 47: 2318–2322.
28. Bivard A, Spratt N, Miteff F, et al. Tissue is more important than time in stroke patients being assessed for thrombolysis. *Front Neurol* 2018; 9: 41.
29. Bivard A, Levi C, Krishnamurthy V, et al. Perfusion computed tomography to assist decision making for stroke thrombolysis. *Brain* 2015; 138: 1919–1931.
30. Powers WJ, Rabinstein AA, Ackerson T, et al. 2018 guidelines for the early management of patients with acute ischemic stroke: a guideline for healthcare professionals From the American Heart Association/American Stroke Association. *Stroke* 2018; 49: e46–e110.
31. Lansberg MG, Albers GW, Beaulieu C, et al. Comparison of diffusion-weighted MRI and CT in acute stroke. *Neurology* 2000; 54: 1557–1561.
32. Boers AMM, Jansen IGH, Beenen LFM, et al. Association of follow-up infarct volume with functional outcome in acute ischemic stroke: a pooled analysis of seven randomized trials. *J Neurointerv Surg* 2018; 10: 1137–1142.
33. del Zoppo GJ, Sharp FR, Heiss W-D, et al. Heterogeneity in the penumbra. *J Cereb Blood Flow Metab* 2011; 31: 1836–51.

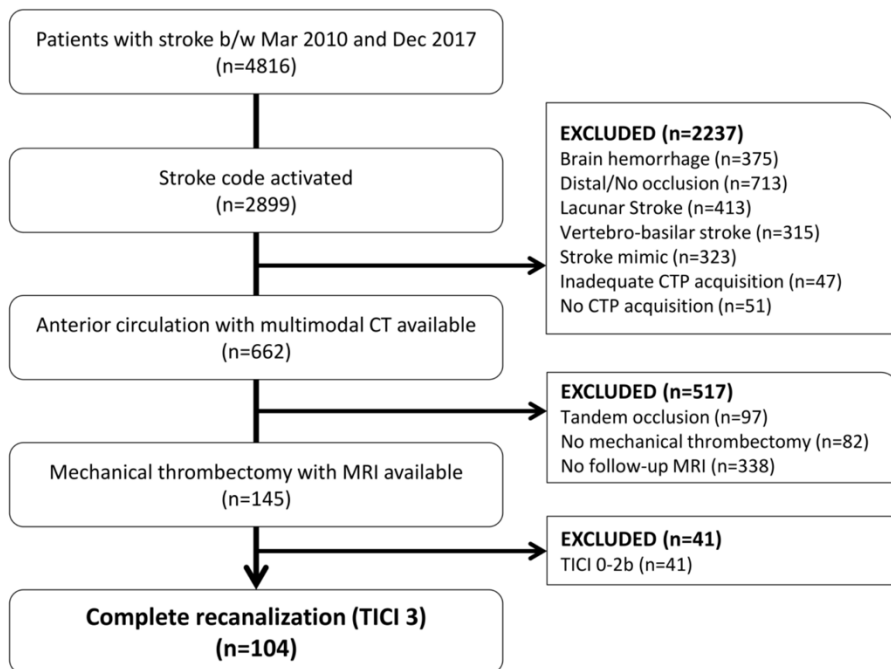
SUPPLEMENTARY MATERIAL

Supplementary table 1

		Model R ² (p value)			
		Linear	Logarithmic	Quadratic	Cubic
Best threshold	aCBF	0.103 (p=0.001)	0.145 (p<0.001)	0.150 (p<0.001)	0.193 (p<0.001)
	rCBF	0.151 (p<0.001)	0.173 (p<0.001)	0.159 (p<0.001)	0.235 (p<0.001)
	aCBV	0.092 (p=0.002)	0.133 (p<0.001)	0.144 (p<0.001)	0.171 (p<0.001)
	rCBV	0.112 (p=0.001)	0.150 (p<0.001)	0.154 (p<0.001)	0.178 (p<0.001)

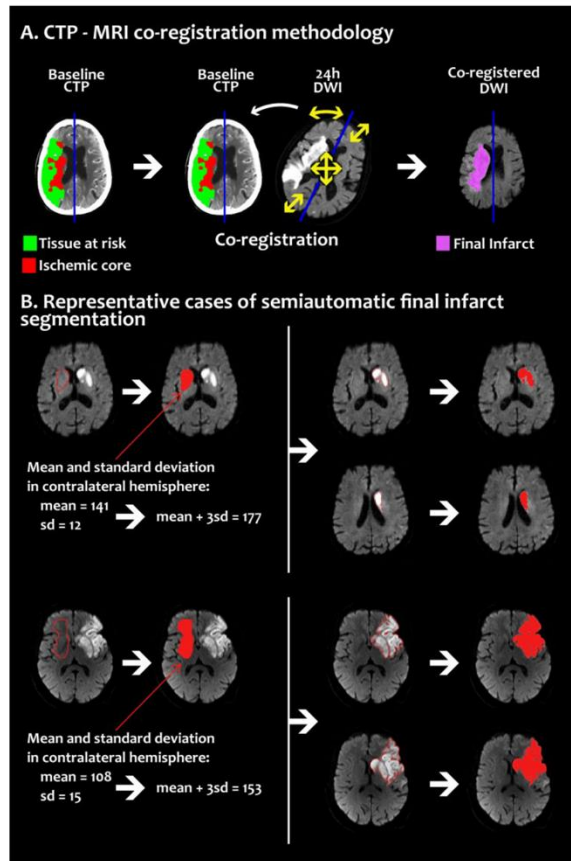
Supplementary table 1 legend: R squared and p values of the fitting of the different models (Linear, Logarithmic, Quadratic and Cubic) to explain the relationship between the best threshold in each patient depending on the time from symptom onset to recanalization. R squared and p value is shown for every absolute and relative threshold.

Supplementary figure 1



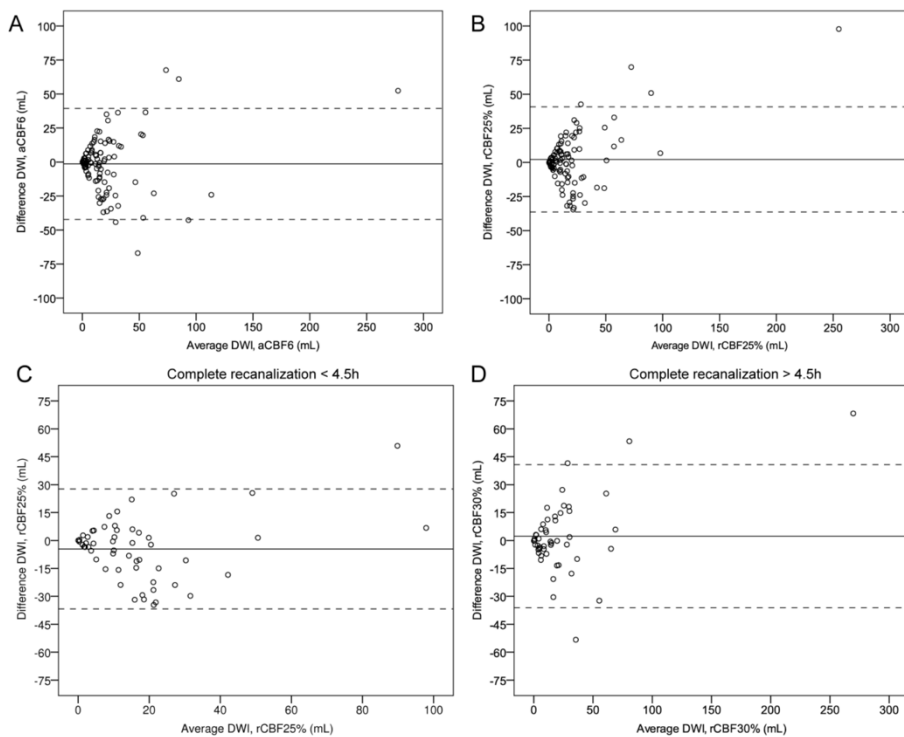
Supplementary figure 1 legend: Flow chart of the study.

Supplementary figure 2



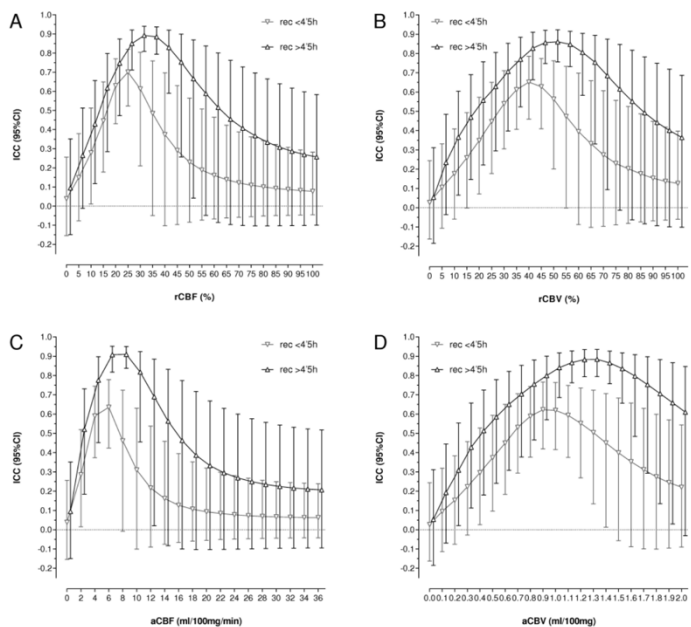
Supplementary figure 2 legend: CT Perfusion and MRI co-registration methodology scheme (A). Representative examples of the methodology used for final infarct segmentation (B). Mean and standard deviation (sd) were extracted from a manual region of interest in the contralateral hemisphere and the mean plus 3 sd was used as a threshold to define final infarct.

Supplementary figure 3



Supplementary figure 3 legend: 2A and 2B: Bland-Altman plots for the two best definitions of NVT, aCBF6 (2A) and rCBF25% (2B). 2C and 2D: Bland-Altman plots for the best definition of NVT in patients with complete recanalization before (rCBF25%) (2C) and after (rCBF30%) (2D) 4.5 hours, respectively.

Supplementary figure 4



Supplementary figure 4 legend: Intraclass correlation coefficient (ICC) and 95% confidence intervals (95%CI) between the volume of ischemic core non-viable tissue (NVT) defined on CT Perfusion and final infarct volume defined on DWI depending on time from symptom onset to recanalization (complete recanalization before or after 4.5 hours from symptom onset) including only those patients with not truncated tissue time attenuation curves at the end of the PCT acquisition. Higher ICC values were found in patients with later recanalization for every analyzed threshold: rCBF (A), rCBV (B), aCBF (C) and aCBV(D).

Study 2

Variables influencing the association between CT Perfusion predicted infarct core and clinical outcome in acute stroke. (UNPUBLISHED)

Variables influencing the association between CT perfusion predicted infarct core and clinical outcome in acute stroke

Carlos Laredo^{1,3*}, Aleix Solanes^{2,3*}, Arturo Renú^{1,3}, Salvatore Rudilosso^{1,3}, Laura Lull^{1,3}, Antonio López-Rueda⁴, Napoleón G Macías⁴, Alejandro Rodríguez^{1,3}, Xabier Urra^{1,3}, Víctor Obach^{1,3}, Jose Carlos Pariente³, Ángel Chamorro^{1,3}, Joaquim Radua^{2,3}, Sergio Amaro^{1,3}.

Background and Purpose: After an acute ischemic stroke, patients with a large CT Perfusion (CTP) predicted infarct core (pIC) commonly have poor clinical outcome. However, previous research suggests that this relationship may be relevant for a subgroup of patients determined by pretreatment and treatment-related variables while negligible for others. We analyzed a large cohort of patients to identify these subgroups.

Methods: We included a cohort of 828 patients with acute proximal arterial occlusions in the carotid territory imaged with a whole-brain CTP within 8 hours from stroke onset. pIC was computed on CTP Maps (Cerebral Blood Flow <30%) and poor clinical outcome was defined as a 90-day modified Rankin Scale score higher than 2. Potential mediators of the association between pIC and clinical outcome were evaluated through first order and advanced interaction analyses in the derivation cohort (n=654) for obtaining a prediction model. The derived model was further validated in an independent cohort (n=174).

Results: The volume of pIC was significantly associated with poor clinical outcome (OR=2.19, 95%CI=1.73-2.78, p<0.001). The strength of this association depended on baseline National Institute of Health Stroke Scale, glucose levels, the use of thrombectomy, and the interaction of age with thrombectomy. The model combining these variables showed good discrimination for predicting clinical outcome in both the derivation and validation cohorts [area under the Receiver Operating Characteristic curve 0.780 (95%CI=0.746-0.815) and 0.782 (95%CI=0.715-0.850), respectively].

Conclusions: These results highlight the need for an individualized evaluation of pIC for predicting clinical outcome in patients imaged within 8 hours from stroke onset.

Keywords: CT Perfusion; Infarct Core; Clinical Outcome.

* Carlos Laredo and Aleix Solanes contributed equally

1. Comprehensive Stroke Center, Hospital Clinic of Barcelona, Barcelona, Spain.
2. Imaging of Mood- and Anxiety-Related Disorders (IMARD) Group, Center for Networking Biomedical Research in Mental Health (CIBERSAM), Spain.
3. August Pi i Sunyer Biomedical Research Institute (IDIBAPS), Barcelona, Spain.
4. Department of Radiology, Hospital Clinic of Barcelona, Spain.

Introduction

CT Perfusion (CTP) is extensively used in the acute stroke setting to obtain a predicted infarct core (pIC) volume, which is a perfusion based estimation of the non-viable tissue.¹ However, despite the overall association between pIC and clinical outcome metrics, a number of pretreatment and treatment-related variables have been shown to modify these relationships including age, baseline National Institute of Health Stroke Scale (NIHSS), Alberta Stroke Program Early CT score (ASPECTS), time to CTP acquisition, degree of reperfusion, collaterals or hyperglycemia.²⁻⁸ A better delineation of the interaction between these variables would be relevant for assuring better outcome predictions. We aimed to identify which pretreatment and treatment-related variables are the most relevant modifiers of the association between pIC and clinical outcome in a cohort of acute ischemic stroke patients with large-vessel anterior circulation occlusions.

Materials and methods

Patients

The study population included consecutive acute stroke patients admitted in a referral comprehensive stroke center between March-2010 and December-2017 (derivation cohort) and between January-2018 and December-2018 (validation cohort) who had a whole-brain CTP scan within the first 8 hours from stroke onset showing a perfusion deficit due to a proximal arterial occlusion in the carotid territory (flow-chart in Online Figure I). Ethics approval was acquired from the local Clinical Research

Ethics Committee of the institution. Patient consent was not required due to the retrospective nature of the study. Demographics, clinical course, stroke etiology, reperfusion-therapy modality and clinical outcome were prospectively recorded. Reperfusion therapies were administered following contemporary guideline recommendations. Poor outcome was defined as a modified Rankin Scale score (mRS) higher than 2 at 3 months.

The imaging protocol included a baseline multimodal whole-brain CT scan (SIEMENS Somatom 128-section dual-source CT scanner), which included a Non-Contrast CT, a CT angiography and a CTP (98 mm z-coverage, total acquisition time of 59s). CTP maps were calculated through a model-free singular value decomposition algorithm with a delay and dispersion correction (MIStar, Apollo Medical Imaging Technology, Melbourne, Australia). A delay time threshold of 3s was used to obtain the hypoperfusion area and a relative Cerebral Blood Flow threshold of 30% was used to define the pIC. ASPECTS on Non-Contrast CT, collaterals and recanalization were defined according to validated methods (more details in the Online supplement).

Statistics

We created a multiple logistic model with the data from the derivation cohort. The dependent variable was the clinical outcome at 90 days, and the independent variables were pIC volume and the interaction between pIC and several potential modulators. We followed an advanced analysis of interaction (AAI) to select significant first and second-order interactions in the regression (Online Figure II). Before inclusion in the regression, we

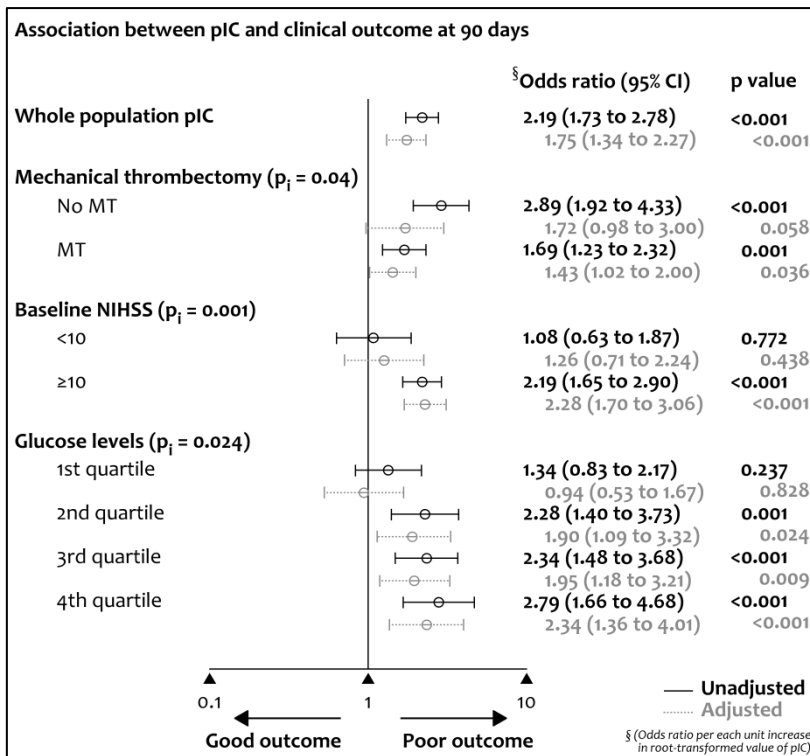


Figure 1 Forest plot of the association between pIC and poor outcome. Unadjusted and adjusted Odds Ratios (OR) and 95% Confidence Intervals of the association between pIC and clinical outcome in the whole population and in subgroups defined by significant interaction variables. Age, glucose levels and NIHSS were used for obtaining adjusted-OR.

mRS: modified Rankin Scale score;
MT: Mechanical thrombectomy;
NIHSS: National Institutes of Health Stroke Scale;
p_i: interaction p value;
pIC: predicted infarct core.

applied the fourth root transformation to pIC volume to approach normality. We conducted ten two-fold internal cross-validations to assess the model's internal validity with the area under the Receiver Operating Characteristic (ROC) curve. This statistic may range from 0.5 (tossing a coin) to 1 (perfect prediction). The cross-validation yielded 2000 models, and we chose the model most similar to the others according to the maximum Dice coefficient. Finally, we estimated the validity of the model in the validation cohort with the area under the ROC curve. We conducted all analyses with SPSS v.20 (IBM, Armonk, NY) and R (v.3.4.4, <https://www.R-project.org>).

Results

During the 2010-2018 timeframe, 828 patients were admitted to the unit, of which we assigned 654 to the derivation cohort

(2010-2017) and 174 to the validation cohort (2018) (flow-chart in Online Figure 1, description in Online Tables I-II). A larger pIC volume predicted a poorer clinical outcome (Figure 1). The AAI showed that baseline NIHSS, blood glucose levels, mechanical thrombectomy (MT) use, age, and the interaction age×MT significantly modified the strength of the association between pIC and clinical outcome (Figure 1 and Online Table III). The model combining these variables showed good discrimination in both the derivation cohort [area under the ROC curve=0.780 (95%CI=0.746-0.815)] and the validation cohort [area under the ROC curve=0.782 (95%CI=0.715-0.850)] respectively (Figure 2 and Online Table IV). Representative examples of applying the model for different levels of the identified modifiers are shown in Figure 3.

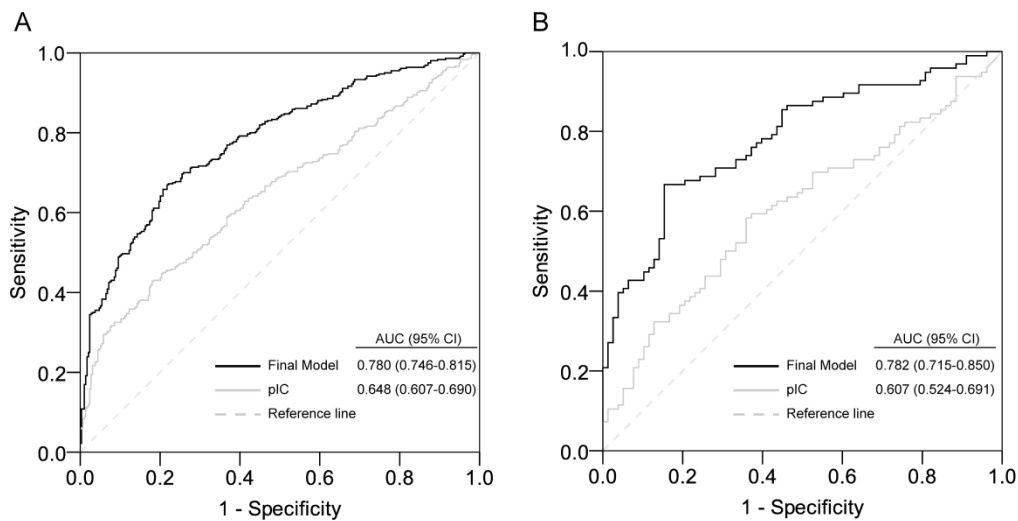


Figure 2. Discrimination of the derived model assessed through ROC Analysis in the derivation (A) and validation (B) cohorts. pIC: predicted Infarct Core.

Discussion

In this study we aimed to assess the interaction between baseline and treatment-related variables and pIC on the prediction of clinical outcome in a cohort of acute stroke patients with proximal arterial occlusions in the carotid territory. Expectedly, we found that higher volumes of pIC were associated with poor clinical outcome,^{6,8} although this association was significantly modified by the combination of baseline stroke severity, pretreatment glucose levels, thrombectomy use and age.³ According to our data, the prognostic relevance of pIC is weakened in the context of milder stroke syndromes, lower baseline glucose levels and in younger patients, especially when the odds of performing of MT are high. These observations support current guidelines and discourage the use of pIC as screening tool for reperfusion therapies in the non-extended time window.^{1,3}

This study has several limitations. First, patients were treated within the first 8 hours from stroke onset following local guidelines where treatment decisions were not randomized and included the use of information derived from CTP. Although we used a validated software our results may not be generalizable to other CTP postprocessing platforms or in the population of patients reperfused beyond 8 hours. Otherwise, the main strength of the study was the use of a comprehensive statistical methodology to assess the strength of the interactions between pIC and relevant pretreatment and treatment-related variables. Although the obtained prediction model was supported by internal cross-validation and performed similarly well at derivation and validation cohorts, it deserves external validation in larger observational studies.

Overall, these data highlight the limited accuracy of CTP for predicting clinical outcome in the early temporal window and supports the need for an individualized evaluation of pIC.

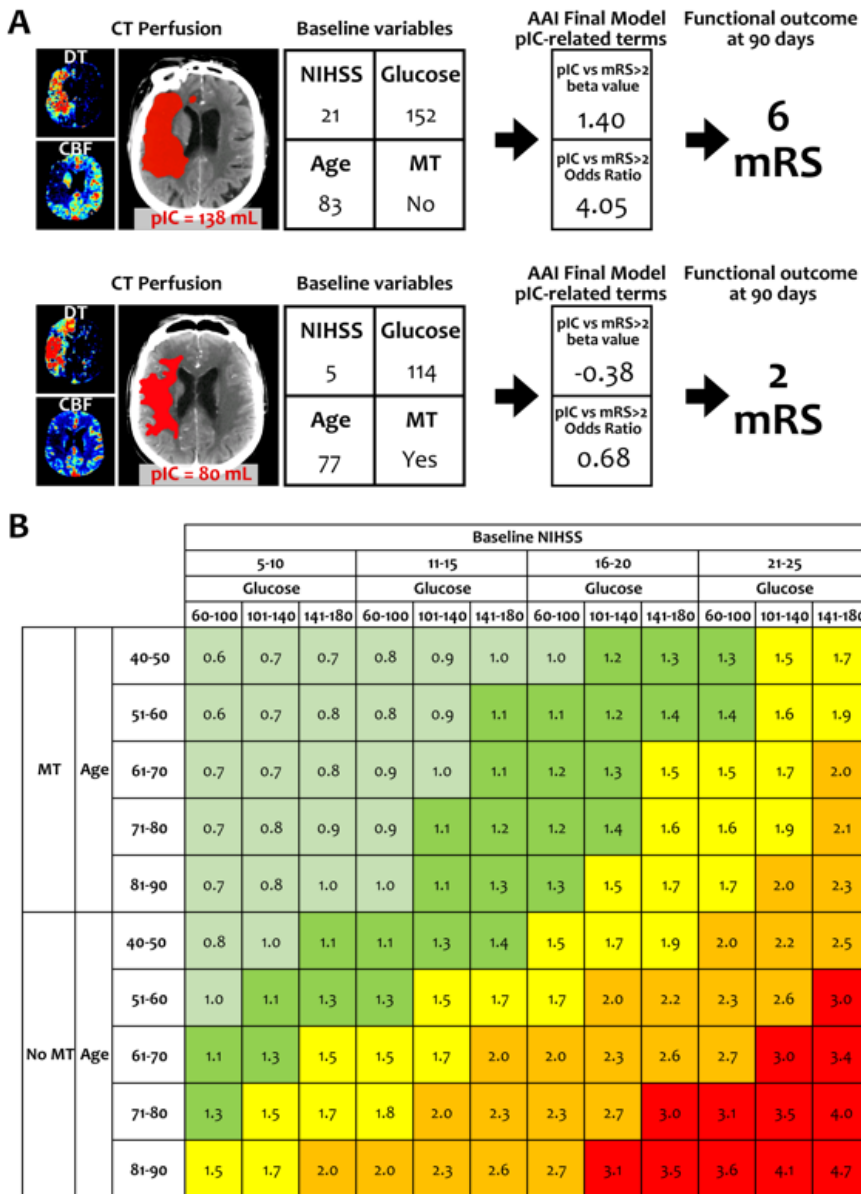


Figure 3. Representative examples of the application of the model in individual patients (A). Summary table for different levels of exposition to the identified modifiers (B). Values are Odds Ratios of the association between predicted infarct core and poor clinical outcome (mRS>2) across different exposition levels of the modifiers. CBF: Cerebral Blood Flow; DT: Delay Time; mRS: modified Rankin Scale score; MT: Mechanical thrombectomy; NIHSS: National Institutes of Health Stroke Scale; pIC: predicted infarct core.

Sources of funding

Spanish Ministry of Economy and Competitiveness (PI13/01268 and PI16/00711, funded by Instituto de Salud Carlos III (ISCIII) and co-funded by European Regional

Development Fund ERDF). CL receives funding from ISCIII (PFIS-FI16/00231). This work was partially developed at the building Centro Esther Koplowitz (CERCA Programme/Generalitat de Catalunya).

Disclosures

The authors declare no conflicts of interest.

References

1- Powers WJ, Rabinstein AA, Ackerson T, Adeoye OM, Bambakidis NC, Becker K, Biller J, Brown M, Demaerschalk BM, Hoh B, et al. Guidelines for the Early Management of Patients With Acute Ischemic Stroke: 2019 Update to the 2018 Guidelines for the Early Management of Acute Ischemic Stroke: A Guideline for Healthcare Professionals From the American Heart Association/American Stroke Association. *Stroke*. 2019;50:e344-e418.

2- Ribo M, Flores A, Mansilla E, Rubiera M, Tomasello A, Coscojuela P, Pagola J, Rodriguez-Luna D, Muchada M, Alvarez-Sabín J, et al. Age-adjusted infarct volume threshold for good outcome after endovascular treatment. *J Neurointerv Surg*. 2014;6:418-22.

3- Goyal M, Ospel JM, Menon B, Almekhlafi M, Jayaraman M, Fiehler J, Psychogios M, Chapot R, van der Lugt A, Liu J, et al. Challenging the Ischemic Core Concept in Acute Ischemic Stroke Imaging. *Stroke*. 2020;51:3147-3155.

4- Wintermark M, Albers GW, Broderick JP, Demchuk AM, Fiebach JB, Fiehler J, Grotta JC, Houser G, Jovin TG, Lees KR, et al. Acute Stroke Imaging Research Roadmap II. *Stroke*. 2013;44:2628-39.

5- Laredo C, Renú A, Tudela R, Lopez-Rueda A, Urra X, Llull L, Macías NG, Rudilosso S, Obach V, Amaro S, et al. The accuracy of ischemic core perfusion thresholds varies according to time to recanalization in stroke patients treated with mechanical thrombectomy: A comprehensive whole-brain computed tomography perfusion study. *J Cereb Blood Flow Metab*. 2020;40:966-977.

6- Albers GW, Goyal M, Jahan R, Bonafe A, Diener HC, Levy EI, Pereira VM, Cognard C, Cohen DJ,

Hacke W, et al. Ischemic core and hypoperfusion volumes predict infarct size in SWIFT PRIME. *Ann Neurol*. 2016;79:76-89.

7- Vagal A, Menon BK, Foster LD, Livorine A, Yeatts SD, Qazi E, d'Este C, Shi J, Demchuk AM, Hill MD, et al. Association Between CT Angiogram Collaterals and CT Perfusion in the Interventional Management of Stroke III Trial. *Stroke*. 2016;47:535-8.

8- Haussen DC, Dehkharghani S, Rangaraju S, Rebello LC, Bouslama M, Grossberg JA, Anderson A, Belagaje S, Frankel M, Nogueira RG. Automated CT Perfusion Ischemic Core Volume and Noncontrast CT ASPECTS (Alberta Stroke Program Early CT Score): Correlation and Clinical Outcome Prediction in Large Vessel Stroke. *Stroke*. 2016;47:2318-22.

SUPPLEMENTAL MATERIAL

Supplemental methods

Patients

Demographics, clinical course, functional outcome and reperfusion-therapy modality (no treatment, intravenous thrombolysis and primary or rescue Mechanical Thrombectomy, MT) were prospectively recorded. Reperfusion therapies were administered following contemporary guideline recommendations, as previously described.¹ Systemic rtPA was given within 4.5 hours from stroke onset at a dose of 0.9 mg per kg (10% administered as an initial bolus followed by an infusion of 0.9mg/dl, maximum total dose of 90 mg). MT was performed within 8 hours in eligible patients with proximal arterial occlusions on CT angiography (CTA). The presence of a malignant profile in CTP (predicted infarct core, pIC, higher than 70ml) and the absence of mismatch in patients with symptoms lasting >4.5 hours from the onset of stroke were exclusion criteria for receiving MT. Qualifying strokes were classified according to the Trial of Org 10 172 in Acute Stroke Treatment (TOAST) criteria.² Neurological deficits were assessed using the National Institutes of Health Stroke Scale (NIHSS) score.³ Functional outcome was scored with the modified Rankin Scale score (mRS) at 3 months and poor clinical outcome was defined as an mRS > 2.

The imaging protocol included a baseline multimodal whole-brain CT scan, which included a Non-Contrast CT (NCCT), a CTA and a CTP. All patients were scanned using a SIEMENS Somatom 128-section dual-source CT scanner (Siemens Healthcare, Erlangen,

Germany), with a 98 mm z-coverage and 31 time points (26 acquired each 1.5s and the last 5 each 4s (total acquisition time, 59s). Images were formatted as 49 2-mm slices. For this analysis, CTP maps were calculated with commercial software MIStar (Apollo Medical Imaging Technology, Melbourne, Australia). A model-free singular value decomposition with a delay and dispersion correction was used to perform the deconvolution of the tissue-enhancement curve and the arterial input function.⁴ Cerebral Blood Flow (CBF), Cerebral Blood Volume (CBV), Mean Transit Time (MTT) and Delay Time (DT) maps were generated. According to previously published data,⁴ a DT threshold of 3s was used to obtain the hypoperfusion area and a relative CBF threshold of 30% of the value in the contralateral tissue was used to define pIC. Alberta Stroke Program Early CT Score (ASPECTS) was assessed on baseline NCCT. Collaterals were scored on CTA according to a validated grading system that ranged from 0 to 3 (0, absent collateral supply; 1, collateral supply filling <50%; 2, collateral supply filling >50% but <100% of the occluded arterial territory; and 3, 100% collateral supply).⁵ In patients receiving MT, early reperfusion was graded on digital subtraction angiography (DSA) according to the modified Thrombolysis in Cerebral Infarction (mTICI) classification (Grade 0, no perfusion; Grade 1, penetration with minimal perfusion; Grade 2a, partial filling of the entire vascular territory; Grade 2b, complete filling, but the filling is slower than normal; Grade 3, complete perfusion). Recanalization was defined as complete if a grade 2b-3 was obtained at the end of the procedure. All imaging studies were evaluated by investigators blinded to clinical data.

Data were stored in a local database and declared to a web-based registry that satisfied all legal requirements for protection of personal data, monitored by the Catalan Health Department. Ethics approval was acquired from the local Clinical Research Ethics Committee from Hospital Clinic of Barcelona under the requirements of Spanish legislation in the field of biomedical research, the protection of personal data (15/1999) and the standards of Good Clinical Practice, as well as with the Helsinki Declaration of 1975/1983. Patient consent was not required due to the retrospective nature of the study design and the lack of patient interaction. We adhered to the STARD (Standards for Reporting of Diagnostic Accuracy) guidelines (<http://www.stard-statement.org/>).

Statistics

Continuous variables were reported as mean (standard deviation, SD) or median (interquartile range, IQR) and were compared with the Student t test, one-way analysis of variance, Mann–Whitney, or Kruskal-Wallis tests as appropriate. Categorical variables were compared with the χ^2 and Fisher exact tests as appropriate. Unadjusted and adjusted logistic regression models were used to obtain the association between pIC and poor clinical outcome. An analysis of interaction was performed in the whole derivation cohort to identify the baseline clinical and radiological variables that significantly modified the association between pIC and clinical outcome. The database included poor clinical outcome as dependent variable and pIC volume was forced as independent variable in each model. The variables included in the adjusted models were those who showed and independent association with poor

clinical outcome in the whole derivation cohort after applying a stepwise backwards procedure. Treatment-related variables and those neuroimaging variables that were highly correlated with pIC were not included in order to avoid losing not-treated patients from the analysis and to prevent collinearity issues (online Table II).

The analysis of interaction was performed in two stages. First, we evaluated the first order interaction between pIC and the potential mediators in unadjusted and adjusted binary logistic regression models and subgroup analyses were performed in the presence of significant interaction term (p value lower than 0.1). Second, we implemented a three steps advanced analysis of interaction (AAI) including first and second-order interactions, as illustrated in online Figure II. In AAI step 1 a binary logistic regression was applied for every interacting variable to predict poor clinical outcome (PO) in a model including four terms: intercept, pIC, the interacting variable and the first-order interaction term pIC-interacting variable (Eq. 1). In this stage all the interacting variables that had a significant first order interaction term in the model were stored. The interaction variable alone was also stored if it was significant together with the interaction term. In the AAI step 2, a binary logistic regression was applied for every pair of interacting variables identified in the previous step into a model with seven terms including second order interaction terms (Eq. 2). In this step all the pair of interacting variables that had a significant second order interaction term in the model were stored. In the AAI third step, a final logistic regression model was constructed with all the significant interacting variables stored in previous

steps, including significant variables alone, first-order interaction terms and second-order interaction terms (Eq. 3). In the final model, the sum of all the beta values of the terms related to pIC provided the strength of the association between pIC and poor outcome taking into account the interacting variables. Finally, before applying the AAI to the whole cohort of patients, two-fold cross-validation (CV) was carried out ten times to test the validity of the AAI approach (Online Figure II A). The allocation of patients in the 2 folds of the internal CV was controlled through balancing the distribution of mRS between both groups. To test if the interacting variables influenced the relationship between pIC and poor outcome, the final model obtained in the training fold was applied to the validation fold and the beta values of the terms related to pIC were stored in a new continuous variable called POWER and the beta value for the interaction term pIC*POWER was stored (Eqs. 4 and 5 respectively). A meta-analysis using fixed and random effects was then applied to the ten 2-folds. The mean of the 20 meta-analytic beta values, variances and global Z and p values were recorded (significant global Z and p values were considered as indicative of model validity). After the internal CV, the AAI procedure was applied to all the database of 654 patients (Online Figure II B). A hundred iterations of the procedure were processed (20 models per iteration, 2000 models) and the Dice coefficient was calculated for every pair of 2000 models. Finally, the models with a maximum Dice coefficient were stored and the mean beta values for every variable were computed to obtain a representative unique final model. Finally, the discrimination of the AAI derived model was

assessed through ROC analyses in the derivation and validation cohorts.

All the analyses were performed using SPSS v.20 (IBM Corp., Armonk, NY) and R (v.3.4.4, R foundation for Statistical Computing, Vienna, Austria, <https://www.R-project.org>).

(Eq. 1)

$$PO = A + B * pIC + C * var + D * pIC * var$$

(Eq. 2)

$$PO = A + B * pIC + C * var_1 + D * var_2 + E * pIC * var_1 + F * pIC * var_2 + G * pIC * var_1 * var_2$$

(Eq. 3)

$$PO = A + B * pIC + \sum_n (C_n * var_n) + \sum_n (D_n * pIC * var_n) + \sum_n \sum_m (E_{nm} * pIC * var_n * var_m)$$

(Eq. 4)

$$POWER = B + \sum_n D_n + \sum_n \sum_m E_{nm}$$

(Eq. 5)

$$PO = A + B * pIC + C * POWER + D * pIC * POWER$$

Supplemental references

- 1.- Laredo C, Renú A, Tudela R, Lopez-Rueda A, Urra X, Llull L, Macías NG, Rudilosso S, Obach V, Amaro S, et al. The accuracy of ischemic core perfusion thresholds varies according to time to recanalization in stroke patients treated with mechanical thrombectomy: A comprehensive whole-brain computed tomography perfusion study. *J Cereb Blood Flow Metab.* 2020;40:966-977.
- 2.- Adams HP Jr, Bendixen BH, Kappelle LJ, Biller J, Love BB, Gordon DL, Marsh EE 3rd. Classification of subtype of acute ischemic stroke. Definitions for use in a multicenter clinical trial.

TOAST. Trial of Org 10172 in Acute Stroke Treatment. *Stroke* 1993; 24: 35–41.

3.- National Institute of Neurological Disorders and Stroke rt-PA Stroke Study Group. Tissue Plasminogen Activator for Acute Ischemic Stroke. *N Engl J Med* 1995; 333: 1581–1588.

4.- Lin L, Bivard A, Krishnamurthy V, Levi CR, Parsons MW. Whole-Brain CT Perfusion to

Quantify Acute Ischemic Penumbra and Core. *Radiology*. 2016;279(3): 876-87.

5.- Tan IY, Demchuk AM, Hopyan J, Zhang L, Gladstone D, Wong K, Martin M, Symons SP, Fox AJ, Aviv RI. CT angiography clot burden score and collateral score: correlation with clinical and radiologic outcomes in acute middle cerebral artery infarct. *AJNR Am J Neuroradiol* 2009; 30: 525-531.

Supplemental Tables

Online Table I. Demographics, baseline and procedure related variables for all patients and according to treatment modality

	All patients N=654	No IVT/MT N=92	IVT alone N=129	MT± IVT N=433	P
Age (years)	72 (62-80)	75 (66-80)	74 (64-79)	73 (61-80)	0.354
Prior mRS	0 (0-1)	0 (0-1)	0 (0-0)	0 (0-1)	0.187
Females, n (%)	308 (47)	44 (48)	47 (45)	206 (48)	0.863
Hypertension, n (%)	405 (62)	59 (64)	86 (67)	260 (60)	0.356
Diabetes, n (%)	118 (18)	23 (25)	26 (20)	69 (16)	0.095
Dyslipidemia, n (%)	268 (41)	35 (38)	55 (43)	178 (41)	0.788
Atrial Fibrillation, n (%)	190 (29)	29 (32)	30 (23)	131 (30)	0.262
Glucose (mg/dl)	124 (107-146)	125 (109-160)	128 (111-154)	119 (105-142)	0.008
NIHSS, median (IQR)	16 (10-20)	15 (6-21)	16 (9-20)	17 (11-20)	0.067
ASPECTS, median (IQR)	9 (8-10)	8 (6-10)	8 (7-10)	9 (8-10)	<0.001
Collateral score	2 (1-3)	2 (1-3)	2 (1-2)	2 (1-3)	0.015
Time to CTP (min)	181 (103-288)	245 (114-636)	179 (110-251)	179 (100-285)	0.002
Time to MT onset (min)		-	-	251 (180-360)	-
Recanalization (yes), n (%)		-	-	376 (87)	-
Time to Recanalization (min)		-	-	300 (217-398)	-
TOAST classification					0.160
Atherothrombotic, n (%)	110 (17)	15 (16)	19 (15)	76 (18)	
Cardioembolic, n (%)	327 (50)	52 (57)	56 (43)	219 (51)	
Other etiologies, n (%)	217 (33)	25 (27)	54 (42)	138 (32)	
Location of the occlusion					<0.001
Tandem, n (%)	90 (14)	11 (12)	18 (14)	61 (14)	
ICA-T or M1, n (%)	446 (68)	50 (54)	79 (61)	317 (73)	
M2, n (%)	118 (18)	31 (34)	32 (25)	55 (13)	
pIC (ml)	20 (8-37)	23 (6-83)	28 (9-81)	19 (8-36)	0.002

Data are median (IQR) unless otherwise specified.

ASPECTS: Alberta Stroke Program Early CT Score; CTP: Computed Tomography Perfusion; IVT: Intravenous Treatment; mRS: modified Rankin Scale score; MT: Mechanical Thrombectomy; NIHSS: National Institutes of Health Stroke Scale; pIC: predicted Infarct Core; TOAST: Trial of ORG 10172 in acute stroke treatment.

Online Table II. Demographics, baseline and procedure related variables according to clinical outcome at day 90.

	mRS≤2 N=294	mRS>2 N=360	p	p*
Age (years)	69 (59-78)	74 (65-80)	<0.001	<0.001
Prior mRS	0 (0-1)	0 (0-1)	<0.001	-
Females, n (%)	130 (44)	178 (49)	0.183	-
Smoking, n (%)	37 (13)	32 (9)	0.126	-
Hypertension, n (%)	166 (57)	239 (66)	0.009	-
Diabetes, n (%)	43 (15)	75 (21)	0.040	-
Dyslipidemia, n (%)	121 (41)	147 (41)	0.933	-
Atrial Fibrillation, n (%)	76 (26)	114 (32)	0.103	-
Glucose (mg/dl)	116 (102-136)	127 (111-152)	<0.001	0.002
NIHSS	13 (8-18)	18 (13-22)	<0.001	<0.001
ASPECTS	9 (8-10)	9 (7-10)	<0.001	-
Collateral score	2 (2-3)	2 (1-2)	<0.001	0.097
Time to CTP (min)	172 (107-245)	194 (116-289)	0.089	-
TOAST classification			0.541	-
Atherothrombotic, n (%)	49 (17)	61 (17)		
Cardioembolic, n (%)	141 (48)	186 (52)		
Other etiologies, n (%)	104 (35)	113 (31)		
Location of the occlusion			0.474	-
Tandem, n (%)	39 (13)	51 (14)		
ICA-T or M1, n (%)	196 (67)	250 (69)		
M2, n (%)	59 (20)	59 (17)		
pIC (ml)	14 (6-29)	27 (10-67)	<0.001	0.002

Data are median (IQR) unless otherwise specified. The final multivariate model for obtaining adjusted p values (p*) was constructed through a stepwise backwards procedure after removing the treatment-related variables (in order to avoid losing not-treated patients from the analysis) and also the neuroimaging based variables that were highly correlated with pIC (to avoid collinearity). The variables that remained in the final multivariate model were used for the adjustment of the association between pIC and poor outcome at 90 days in the whole population and in subgroups shown in Figure 1 (Main text).

ASPECTS: Alberta Stroke Program Early CT Score; CTP: Computed Tomography Perfusion; mRS: modified Rankin Scale score; NIHSS: National Institutes of Health Stroke Scale; pIC: predicted Infarct Core; TOAST: Trial of ORG 10172 in acute stroke treatment.

Online Table III. Clinical variables and coefficients of the final derived model

Variable	Coefficient
Intercept	-0.629416935
pIC	-1.549562775
pIC:Age	0.015214074
pIC:Glucose	0.003234035
pIC:NIHSS	0.056892900
pIC:MT	0.021245386
pIC:MT:Age	-0.008793370

MT: Mechanical Thrombectomy; NIHSS: National Institutes of Health Stroke Scale; pIC: predicted Infarct Core.

Online Table IV. Results of the metagen analysis on the ten two-folds of the internal cross-validation procedure.

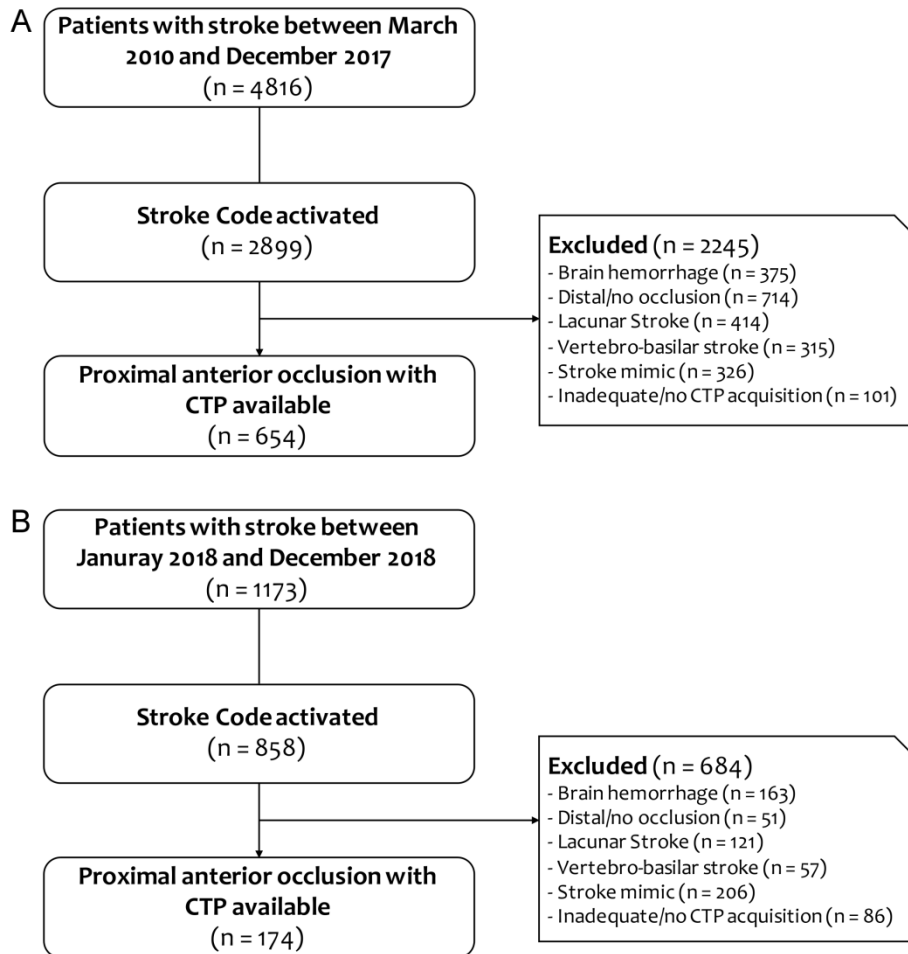
fold beta POWER*p IC	fold SE POWER* pIC	fold Z POWER*p IC	fold p POWER *pIC	meta weight	meta beta POWER *pIC	meta VAR POWER *pIC	meta Z POWER* pIC	meta p POWER *pIC
1,43	0,49	2,9	0,004	4,09	1,11	0,09	3,8	0,0001
0,94	0,36	2,6	0,010	7,59				
1,46	0,45	3,3	0,001	5,01	1,15	0,07	4,2	0,0000
0,97	0,34	2,8	0,005	8,47				
0,42	0,43	1,0	0,324	5,49	0,40	0,14	1,1	0,2799
0,34	0,76	0,5	0,653	1,73				
1,39	0,45	3,1	0,002	4,91	1,37	0,13	3,8	0,0002
1,35	0,62	2,2	0,030	2,59				
0,78	0,46	1,7	0,085	4,83	0,85	0,09	2,8	0,0048
0,91	0,41	2,2	0,025	6,06				
1,29	0,35	3,7	0,000	8,31	0,81	0,04	4,0	0,0001
0,40	0,25	1,6	0,107	16,25				
0,56	0,47	1,2	0,240	4,48	0,45	0,17	1,1	0,2797
0,09	0,85	0,1	0,912	1,39				
0,14	0,38	0,4	0,722	6,93	0,73	0,09	2,5	0,0125
1,38	0,46	3,0	0,003	4,79				
-0,72	0,86	-0,8	0,404	1,34	0,38	0,30	0,7	0,4851
1,36	0,70	1,9	0,053	2,02				
0,98	0,38	2,6	0,010	6,88	0,78	0,10	2,5	0,0120
0,38	0,55	0,7	0,489	3,36				

Beta values, standard errors, Z values and p values for the 20 models constructed in the internal cross-validation process to explore the validity of the Advanced Analysis of Interaction are shown in the first four columns. Metagen weights, beta values, variances, Z values and p values of the 10 two-folds are shown in the last 5 columns.

pIC: predicted Infarct Core; SE: Standard Error; VAR: Variance.

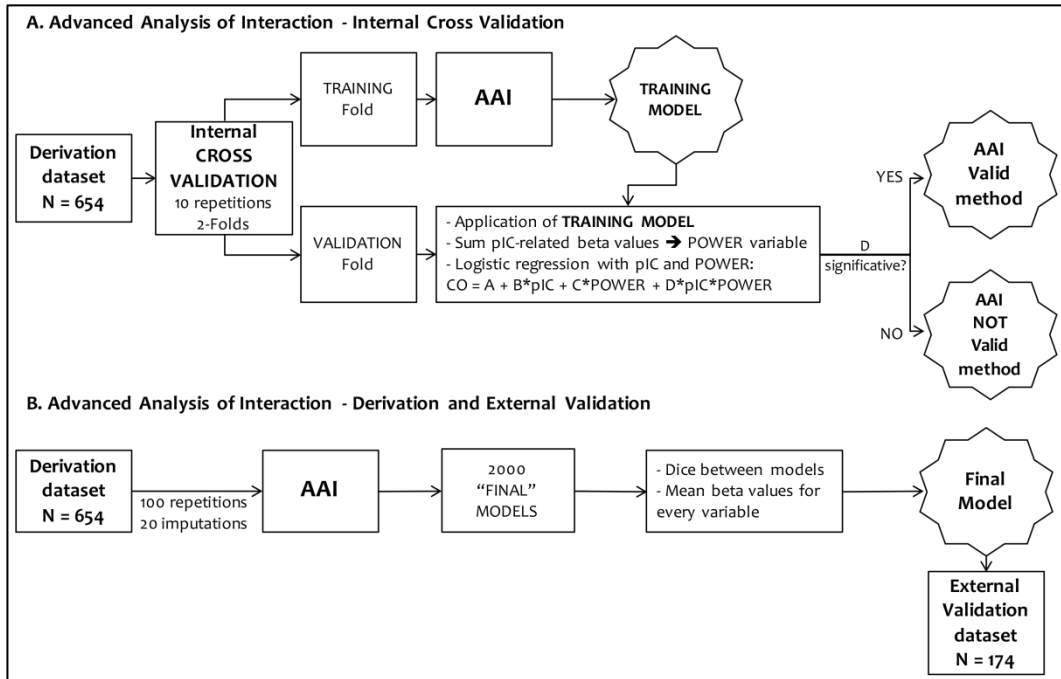
Supplemental Figures

Online Figure I. Flow chart of the included population.



Derivation (A) and validation (B) cohorts.
CTP: Computer Tomography Perfusion.

Online Figure II: Graphical representation of the study design and analysis.



AAI: Advanced Analysis of Interaction; CO: Clinical Outcome; pIC: predicted Infarct Core.

Study 3

Brain hemorrhage after endovascular reperfusion therapy of ischemic stroke: a threshold-finding whole-brain perfusion CT study.

Brain hemorrhage after endovascular reperfusion therapy of ischemic stroke: a threshold-finding whole-brain perfusion CT study

Arturo Renú¹, Carlos Laredo¹, Raúl Tudela², Xabier Urria¹, Antonio Lopez-Rueda³, Laura Llull¹, Laura Oleaga³, Sergio Amaro¹ and Ángel Chamorro¹

Abstract

Endovascular reperfusion therapy is increasingly used for acute ischemic stroke treatment. The occurrence of parenchymal hemorrhage is clinically relevant and increases with reperfusion therapies. Herein we aimed to examine the optimal perfusion CT-derived parameters and the impact of the duration of brain ischemia for the prediction of parenchymal hemorrhage after endovascular therapy. A cohort of 146 consecutive patients with anterior circulation occlusions and treated with endovascular reperfusion therapy was analyzed. Recanalization was assessed at the end of reperfusion treatment, and the rate of parenchymal hemorrhage at follow-up neuroimaging. In regression analyses, cerebral blood volume and cerebral blood flow performed better than Delay Time maps for the prediction of parenchymal hemorrhage. The most informative thresholds (receiver operating curves) for relative cerebral blood volume and relative cerebral blood flow were values lower than 2.5% of normal brain. In binary regression analyses, the volume of regions with reduced relative cerebral blood volume and/or relative cerebral blood flow was significantly associated with an increased risk of parenchymal hemorrhage, as well as delayed vessel recanalization. These results highlight the relevance of the severity and duration of ischemia as drivers of blood-brain barrier disruption in acute ischemic stroke and support the role of perfusion CT for the prediction of parenchymal hemorrhage.

Keywords

Brain imaging, brain ischemia, hemodynamics, intracerebral hemorrhage, reperfusion

Received 4 May 2015; Revised 13 July 2015; Accepted 14 July 2015

Introduction

Endovascular therapy (ET) is increasingly used for acute ischemic stroke treatment due to proximal vessel occlusions and its clinical benefit over best medical therapy in selected patients has been recently shown.^{1–3} The risk of intracerebral hemorrhage increases with reperfusion therapies and is associated with increased morbidity and mortality.⁴ Therefore, the identification of clinical and radiological predictors of hemorrhagic complications in patients with acute stroke receiving reperfusion therapies is highly relevant.

The pathophysiological mechanisms involved in the appearance of cerebral hemorrhage associated with reperfusion therapies are multiple, including several processes such as the severity and duration of brain

ischemia, toxicity secondary to thrombolytic drugs and procedure-related direct vessel damage.^{5,6} Of those mechanisms, the severity of brain ischemia can be reliably quantified using dynamic contrast-enhanced magnetic resonance imaging (MRI) or computerized

¹Comprehensive Stroke Center, Department of Neuroscience, Hospital Clinic, University of Barcelona and August Pi i Sunyer Biomedical Research Institute (IDIBAPS), Barcelona, Spain

²CIBER de Bioingeniería, Biomateriales y Nanomedicina (CIBER-BBN), Group of Biomedical Imaging of the University of Barcelona, Barcelona, Spain

³Radiology Department, Hospital Clinic, Barcelona, Spain

Corresponding author:

Sergio Amaro, Hospital Clinic, Villarroel 170, 08036 Barcelona, Spain.
 Email: samaro@clinic.ub.es

tomography (CT) by measuring cerebral blood flow (CBF), cerebral blood volume (CBV) or time-based variables such as Tmax, mean transit time (MTT), time to peak (TTP) or delay time (DT). MRI-based clinical studies of patients with acute stroke treated or not with thrombolysis have shown that very severe reductions of CBV (termed as *Very Low CBV*) are strongly associated with the risk of PH,⁷⁻⁹ particularly when delayed reperfusion occurs after thrombolysis.⁸ Using perfusion CT, the risk of hemorrhagic transformation has been related to a myriad of perfusion measures such as low relative CBV values,¹⁰ low relative CBF values,¹¹ longer relative MTT or Tmax values,^{11,12} and severe hypoperfusion detected in TTP maps.¹³ Specifically in patients receiving endovascular reperfusion therapies, reduced pretreatment CBV or CBF values measured with perfusion CT have been associated with poor clinical outcomes,¹⁴ including the risk of development of intracranial hemorrhage.^{15,16} However, the best perfusion CT parameters and thresholds for the prediction of PH and their relationship with the occurrence and timing of reperfusion have not been sufficiently addressed in this patient population. Moreover, the identification and validation of these biomarkers may be relevant for risk stratification of acute stroke patients receiving multimodal reperfusion therapies and for the evaluation of neuroprotective therapies in the setting of clinical trials.

Here we performed a comprehensive analysis of whole-brain perfusion CT maps to assess the relevance of the severity and duration of brain ischemia in predicting the risk of parenchymal hemorrhage in acute stroke secondary to proximal arterial occlusion treated with endovascular reperfusion therapies. Expressly, we aimed to examine the optimal parameters and thresholds of perfusion maps for the prediction of PH after ET and to evaluate the impact of the timing from the onset of ischemia to reperfusion on the risk of PH.

Materials and methods

Patients

Patients were part of a prospectively collected clinical registry of acute ischemic stroke treated with reperfusion therapies in a single Comprehensive Stroke Center. The study population included consecutive patients with occlusions in the carotid territory treated with endovascular recanalization therapy between March 2010 and July 2013. Additional inclusion criteria for this analysis were: (1) the availability of a technically adequate pre-treatment whole-brain perfusion CT scan, and (2) the availability of a post-treatment follow-up neuroimaging adequate for evaluating the development of hemorrhagic transformation. Post-treatment

follow-up neuroimaging included Dual Energy CT (DE-CT) or MRI. DE-CT scan was required instead of plain CT scan to allow an accurate differentiation between blood and contrast media extravasation.¹⁷ A total of 146 patients fulfilled these criteria and were finally included in the study. A contemporary group of 51 patients was not included because of vertebro-basilar location of the arterial occlusion (n=24), absence of baseline perfusion CT imaging (n=7), technically inadequate perfusion CT acquisition (n=10), no availability of follow-up DE-CT or MRI (n=10). ET was performed in patients with a proximal artery occlusion on CT angiography if the patients and/or their legal representatives signed a written informed consent accepting to receive ET and to be included in the registry. The presence of a malignant profile in perfusion CT and the absence of mismatch in patients with symptoms lasting >4.5 h from the onset of stroke were exclusion criteria for receiving ET. This pre-treatment perfusion evaluation was performed using a commercially available semi-automated perfusion analysis software (Siemens) based on the maximum slope model of perfusion. Infarct core was segmented based on a CBV threshold of 0.6 relative to the contralateral white matter and ischemic penumbra was segmented based on a TTP relative threshold of 6 s compared to contralateral hemisphere for identification of critically hypoperfused tissue. In patients with proximal occlusions, malignant profile was defined as infarct core higher than 70 ml, and mismatch profile was defined as the presence of a hypoperfusion lesion that was higher or equal than 120% of the infarct core. Data were stored in a local database and declared to a Web-based registry that satisfied all legal requirements for protection of personal data, monitored by the Catalan Health Department. The study protocol was also approved by the local Clinical Research Ethics Committee from Hospital Clínic of Barcelona under the requirements of Spanish legislation in the field of biomedical research, the protection of personal data (15/1999) and the standards of Good Clinical Practice, as well as with the Helsinki Declaration of 1975/1983.

Patients were admitted into an intermediate care Stroke Unit and were managed by certified stroke neurologists following the European Stroke Organization Guidelines. The qualifying strokes were classified according to the Trial of Org 10172 in Acute Stroke Treatment (TOAST) criteria after a complete diagnostic workup.¹⁸ Demographics, risk factors, laboratory tests, neuroimaging, concomitant therapies, clinical course, and functional outcome were prospectively collected. Neurological status was monitored with the National Institutes of Health Stroke Scale (NIHSS) score and functional outcome was quantified with the modified Rankin Scale (mRS) score at 3 months.

Imaging protocol

The imaging protocol included a baseline multimodal whole-brain CT scan, which included a plain CT (140 Kv, 127 mAs, FoV 225 mm, matrix 512×512 , slice thickness 5 mm), a CT angiography (120 Kv, 663 mAs, FoV 261 mm, matrix 512×512 , slice thickness 0.6 mm), and a perfusion CT performed before ET. When systemic recombinant tissue plasminogen activator (rt-PA) was administered, the multimodal neuroimaging was performed at the end of rt-PA infusion. The Alberta Stroke Program Early CT Score (ASPECTS) was assessed on baseline CT, and collaterals were scored on CT angiography according to a validated grading system (Tan scale) that ranged from 0 to 3 (0, absent collateral supply; 1, collateral supply filling $<50\%$; 2, collateral supply filling $>50\%$ but $<100\%$ of the occluded arterial territory; and 3, 100% collateral supply).¹⁹ After ET, a DE-CT and/or an MRI were performed within 72 h [median 38 (IQR 17–72) h] of hospital admission. The implemented DE-CT protocol allowed simultaneous imaging acquisition at 100 kV/250 mAs and 140 kV/250 mAs, and a 20×0.6 mm collimation. The MRI included diffusion-weighted images (DWI, parameters: Repetition time (TR)/echo time (TE) 10,800/89 ms, matrix 192×192 , Field of View (FoV) 240 mm, slice thickness 3 mm, directions x,y,z, b-values: 0 and $1000 \text{ mm}^2/\text{s}^2$) and gradient-echo T2*-weighted (GRE: TR/TE 764/26 ms; matrix 384×512 ; FoV 240 mm; slice thickness 5 mm) sequences. The bleeding complications were scored on follow-up brain imaging (up to 72 h) according to the European Cooperative Acute Stroke Study (ECASS) criteria as hemorrhagic infarction (HI) and parenchymal hematoma (PH) type 1 and type 2.²⁰ Symptomatic intracranial hemorrhage was defined as any PHs associated with an increment of at least 4 points in the NIHSS score. Investigators blinded to clinical data and baseline perfusion CT analysis (AR, SA) evaluated in consensus the post-treatment imaging studies.

Final vessel patency was graded on digital subtraction angiography (DSA) at the end of ET according to the Thrombolysis in Cerebral Infarction (TICI) classification (Grade 0, no perfusion; Grade 1, penetration with minimal perfusion; Grade 2a, partial filling of the entire vascular territory; Grade 2b, complete filling, but the filling is slower than normal; Grade 3, complete perfusion). For this analysis recanalization was defined as a grade 2–3 if it was obtained at the end of ET and was further classified as early if obtained within the first 6 h from symptom onset or delayed if obtained after 6 h.

Perfusion CT imaging analysis

Threshold-finding perfusion CT analysis. A total of 146 patients who fulfilled the inclusion criteria for the

study were analyzed to obtain the optimal baseline perfusion parameters and thresholds for the prediction of PH after ET, which was the main outcome of this study. All patients were scanned using a SIEMENS Somatom Definition Flash 128-section dual-source multidetector scanner (Siemens Healthcare, Erlangen, Germany), with a 98 mm z-coverage and 26 time points acquired each 1.5 s (total acquisition time, 39 s). Fifty milliliters of nonionic iodinated contrast was administered intravenously at 5 mL/s by using a power injector, followed by a saline flush of 20 ml at an injection rate of 2 ml/s. Perfusion CT imaging parameters were 80 kV (peak), 250 mAs, 1.5-s rotation, FoV 18 mm, matrix 512×512 , and 2-mm thickness (49 slices in total). Perfusion CT maps were then calculated by commercial software MISTar (Apollo Medical Imaging Technology, Melbourne, Australia) using a model-free singular value decomposition (SVD) algorithm with a delay and dispersion correction.²¹ The software automatically performs motion correction and selects an arterial input function (AIF) from an unaffected artery (usually the anterior cerebral artery) and a venous output function (VOF) from a large draining vein (the sagittal sinus). The software generates CBF, CBV, MTT and DT maps. Of note, the delay corrected deconvolution method produces DT maps rather than the more extensively used Tmax maps. With this methodology, a DT over 2 s is equivalent to a Tmax over 6 s when a SVD method without delay correction is employed.²¹ An image processing pipeline using in-house fully automated software running in Matlab (v.2013a, Mathworks, Natick, MA) was developed in order to implement a comprehensive analysis of the perfusion maps. An absolute threshold of 2 s was selected on the DT map to obtain the hypoperfused tissue (perfusion lesion). Inside this area, a range of relative and absolute thresholds was explored in the CBF, CBV and DT maps at constant increments, as shown in Table 1. The relative thresholds were calculated as a percentage of mean perfusion values from the complete unaffected/contralateral hemisphere. To assess the consistency of the optimal parameter thresholds for predicting PH found in the whole population, a sensitivity analysis including only those patients in whom tissue time attenuation curves (TACs) were not truncated at the end of the perfusion CT acquisition was performed. For this subset analysis, truncated curves were defined as those in which the TACs did not achieve a plateau state at the final time point of the acquisition, and not truncated curves as those that were effectively completed. Investigators blinded to clinical data and post-treatment neuroimaging studies (C.L.; R.T.) performed the post-processing and analysis of baseline perfusion CT data.

Table 1. Range of explored thresholds in CT maps.

PCT map	Parameter	Range of explored thresholds	Increments
CBV	aCBV	0 to 2.0 ml/100 g	0.1 ml/100 g
	rCBV	0 to 100%	2.5%
CBF	aCBF	0 to 36 ml/100 g/min	2 ml/100 g/min
	rCBF	0 to 100%	2.5%
DT	aDT	0 to 20 s	1 second

PCT: perfusion CT; CBV: cerebral blood volume; aCBV: absolute CBV; rCBV: relative CBV; CBF: cerebral blood flow; aCBF: absolute CBF; rCBF: relative CBF; DT: delay time; aDT: absolute DT.

Perfusion CT-MRI coregistered regions of interest analysis. Patients who developed PH at follow-up and had both baseline perfusion CT and follow-up MRI ($n=19$) were additionally analyzed to explore the differences in baseline perfusion values between three coregistered regions of interest delineated in MRI: non-infarcted tissue, infarcted tissue, and tissue with hemorrhagic transformation. The MR imaging protocol included DWI and GRE sequences. Each MR image (DWI and GRE) was coregistered to the corresponding perfusion CT map using a rigid co-registration protocol implemented with Statistical Parametric Mapping (SPM8, Functional Imaging Laboratory, University College London, London, UK). DWI and GRE lesions were delineated using AMIRA software by means of a semi-automated thresholding method to identify regions of interest with high DWI and low GRE signal intensity. DWI lesions were defined as pixels exceeding the DWI signal intensity of the contralateral hemisphere by more than three standard deviations and GRE lesions as pixels with intensity below 20% of the mean in the contralateral hemisphere. DWI and GRE Regions of Interest (ROI) were then placed in the coregistered perfusion CT maps and automatically mirrored to the contralateral hemisphere. The mean values of CBF, CBV and DT in the respective individual perfusion CT maps were extracted and compared within these ROIs.

Statistics

Continuous variables were reported as mean (standard deviation, SD) or median (interquartile range, IQR) and were compared with the Student *t*-test, ANOVA, Mann-Whitney, or Kruskal-Wallis tests as appropriate. Categorical variables were compared with the χ^2 and Fisher exact tests. Receiver-operating characteristic (ROC) curve analysis was performed to determine the most accurate perfusion CT parameter, and the optimal threshold for each parameter for the prediction of PH. After transformation to the third root to approach

normality, the selected perfusion CT parameters were included in binary logistic regression models to evaluate their association with the risk of PH. In each model, the coefficient of determination (R^2), and information criteria indicators, such as the Akaike's information criterion (AIC) and the Bayesian information criterion (BIC) were calculated to compare their predictive effects on the risk of PH. A better model is evidenced by a lower AIC, a lower BIC, and a higher R^2 .²² Univariate logistic regression models were used to assess the value of the selected perfusion measures (relative CBV and CBF) to predict the risk of PH. Afterwards, multivariate logistic regression models were used to adjust the estimations for the effect of time from stroke onset to recanalization, baseline NIHSS and pre-stroke antithrombotic use (*p* values lower than 0.10 on univariate analysis), and for other potential relevant confounding variables such as age, gender and treatment modality (primary ET versus rescue ET). The analyses were performed using SPSS Version 19.0 and the level of significance was established at the 0.05 level (2-sided).

Results

A total of 146 patients were included in the analysis, of whom 27 (18.5%) had parenchymal hemorrhage (PH) at follow-up neuroimaging performed within 72 h of hospital admission [PH-1 $n=13$ (9.6%), PH-2 $n=14$ (9.6%)], and 41 (28.1%) HI [IH-1 $n=20$ (13.7%), IH-2 $n=21$ (14.4%)]. A total of 14 (9.6%) PHs were identified at the first post-treatment neuroimaging (within 24 h), and only 7 (4.8%) were symptomatic. Subarachnoid hemorrhage after ET was observed in 20 of the 146 included patients (14%), and in 9 of the 27 patients with PH (33%). Descriptive data on demographics and baseline variables according to the presence of PH are shown in Table 2. Of note, patients with PH had higher baseline NIHSS, lower baseline ASPECTS scores and longer times from stroke onset to recanalization, in comparison with patients who did not have PH. The location of arterial occlusions prior to ET, the modality of ET (rescue ET versus primary ET), baseline glucose and baseline systolic blood pressure levels were similar across groups. Overall, the presence of any PH type at follow-up was associated with an increased mRS score at 90 days (OR for shifting to a worse mRS category 3.417, 95% CI 1.596–7.312, $p=0.002$).

Perfusion parameters and risk of PH: ROC and regression analysis

The optimal baseline perfusion parameters and thresholds for the prediction of PH after ET were evaluated in

Table 2. Demographics, baseline and procedure related variables according to the occurrence of PH.

	No PH N = 119	PH N = 27	p
Age (years), median (IQR)	72 (62–79)	67 (57–81)	0.954
Males, n (%)	53 (45)	13 (48)	0.734
Smoking, n (%)	28 (24)	5 (19)	0.560
Hypertension, n (%)	71 (60)	18 (67)	0.501
Diabetes, n (%)	23 (19)	3 (11)	0.314
Dyslipidemia, n (%)	49 (41)	11 (41)	0.967
Atrial fibrillation, n (%)	36 (30)	10 (37)	0.493
Previous stroke, n (%)	10 (8)	4 (15)	0.307
Previous antithrombotic treatment, n (%)	51 (43)	18 (68)	0.025
Baseline SBP (mmHg), mean (SD)	148 (23)	147 (27)	0.805
Glucose (mg/dl), median (IQR)	118 (102–137)	125 (108–150)	0.442
Pre-angio NIHSS, median (IQR)	15 (10–19)	18 (14–21)	0.020
Baseline ASPECTS, median (IQR)	8 (7–9)	7 (6–8)	0.005
ASPECTS 8–10, n (%)	66 (59)	7 (26)	0.002
Good collaterals (collateral score 2-3), n (%)	72 (61)	15 (56)	0.601
Alteplase + ET, n (%)	79 (66)	16 (59)	0.483
Primary ET, n (%)	40 (34)	11 (41)	0.483
Time to perfusion CT (min), md (IQR)	173 (105–255)	224 (124–309)	0.177
Time to ET onset (min), md (IQR)	263 (195–352)	290 (208–400)	0.358
Duration of ET procedure (min), md (IQR)	32 (15–74)	58 (35–80)	0.046
Type of ET treatment			
Stent-retrievers, n (%)	107 (90)	27 (100)	0.124
Merci device, n (%)	8 (7)	1 (4)	0.478
Carotid stenting, n (%)	14 (12)	0 (0)	0.073
Local alteplase, n (%)	1 (0)	0 (0)	1.000
Device passes per procedure, median (IQR)	2 (1–4)	3 (1–3)	0.157
Recanalization (yes), n (%)	109 (92)	24 (89)	0.656
Time to recanalization (min), median (IQR)	300 (240–367)	360 (278–453)	0.022
Recanalization groups			0.049
Recanalization < 6 h, n (%)	78 (66)	11 (41)	
Recanalization > 6 h, n (%)	31 (26)	13 (48)	
No rec, n (%)	10 (8)	3 (11)	
TOAST classification			0.858
Atherothrombotic origin, n (%)	21 (18)	6 (22)	
Cardioembolic origin, n (%)	61 (51)	13 (48)	
Other etiologies, n (%)	37 (31)	8 (30)	
Location of the occlusion			0.666
Tandem occlusions, n (%)	18 (15)	6 (22)	
ICA-T or MI, n (%)	81 (68)	17 (63)	
M2, n (%)	20 (17)	4 (15)	

PH: parenchymal hematoma; SBP: systolic blood pressure; NIHSS: National Institutes of Health Stroke Scale; ASPECTS indicates Alberta Stroke Program Early CT Score; ET: endovascular therapy; TOAST: Trial of Org 10 172 in Acute Stroke Treatment; ICA-T: internal carotid artery.

the 146 included patients by means of regression and ROC analyses. In regression analyses, CBF and CBV maps were more accurate than time-based maps for the prediction of the occurrence of PH at follow up neuroimaging, as shown in Table 3. In ROC analyses, the

optimal thresholds for both relative CBV and CBF parameters were perfusion values lower than 2.5% of normal brain in the contralateral hemisphere, and the best absolute thresholds were 0.1 ml/100 g for CBV and 2 ml/100 g/min for CBF. The best volumetric cut-off

Table 3. Regression analysis.

Perfusion CT map	AIC	BIC	R ² (%)
rCBV	93.993	99.448	10.8
rCBF	92.578	98.033	11.3
aCBV	91.484	96.939	10.8
aCBF	99.810	105.264	10.6
DT	119.905	152.360	5.2

Performance of different models for the prediction of PH fitted with relative CBV, relative CBF, absolute CBF, absolute CBV and absolute DT. In each model, the AIC, the BIC and the coefficient of determination R² were calculated to quantify the predictive effects of each parameter on the risk of PH. A better model is evidenced by a lower AIC, a lower BIC, and a higher R². CBV: cerebral blood volume; aCBV: absolute CBV; rCBV: relative CBV; CBF: cerebral blood flow; aCBF: absolute CBF; rCBF: relative CBF; DT: delay time; AIC: Akaike's information criterion; BIC: Bayesian information criterion; R²: coefficient of determination.

points within each perfusion CT map for the prediction of PH are summarized in Table 4, and representative cases are shown in Figure 1. The sensitivity, specificity, positive predictive values and negative predictive values of the optimal thresholds found in this study are also specified in Table 4. Overall, these thresholds had high negative predictive values and moderate sensibility and specificity values.

A total of 83 (57%) patients had non-truncated curves, and 14 (17%) of them had PH at follow-up. In this subset of patients, a sensitivity analysis showed that the optimal thresholds obtained with ROC analyses were perfusion values lower than 2.5% of normal brain in the contralateral hemisphere for relative CBV [Area Under the Curve (AUC) 0.622, 95%CI 0.458–0.787] and CBF (AUC 0.627, 95%CI 0.462–0.791) parameters, and the best absolute thresholds were 0.1 ml/100 g for CBV (AUC 0.628, 95%CI 0.462–0.794) and 2 ml/100 g/min for CBF (AUC 0.623, 95%CI 0.455–0.791), as in the whole study sample. The best perfusion threshold for DT was 8 s (AUC 0.600, 95%CI 0.428–0.773).

Perfusion parameters and risk of PH: perfusion CT-MRI coregistered regions of interest analysis

A perfusion CT-MRI coregistered regions of interest analysis was performed including those patients with PH who had baseline perfusion CT and follow-up MR imaging (n = 19 of 27). In this subgroup of patients we explored the baseline perfusion CT values of brain regions that at follow up MRI were classified as infarcted tissue without hemorrhagic transformation, tissue with hemorrhagic transformation, and non-infarcted contralateral tissue. As shown in Figure 2, infarct regions that developed PH at follow-up showed lower values of CBV and CBF, but similar

values of DT at baseline, compared with infarct regions that did not develop PH. As expected, normal tissue had higher CBV and CBF values, and shorter DT values than finally infarcted tissue (either with or without hemorrhagic transformation).

Time to recanalization from stroke onset and risk of PH

From the 146 included patients, a total of 133 (91%) recanalized at the end of ET, and 13 (9%) did not recanalize. Early recanalization (<6 h from stroke onset) was observed in 89 (61%) patients, and delayed recanalization (>6 h) in 44 (30%). In reference to patients with early recanalization, the rate of PH was significantly higher in patients with delayed recanalization (OR 2.97, 95%CI 1.20–7.35; p = 0.018), but not in those without recanalization (OR 2.12, 95%CI 0.51–8.95; p = 0.303). In models adjusted for baseline stroke severity, the rate of poor outcome was increased in patients with delayed recanalization (OR 2.45, 95%CI 1.10–5.44; p = 0.028) and in those without recanalization (OR 6.66, 95%CI 1.57–28.22; p = 0.010), in reference to patients achieving early recanalization. In the subset of patients with recanalization, longer onset to reperfusion times (OTR) were associated with a gradually increased risk of poor outcome (OR 1.15 per each decile of OTR increase, 95%CI 1.03–1.30; p = 0.025) and with an increased risk of PH (OR 1.22 per each decile of OTR increase, 95%CI 1.03–1.44; p = 0.023).

Multivariate models for the prediction of PH

Relative CBF and CBV parameters instead of absolute values were used for multivariate analyses. As shown in Figure 3, the volume of regions with low relative CBV and/or CBF was associated with an increased risk of PH and the associations remained significant in models adjusted for the effect of recanalization status at follow up, age, gender, baseline stroke severity, treatment modality and prior antithrombotic use. Delayed recanalization (>6 h), but not early recanalization (<6 h) or absence of recanalization, was also associated with an increased risk of PH. After excluding patients without recanalization (n = 13), the associations of low rCBV, low rCBF and OTR time with the risk of PH remained significant in unadjusted and adjusted models.

The interaction between recanalization status and the volume of regions with low rCBV (p = 0.294) or low rCBF (p = 0.479) was not significant. Moreover, in patients with recanalization at the end of ET, the interaction between OTR time and the volume of regions with low rCBV (p = 0.286) or low rCBF (p = 0.456) was neither significant. Finally, there was

Table 4. ROC analysis: best thresholds and volumetric cut-off points for the prediction of PH within each perfusion CT map.

Perfusion CT map	Best perfusion threshold	AUC (95% CI); p	Best volumetric cutpoint	Se/Sp/PPV/NPV
rCBV	2.5%	0.724 (0.611–0.837); p = 0.001	1.49 ml	65/77/46/88
rCBF	2.5%	0.723 (0.610–0.837); p = 0.001	0.64 ml	73/68/40/89
aCBV	0.1 ml/100 g	0.717 (0.599–0.835); p = 0.001	1.91 ml	65/77/46/88
aCBF	2 ml/100 g/min	0.724 (0.609–0.838); p = 0.001	1.07 ml	81/57/36/91
DT	6 s	0.659 (0.544–0.773); p = 0.014	44.4 ml	62/71/39/86

ROC: Receiver Operating characteristics; CBV: cerebral blood volume; aCBV: absolute CBV; rCBV: relative CBV; CBF: cerebral blood flow; aCBF: absolute CBF; rCBF: relative CBF; DT: delay time; AUC: area under the curve; Se: sensitivity; Sp: specificity; PPV: positive predictive value; NPV: negative predictive value.

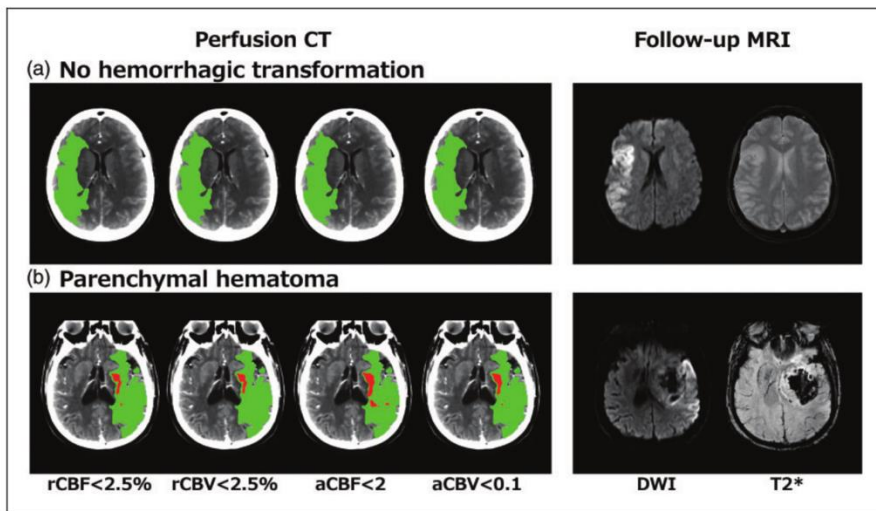


Figure 1. Illustrative cases showing regions of severe ischemia (red areas) assessed with the best identified thresholds on each perfusion map, in relation with hypoperfused tissue (green areas) and follow up MRI. (a) Patient without regions of severe ischemia and absence of hemorrhagic transformation in follow-up neuroimaging. (b) Patient with regions of severe ischemia in baseline perfusion CT who developed a parenchymal hematoma (PH-2) in follow-up MRI.

no significant association between the volume of regions with low CBV and/or CBF values in regression analyses restricted to symptomatic PH (data not shown).

Discussion

In this threshold-finding study we implemented a comprehensive analytic approach of whole-brain perfusion CT data to identify the best hemodynamic parameters for prediction of PH after ET in a homogeneous cohort of patients with proximal occlusions in the carotid territory. The present study demonstrated a consistent association between regions with severe reductions of relative CBV and/or CBF and an increased risk of PH. The study also suggested that delayed recanalization may also be associated with hemorrhagic

complications, in contrast with earlier recanalization or permanent arterial occlusion. Collectively, these results highlighted the relevance of the severity and duration of ischemia as drivers of blood-brain barrier (BBB) disruption in acute ischemic stroke, and supported the role of perfusion CT in the prediction of the risk of PH after ET.

Experimental cerebral ischemia impairs vascular integrity and results in the loss of microvascular structures and erythrocyte extravasation,^{23,24} in a process which is dependent on the intensity and duration of the lack of flow.²⁵ In human stroke, blood flow can be reliably quantified with dynamic contrast-enhanced neuroimaging, such as perfusion CT.²¹ In this perfusion CT based study, CBV and CBF derived thresholds were more informative of the risk of PH than those extracted from DT maps. The best CBV or CBF thresholds for

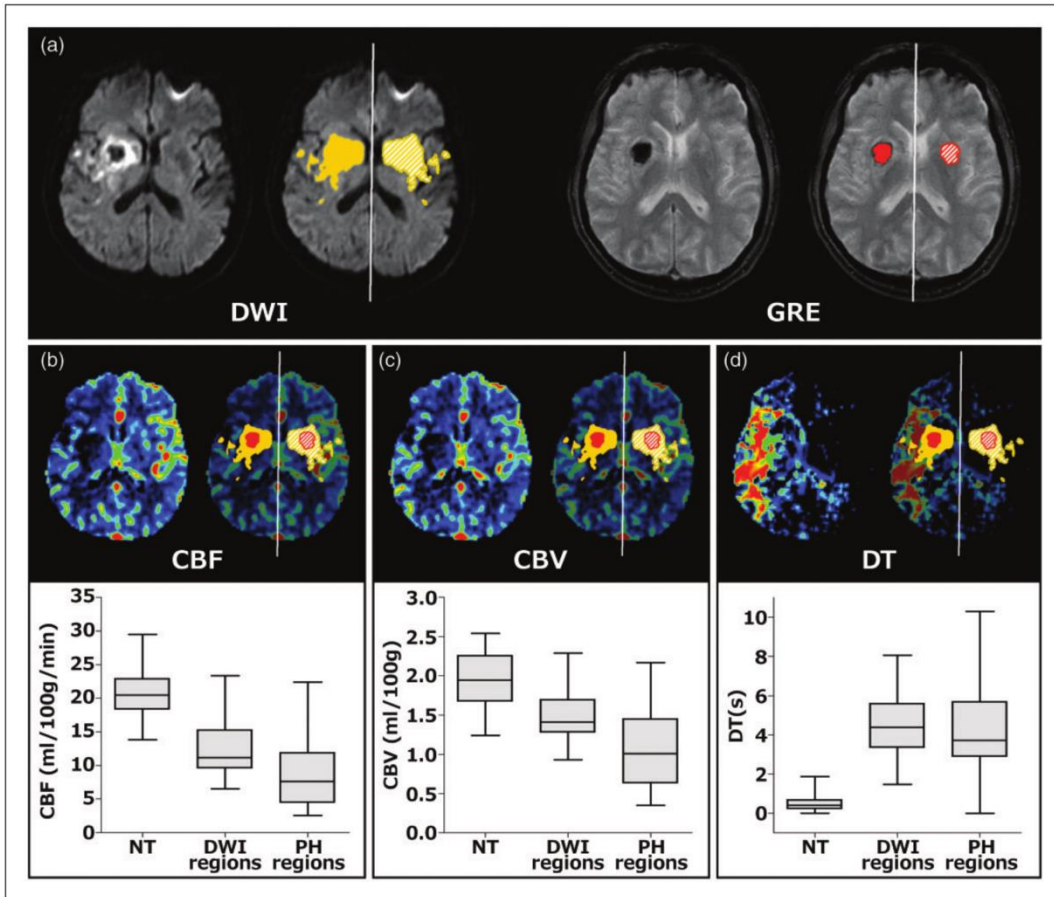


Figure 2. Differences in pre-treatment baseline perfusion values between regions classified as non-infarcted tissue (normal tissue, NT), infarcted tissue (DWI regions, yellow label), and tissue with hemorrhagic transformation (PH regions, red label) in follow-up MRI of patients who developed parenchymal hematomas (PH) ($n = 19$). (a) DWI and PH regions of interests were delineated, placed in the co-registered perfusion CT maps and automatically mirrored to the contralateral hemisphere (mirrored DWI region of interest: yellow striped label; mirrored PH region of interest: red striped label); (b) Baseline perfusion CT cerebral blood flow (CBF) absolute values were significantly lower in regions which developed PH (median 7.6, IQR 4.4–11.9) at follow-up neuroimaging, in comparison with regions which developed infarction but no PH (median 11.2, IQR 9.4–15.8, $p = 0.002$), or in comparison with contralateral normal tissue (median 20.5, IQR 18.3–23.0, $p < 0.001$). (c) Baseline perfusion CT cerebral blood volume (CBV) absolute values were significantly lower in regions which developed PH (median 1.0, IQR 0.6–1.5) at follow-up neuroimaging, in comparison with regions which developed infarction but no PH (median 1.4, IQR 1.3–1.7, $p = 0.003$), or in comparison with contralateral normal tissue (median 1.7, IQR 1.9–2.3, $p < 0.001$). (d) PH regions disclosed similar pretreatment baseline DT values (median 4.4, IQR 3.2–5.6) than DWI regions (median 3.7, IQR 2.7–5.9; $p = 0.313$), and higher values than normal tissue (median 0.4, IQR 0.2–0.7, $p < 0.001$).

predicting the development of PH were values lower than 2.5% of mean CBF and CBV values in normal brain. These results contrast with a previous threshold-finding study where the optimal observed perfusion CT derived parameters and thresholds were a $T_{max} > 14$ s, a rCBF lower than 30% and a rCBV lower than 35% of normal brain tissue.¹² Beyond the differences in perfusion CT acquisition and post-processing protocols that were used in these studies, herein we included a highly homogeneous stroke population treated with endovascular reperfusion therapy. This selected population contrast with the former study in which only half of

the patients received systemic thrombolysis thus precluding the high rate of early reperfusion encountered in our study. In concordance with previous MRI derived data,⁷ the thresholds identified in this perfusion CT study did better than the total volumes of non-viable tissue, total hypoperfused tissue or tissue at risk, as defined with validated thresholds. Overall, these data may indicate that the amount of tissue with an extreme reduction of perfusion would be the most relevant hemodynamic parameter for promoting early BBB damage, particularly when multimodal reperfusion therapy is administered to achieve early

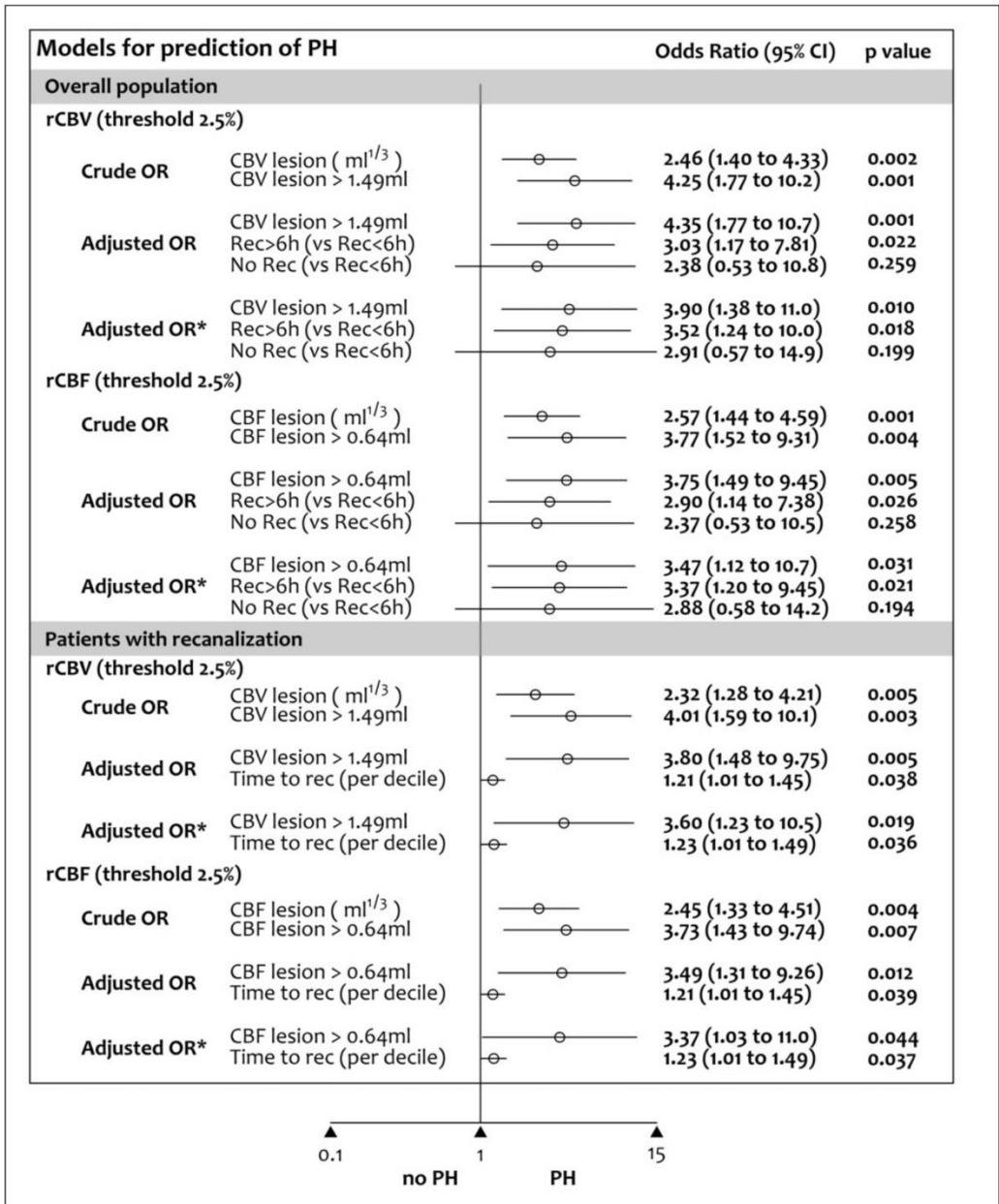


Figure 3. Models for prediction of parenchymal hematoma at follow-up neuroimaging.

PH: parenchymal hematoma; rCBV: relative Cerebral Blood Volume; rCBF: relative Cerebral Blood Flow; Rec: recanalization. Circles and horizontal lines represent OR point estimates and 95% confidence intervals (95%CI), respectively.

Crude OR: OR and 95% CI obtained by unadjusted models. Adjusted OR: OR and 95% CI obtained by models adjusted for recanalization status. Adjusted OR*: OR and 95% CI obtained by models adjusted for recanalization status, age, gender, baseline stroke severity, treatment modality and pre-stroke antithrombotic use.

recanalization. Nevertheless, further studies are warranted to assess the effect of the severity of hypoperfusion in acute stroke patients according to the occurrence of early reperfusion or to the administration of different reperfusion strategies.

The aim of recanalization therapies is to achieve an early reperfusion of the ischemic tissue to prevent brain infarction. However, the reperfusion of a severely ischemic tissue may lead to harmful consequences, which include brain edema, hemorrhagic complications or a

combination of them. This deleterious process is called reperfusion injury and implies a myriad of mechanisms such as oxidative stress, inflammation and activation of proteolytic enzymes that finally involve the disruption of the BBB.²⁶ In the experimental setting, the duration of ischemia prior to reperfusion is strongly related to the risk of hemorrhagic complications.²⁷ Postischemic reperfusion can impair vascular function and exacerbate ischemic injury after longer durations of ischemia and reperfusion.²⁸ In experimental models of thromboembolic middle cerebral artery occlusion in rats the duration of brain ischemia prior to reperfusion parallels an increased risk and severity of hemorrhagic transformation. Thus, after 6 h of occlusion the risk of PH was significantly increased in comparison with shorter occlusion times (3 h) or permanent occlusion.²⁹ Accordingly, in humans with cardioembolic stroke, recanalization occurring beyond 6 h is associated with an increased risk of hemorrhagic transformation.³⁰ Moreover, a longer time from stroke onset to the administration of recanalization therapies is associated with the presence of permeability derangements on post-treatment dynamic contrast-enhanced multimodal MRI,³¹ a reliable predictor of hemorrhagic complications in acute stroke.³² In agreement with these clinical and experimental data, we found that the risk of PH was increased in patients with delayed recanalization (over 6 h of stroke onset). Moreover, even in patients achieving early recanalization at the end of ET, we also found a significant association between the time delay to recanalization and the risk of PH. Reassuringly, this association was maintained in models adjusted by the effect of relevant confounders. However, the limited number of events in patients with delayed or absence of recanalization precludes the generalizability of this association and calls for the implementation of further adequately powered prospective studies. Overall, the data further support that reperfusion may be more deleterious for the integrity of the BBB in patients with longer duration of ischemia. There remains to be shown in clinical trials whether this potential pernicious effect of delayed reperfusion may be ameliorated with neuroprotective or vasculoprotective therapies. According to our data, patients with regions of severe ischemia and longer expected delays from stroke onset to recanalization may represent a target population for these therapies. Importantly, it is essential to remark that this study was not designed to assess the role of perfusion CT in the selection of patients for endovascular reperfusion therapies. Given the strong beneficial effects in terms of clinical outcome of endovascular reperfusion therapies recently shown in clinical trials, the presence of regions of severe reductions of CBF or CBV in perfusion CT should not preclude the treatment of patients otherwise eligible for receiving endovascular reperfusion therapies.

The low positive predictive value and high negative predictive value of the best performing thresholds indicate that severe ischemia may be a necessary but not sufficient mediator for PH. Previous MRI-based clinical studies showed that delayed reperfusion of regions with severe reductions of CBV was strongly associated with PH in patients receiving systemic thrombolysis.^{8,33} Others showed that early reperfusion had no influence on the risk of PH in acute stroke patients treated or not with thrombolysis.⁹ In agreement with the latter study, we did not find a significant interaction between perfusion CT markers of severe ischemia and timing of recanalization in the prediction of PH although the lack of this relationship may be related to an underpowered sample size. Whether reperfusion driven by ET would be more deleterious in patients with larger areas of very severe ischemic deficits should be assessed in further studies.

For this analysis we evaluated the incidence of PH in follow-up neuroimaging explorations performed within the first 72 h of therapy to gather a sufficient number of events to be analyzed. The use of this time point may partly explain why in this cohort of patients PH rates were higher than that reported in recent studies of ET. Likewise, MR imaging including gradient-recall echo sequence is more sensitive and more reliable than CT for detecting hemorrhagic transformation in the acute phase of ischemic stroke.³⁴ In this study, hemorrhagic transformation was evaluated in gradient-recall echo MRI in 19 (70%) and in CT in 8 (30%) of the patients who developed PH. Of note, the rate of PH at the first neuroimaging after ET (within 24 h; $n = 14$, 9.6%) and the rate of symptomatic PHs ($n = 7$, 4.8%) were similar to those reported in the literature.³⁵⁻³⁷ We did not find a significant association between the volume of regions with low CBV and/or CBF values in regression analyses restricted to symptomatic hemorrhagic transformation, although this study was not powered to analyse their association with perfusion measures due to the low number of symptomatic PHs. Additional studies should be performed to determine the association of these biomarkers with clinically relevant hemorrhagic transformation after ischemic stroke.

The use of whole-brain perfusion CT was a strong point of the study as it allowed obtaining perfusion measures of most of the affected brain tissue. The inclusion of patients treated with ET also allowed an accurate estimation of times from stroke onset to recanalization. Moreover, patients were collected consecutively and managed following a homogeneous therapeutic protocol. Nonetheless, the study has several limitations. First, the assessment of perfusion with dynamic CT in acute stroke is a static evaluation of a multifaceted and time-dependent process. Secondly, perfusion measures may be affected by multiple factors,

including the acquisition protocols, the brain coverage and the post-processing platforms.³⁸ Regarding the acquisition protocols, a limited acquisition time (<60 s) may result in a delayed arrival of contrast agent with a consequent truncation of tissue TACs that may preclude accurate calculation of perfusion CT parameters with a shift towards overestimation of perfusion deficits. To minimize the effect of delayed bolus arrival due to the relatively short scan acquisition time used in this study, perfusion CT maps were calculated using a validated deconvolution algorithm with delay and dispersion correction.^{21,39} These delay-insensitive algorithms have been shown to be more reliable and accurate for measuring hypoperfused and non viable tissue volumes than delay-sensitive software.³⁹ Moreover, the consistency of the thresholds found in the whole population was confirmed in a sensitivity subgroup analysis that included only those patients without truncated TACs. As a note of caution, the parameter thresholds obtained in this study may depend on the post-processing platform and the acquisition protocols that were employed and may not be generalizable to other methodologies. Additionally, we were not able to obtain direct measures of the permeability of the blood-brain barrier due to the short perfusion CT acquisition protocol. Indeed, the quantification of the passage of contrast agents from the vascular compartment to the brain across the vascular endothelium as a marker of BBB derangement is overestimated when first-pass perfusion CT data is used, and delayed acquisitions (up to 210 s) are necessary to obtain unbiased measures. Furthermore, it will be of potential interest to evaluate the relationship between very severe reductions of CBF/CBV and direct measurements of BBB damage, as those obtained by means of the quantification of BBB permeability using dynamic contrast-enhanced MRI or adequately extended perfusion CT acquisitions. As an additional limitation, the post-processing software (Siemens) used for the real-time selection of patients for receiving endovascular reperfusion therapy was different from the post-processing software (MISStar) used to execute the comprehensive analysis of perfusion maps. Finally, we considered the recanalization status at the end of ET as a surrogate measure of reperfusion, although these two phenomena may not always occur simultaneously.⁴⁰

In summary, this study shows that the identification of severe perfusion deficits evaluated with perfusion CT is predictive of the risk of hemorrhagic complications after endovascular reperfusion therapy of acute ischemic stroke. Moreover, delayed recanalization seems to be associated with an increased risk of parenchymal hemorrhage after thrombectomy. These two factors should be considered in the evaluation of strategies aimed to protect the blood-brain barrier in addition

to early and complete recanalization in this patient population. Nevertheless, the presence of regions of severe reductions of CBF or CBV in perfusion CT should not preclude the treatment of patients otherwise eligible for receiving endovascular reperfusion therapies.

Funding

The author(s) disclosed receipt of the following financial support for the research, authorship, and/or publication of this article: This work was supported by a grant from the Spanish Ministry of Economy and Competitiveness (PI13/01268, funded as part of the Plan Nacional R + D + I and cofinanced by ISCIII-Subdirección General de Evaluación and by the FEDER).

Declaration of conflicting interests

The author(s) declared no potential conflicts of interest with respect to the research, authorship, and/or publication of this article.

Authors' contributions

AR and CL contributed equally to this work. AR and CL obtained the clinical data, performed the post-processing of the perfusion maps and wrote the first draft of the manuscript. RT, ALR and LO supervised the post-processing of perfusion maps and the image analysis. XU and LLI obtained the clinical data. SA and AC designed the study, interpreted the data and wrote the final draft of the manuscript.

References

1. Campbell BC, Mitchell PJ, Kleinig TJ, et al. the EXTEND-IA Investigators. Endovascular therapy for ischemic stroke with perfusion-imaging selection. *N Engl J Med* 2015; 372: 1009–1018.
2. Goyal M, Demchuk AM, Menon BK, et al. the ESCAPE Trial Investigators. Randomized assessment of rapid endovascular treatment of ischemic stroke. *N Engl J Med* 2015; 372: 1019–1030.
3. Jovin TG, Chamorro A, Cobo E, et al. Thrombectomy within 8 hours after symptom onset in ischemic stroke. *N Engl J Med* 2015; 372: 2296–2306.
4. Strbian D, Sairanen T, Meretoja A, et al. Helsinki Stroke Thrombolysis Registry Group. Patient outcomes from symptomatic intracerebral hemorrhage after stroke thrombolysis. *Neurology* 2011; 77: 341–348.
5. Mokin M, Kan P, Kass-Hout T, et al. Intracerebral hemorrhage secondary to intravenous and endovascular intraarterial revascularization therapies in acute ischemic stroke: an update on risk factors, predictors, and management. *Neurosurg Focus* 2012; 32: E2.
6. Mazighi M, Chaudhry SA, Ribo M, et al. Impact of onset-to-reperfusion time on stroke mortality: a collaborative pooled analysis. *Circulation* 2013; 127: 1980–1985.
7. Campbell BC, Christensen S, Butcher KS, et al. EPITHET Investigators. Regional very low cerebral blood volume predicts hemorrhagic transformation

- better than diffusion-weighted imaging volume and thresholded apparent diffusion coefficient in acute ischemic stroke. *Stroke* 2010; 41: 82–88.
8. Campbell BC, Christensen S, Parsons MW, et al. EPITHET and DEFUSE Investigators. Advanced imaging improves prediction of hemorrhage after stroke thrombolysis. *Ann Neurol* 2013; 73: 510–519.
 9. Hermitte L, Cho TH, Ozenne B, et al. Very low cerebral blood volume predicts parenchymal hematoma in acute ischemic stroke. *Stroke* 2013; 44: 2318–2320.
 10. Jain AR, Jain M, Kanthala AR, et al. Association of CT perfusion parameters with hemorrhagic transformation in acute ischemic stroke. *AJNR Am J Neuroradiol* 2013; 34: 1895–1900.
 11. Souza LC, Payabvash S, Wang Y, et al. Admission CT perfusion is an independent predictor of hemorrhagic transformation in acute stroke with similar accuracy to DWI. *Cerebrovasc Dis* 2012; 33: 8–15.
 12. Yassi N, Parsons MW, Christensen S, et al. Prediction of poststroke hemorrhagic transformation using computed tomography perfusion. *Stroke* 2013; 44: 3039–3043.
 13. Shinoyama M, Nakagawara J, Yoneda H, et al. Initial ‘TTP Map-Defect’ of computed tomography perfusion as a predictor of hemorrhagic transformation of acute ischemic stroke. *Cerebrovasc Dis Extra* 2013; 3: 14–25.
 14. Rai AT, Raghuram K, Carpenter JS, et al. Pre-intervention cerebral blood volume predicts outcomes in patients undergoing endovascular therapy for acute ischemic stroke. *J Neurointerv Surg* 2013; 5(Suppl 1):25.32.
 15. Bhatt A, Vora NA, Thomas AJ, et al. Lower pretreatment cerebral blood volume affects hemorrhagic risks after intra-arterial revascularization in acute stroke. *Neurosurgery* 2008; 63: 874–879.
 16. Gupta R, Yonas H, Gebel J, et al. Reduced pretreatment ipsilateral middle cerebral artery cerebral blood flow is predictive of symptomatic hemorrhage post-intra-arterial thrombolysis in patients with middle cerebral artery occlusion. *Stroke* 2006; 37: 2526–2530.
 17. Renú A, Amaro S, Laredo C, et al. Relevance of blood-brain barrier disruption after endovascular treatment of ischemic stroke: dual-energy computed tomographic study. *Stroke* 2015; 46: 673–679.
 18. Adams HP Jr, Bendixen BH, Kappelle LJ, et al. Classification of subtype of acute ischemic stroke. Definitions for use in a multicenter clinical trial. TOAST. Trial of ORG 10172 in Acute Stroke Treatment. *Stroke* 1993; 24: 35–41.
 19. Tan IY, Demchuk AM, Hopyan J, et al. CT angiography clot burden score and collateral score: correlation with clinical and radiologic outcomes in acute middle cerebral artery infarct. *Am J Neuroradiol* 2009; 30: 525–531.
 20. Fiorelli M, Bastianello S, von Kummer R, et al. Hemorrhagic transformation within 36 hours of a cerebral infarct: relationships with early clinical deterioration and 3-month outcome in the European Cooperative Acute Stroke Study I (ECASS I) cohort. *Stroke* 1999; 30: 2280–2284.
 21. Bivard A, Levi C, Spratt N, et al. Perfusion CT in acute stroke: a comprehensive analysis of infarct and penumbra. *Radiology* 2013; 267: 543–550.
 22. Vrieze SI. Model selection and psychological theory: a discussion of the differences between the Akaike information criterion (AIC) and the Bayesian information criterion (BIC). *Psychol Methods* 2012; 17: 228–243.
 23. Hamann GF, Okada Y and del Zoppo GJ. Hemorrhagic transformation and microvascular integrity during focal cerebral ischemia/reperfusion. *J Cereb Blood Flow Metab* 1996; 16: 1373–1378.
 24. Hamann GF, Liebetrau M, Martens H, et al. Microvascular basal lamina injury after experimental focal cerebral ischemia and reperfusion in the rat. *J Cereb Blood Flow Metab* 2002; 22: 526–533.
 25. del Zoppo GJ, von Kummer R and Hamann GF. Ischaemic damage of brain microvessels: inherent risks for thrombolytic treatment in stroke. *J Neurol Neurosurg Psychiatry* 1998; 65: 1–9.
 26. Maier CM, Hsieh L, Crandall T, et al. Evaluating therapeutic targets for reperfusion-related brain hemorrhage. *Ann Neurol* 2006; 59: 929–938.
 27. Jickling GC, Liu D, Stamova B, et al. Hemorrhagic transformation after ischemic stroke in animals and humans. *J Cereb Blood Flow Metab* 2014; 34: 185–199.
 28. Palomares SM and Cipolla MJ. Vascular protection following cerebral ischemia and reperfusion. *J Neurol Neurophysiol* 2011; 20: S1–004.
 29. Copin JC and Gasche Y. Effect of the duration of middle cerebral artery occlusion on the risk of hemorrhagic transformation after tissue plasminogen activator injection in rats. *Brain Res* 2008; 1243: 161–166.
 30. Molina CA, Montaner J, Abilleira S, et al. Timing of spontaneous recanalization and risk of hemorrhagic transformation in acute cardioembolic stroke. *Stroke* 2001; 32: 1079–1084.
 31. Bang OY, Saver JL, Alger JR, et al. UCLA MRI Permeability Investigators. Patterns and predictors of blood-brain barrier permeability derangements in acute ischemic stroke. *Stroke* 2009; 40: 454–461.
 32. Leigh R, Jen SS, Hillis AE, et al. STIR and VISTA Imaging Investigators. Pretreatment blood-brain barrier damage and post-treatment intracranial hemorrhage in patients receiving intravenous tissue-type plasminogen activator. *Stroke* 2014; 45: 2030–2035.
 33. Alsop DC, Makovetskaya E, Kumar S, et al. Markedly reduced apparent blood volume on bolus contrast magnetic resonance imaging as a predictor of hemorrhage after thrombolytic therapy for acute ischemic stroke. *Stroke* 2005; 36: 746–750.
 34. Arnould MC, Grandin CB, Peeters A, et al. Comparison of CT and three MR sequences for detecting and categorizing early (48 hours) hemorrhagic transformation in hyperacute ischemic stroke. *AJNR Am J Neuroradiol* 2004; 25: 939–944.
 35. Abilleira S, Cardona P, Ribó M, et al. Catalan Stroke Code and Reperfusion Consortium. Outcomes of a contemporary cohort of 536 consecutive patients with acute ischemic stroke treated with endovascular therapy. *Stroke* 2014; 45: 1046–1052.
 36. Nogueira RG, Gupta R, Jovin TG, et al. Predictors and clinical relevance of hemorrhagic transformation after endovascular therapy for anterior circulation large

- vessel occlusion strokes: a multicenter retrospective analysis of 1122 patients. *J Neurointerv Surg* 2015; 7: 16–21.
37. Yu S, Liebeskind DS, Dua S, et al. for UCLA Stroke Investigators. Postischemic hyperperfusion on arterial spin labeled perfusion MRI is linked to hemorrhagic transformation in stroke. *J Cereb Blood Flow Metab* 2015; 35: 630–637.
 38. Goyal M, Menon BK and Derdeyn CP. Perfusion imaging in acute ischemic stroke: let us improve the science before changing clinical practice. *Radiology* 2013; 266: 16–21.
 39. Kudo K, Sasaki M, Yamada K, et al. Differences in CT perfusion maps generated by different commercial software: quantitative analysis by using identical source data of acute stroke patients. *Radiology* 2010; 254: 200–209.
 40. Soares BP, Tong E, Hom J, et al. Reperfusion is a more accurate predictor of follow-up infarct volume than recanalization: a proof of concept using CT in acute ischemic stroke patients. *Stroke* 2010; 41: 34–40.

4.4

Study 4

Elevated glucose is associated with hemorrhagic transformation after mechanical thrombectomy in acute ischemic stroke patients with severe pretreatment hypoperfusion.



Elevated glucose is associated with hemorrhagic transformation after mechanical thrombectomy in acute ischemic stroke patients with severe pretreatment hypoperfusion

Carlos Laredo¹, Arturo Renú¹, Laura Llull¹, Raúl Tudela², Antonio López-Rueda³, Xabier Urrea¹, Napoleón G. Macías³, Salvatore Rudilosso¹, Víctor Obach¹, Sergio Amaro^{1✉} & Ángel Chamorro^{1✉}

Several pretreatment variables such as elevated glucose and hypoperfusion severity are related to brain hemorrhage after endovascular treatment of acute stroke. We evaluated whether elevated glucose and severe hypoperfusion have synergistic effects in the promotion of parenchymal hemorrhage (PH) after mechanical thrombectomy (MT). We included 258 patients MT-treated who had a pretreatment computed tomography perfusion (CTP) and a post-treatment follow-up MRI. Severe hypoperfusion was defined as regions with cerebral blood volume (CBV) values < 2.5% of normal brain [very-low CBV (VLCBV)-regions]. Median baseline glucose levels were 119 (IQR = 105–141) mg/dL. Thirty-nine (15%) patients had pretreatment VLCBV-regions, and 42 (16%) developed a PH after MT. In adjusted models, pretreatment glucose levels interacted significantly with VLCBV on the prediction of PH (p-interaction = 0.011). In patients with VLCBV-regions, higher glucose was significantly associated with PH (adjusted-OR = 3.15; 95% CI = 1.08–9.19, $p = 0.036$), whereas this association was not significant in patients without VLCBV-regions. CBV values measured at pretreatment CTP in coregistered regions that developed PH or infarct at follow-up were not correlated with pretreatment glucose levels, thus suggesting the existence of alternative deleterious mechanisms other than direct glucose-driven hemodynamic impairments. Overall, these results suggest that both severe hypoperfusion and glucose levels should be considered in the evaluation of adjunctive neuroprotective strategies.

Mechanical thrombectomy (MT) is the most effective treatment for stroke patients with acute large-vessel occlusions in the carotid territory^{1,2}. However, about half of MT-treated patients do not achieve an adequate clinical recovery at follow-up even despite complete recanalization^{1,2}. One of the pathophysiological processes that has been implicated in the lack of response to recanalization therapies is the risk of hemorrhagic transformation due to blood–brain barrier disruption^{3,4}. Indeed, among patients with anterior circulation stroke undergoing endovascular therapy, the presence of hemorrhagic transformation in follow-up neuroimaging, especially in the form of parenchymal hematomas (PH), has been associated with poor long term functional outcome^{5,6}.

¹Comprehensive Stroke Center, Department of Neuroscience, Hospital Clinic, University of Barcelona and August Pi i Sunyer Biomedical Research Institute (IDIBAPS), Villarroel 170, 08036 Barcelona, Spain. ²CIBER de Bioingeniería, Biomateriales y Nanomedicina (CIBER-BBN), Group of Biomedical Imaging of the University of Barcelona, Barcelona, Spain. ³Radiology Department, Hospital Clinic, Barcelona, Spain. ✉email: samaro@clinic.cat; achamorro@clinic.cat

The presence of PH in post-treatment neuroimaging occurs in 5 to 16% of acute stroke patients treated with MT and has been related with several pretreatment variables including severe hypoperfusion and hyperglycemia^{7,8}. The presence of brain regions with very low cerebral blood volume (VLCBV) in pretreatment computed tomography perfusion (CTP) has been consistently associated with the risk of hemorrhagic transformation although the sensitivity and positive predictive values of risk estimations are relatively low compared with its high specificity and negative predictive values^{9–11}. Accordingly, severe hypoperfusion might not be a sufficient risk factor for the occurrence of hemorrhagic transformation and additional concurrent susceptibility conditions might be needed, such as pretreatment hyperglycemia. The presence of hyperglycemia at stroke onset has been associated with a higher risk of hemorrhagic transformation after reperfusion therapies as well as with significant reductions on the benefits of MT^{4,12,13}. The potential mechanisms contributing to exacerbated neurovascular injury and poor outcomes are multifactorial and include augmented oxidative and nitrosative stress, tissue acidosis, mitochondrial dysfunction, thromboinflammation and impairment of cerebral perfusion, among others^{14,15}. However, in preclinical models the interaction between hyperglycemia and reduced cerebral blood volume or blood flow during ischemia and at reperfusion is controversial^{16–23}.

Herein, we aimed to evaluate whether elevated glucose levels modify the association between severe hypoperfusion and hemorrhagic transformation after MT and to describe whether this association might be explained by glucose-driven hemodynamic impairments before reperfusion.

Methods

Patients. Patients were part of a prospectively collected clinical registry of acute ischemic stroke patients treated with reperfusion therapies in a single Comprehensive Stroke Center. The study population included consecutive patients with occlusions in the carotid territory treated with endovascular recanalization therapy between March 2010 and December 2017. Additional inclusion criteria for this analysis were: 1/the availability of a technically adequate pretreatment whole-brain CTP scan, and 2/the availability of a post-treatment follow-up MRI for evaluating the development of hemorrhagic transformation. A total of 258 patients fulfilled these criteria and were finally included in the study (Supplementary Fig. S1 online). MT was performed according to contemporary guidelines in patients with a proximal artery occlusion on CT angiography and a pretreatment ASPECTS equal or higher than 6, as previously reported¹¹. Final vessel patency was graded on digital subtraction angiography (DSA) at the end of MT according to the modified Thrombolysis in Cerebral Infarction (TICI) score and successful recanalization was defined as a grade 2b–3. The study protocol was approved by the local Clinical Research Ethics Committee of Hospital Clinic de Barcelona (registration number HCB/2019/0805) under the requirements of Spanish legislation in the field of biomedical research, the protection of personal data (15/1999) and the standards of Good Clinical Practice, as well as with the 1964 Helsinki declaration and its later amendments or comparable ethical standards. Participants in the study consented for storage of their data in a local database for the purpose of research that was declared into a Web-based registry that satisfied all legal requirements for protection of personal data, for monitoring by the Catalan Health Department.

Patients were admitted into a Stroke Unit and the Trial of Org 10,172 in Acute Stroke Treatment (TOAST) criteria was used to classify all qualifying strokes after diagnostic workup. Clinical data was prospectively collected including: demographics, laboratory tests, risk factors, concomitant therapies, neuroimaging, clinical course and functional outcome. Neurological status was monitored with the National Institutes of Health Stroke Scale (NIHSS) score and functional outcome was quantified using the modified Rankin Scale (mRS) score at 3 months³.

CTP imaging analysis. Patients were scanned using a SIEMENS Somatom Definition Flash 128-section dual-source multidetector scanner (Siemens Healthineers, Erlangen, Germany), with a 98 mm z-coverage and a total acquisition time of 60 s (31 time points), as previously described¹¹. The imaging protocol included a baseline multimodal whole-brain CT scan, which included a Non-Contrast CT (NCCT), a CT angiography and a CTP. Pretreatment ASPECTS was assessed on NCCT, and good collaterals were defined as collateral supply filling > 50% of the occluded arterial territory²⁴. CTP maps were calculated by commercial software MISTar (Apollo Medical Imaging Technology, Melbourne, Australia) using a model-free singular value decomposition algorithm with a delay and dispersion correction. The software generates cerebral blood flow (CBF), cerebral blood volume (CBV), mean transit time (MTT) and Delay Time (DT) maps. An image processing pipeline using in-house fully-automated software running in Matlab (v.2017b, Mathworks, Natick, MA) was developed in order to extract perfusion volumes. An absolute threshold of 3 s was selected on the DT map to obtain the hypoperfused tissue (perfusion lesion)¹¹. Ischemic core was extracted on CBF maps after applying a threshold of relative CBF < 30%. VLCBV was defined as values on CBV maps lower than 2.5% of normal brain in the contralateral hemisphere with a volume of at least 1.5 mL¹¹.

Follow-up MRI. After MT, a follow-up MRI was performed within a median of 41 h (IQR 26–69 h) of hospital admission. The MRI included diffusion-weighted images and Gradient-Echo T2*-weighted sequences. The bleeding complications were scored on follow-up Gradient-Echo T2*-weighted sequences by 2 experienced stroke neurologists (A.R. and S.A.) according to the European Cooperative Acute Stroke Study criteria as hemorrhagic infarction (HI) and PH type 1 and type 2²⁵. In brief, PH1 was defined as bleeding ≤ 30% of the infarcted area with mild space-occupying effect, and PH2 as bleeding > 30% of the infarcted area, with space-occupying effect. Symptomatic intracranial hemorrhage was defined as any PHs associated with an increment of at least 4 points in the NIHSS score. Investigators blinded to clinical data and baseline CTP analysis evaluated in consensus the post-treatment imaging studies. To perform a CTP-MRI regions of interest analysis each CTP map was coregistered to the corresponding follow-up DWI using a rigid coregistration protocol (6-degrees of freedom) implemented with statistical parametric mapping (SPM12, Functional Imaging Laboratory, University College

Statistics. Continuous variables were reported as mean (standard deviation, SD) or median (interquartile range, IQR) and were compared with the Student *t* test, ANOVA, Mann–Whitney, or Kruskal–Wallis tests as appropriate. Categorical variables were compared with the χ^2 and Fisher exact tests. Univariate logistic regression models were used to assess the association between VLCBV-regions, glucose levels and their interaction on the risk of PH and with other predefined clinical endpoints. Multivariate logistic regression models were used to adjust the estimations for the effect of confounders based on exploratory analysis ($p < 0.05$ on univariate analysis) and avoidance of collinearity. A backwards-stepwise procedure was implemented to reach the final models constructed for assessing the role of pretreatment glucose levels on the risk of PH in subgroups defined by VLCBV regions in order to avoid overfitting. The Hosmer–Lemeshow goodness-of-fit statistic was used to assess final model fit. Receiver-operating characteristic (ROC) curve analysis was performed to determine the most accurate cutoff point (Youden's index) of pretreatment glucose levels for the prediction of PH. To evaluate the relationship between glucose levels and CBV values a set of regression models were used including linear, logarithmic, quadratic and cubic curve estimations. The analyses were performed using SPSS Version 22.0 and the level of significance was established at the 0.05 level (2-sided).

Results

Baseline traits of the included population according to PH occurrence. Overall, 258 patients with a median (IQR) NIHSS 17 (10–20) at admission and treated with MT within a median (IQR) of 231 (161–334) minutes from stroke onset were included in the study. Median (IQR) baseline glucose levels were 119 (105–141) mg/dL (6.6 mmol/L [5.8–7.8] mmol/L). Thirty-nine (15%) patients had pretreatment VLCBV-regions, and 42 (16%) developed a PH in follow-up neuroimaging [30 (12%) had PH1 and 12 (5%) had PH2]. Histograms showing the distribution of pretreatment glucose levels and the volume of regions with VLCBV are shown in the Supplementary Figure S2 online, and the baseline traits of the population according to the presence of VLCBV regions are shown in Supplementary Table 1. Table 1 provides descriptive data on baseline clinical and radiological variables associated with the occurrence of PH. In univariate analysis, PH was associated with a higher baseline stroke severity (NIHSS and ASPECTS score), a larger volume of ischemic tissue with VLCBV, a higher proportion of VLCBV regions, cardioembolic stroke etiology, as well as longer times from stroke onset to CTP acquisition, MT onset and successful recanalization. The presence of PH at follow-up was associated with increased odds for shifting to worse mRS score categories (OR 1.89, 95% CI 1.08–3.30, $p = 0.025$).

Predictors of PH in the whole population: multivariate analysis. In multivariate analyses, both the volume of ischemic tissue with VLCBV values and the presence of VLCBV regions were associated with an increased risk of PH (Table 2). Overall, the sensitivity, specificity, positive predictive value and negative predictive value of the presence of VLCBV regions for predicting the occurrence of PH were 31%, 88%, 33% and 87%, respectively. Additional variables that remained associated with PH were successful recanalization beyond 4.5 h from stroke onset and cardioembolic stroke etiology.

Glucose, VLCBV and risk of PH. In the whole population, glucose levels were not associated with the presence of PH. However, pretreatment glucose levels interacted significantly with VLCBV for the prediction of PH ($p = 0.011$). In patients with VLCBV-regions (see Supplementary Table 2 for subgroup descriptive variables), glucose levels were associated with an increased risk of PH (OR = 2.18 per IQR increase in glucose levels; 95% CI = 1.13–4.200, $p = 0.020$), whereas this association was not significant in patients without VLCBV-regions. The direction of these observations remained unchanged in multivariate models adjusted for the effect of confounders (Fig. 1). Neither glucose nor VLCBV interacted significantly with mTICI score at the end of MT ($p = 0.622$ and $p = 0.389$, respectively) or with time from stroke onset to successful recanalization on the prediction of PH ($p = 0.202$ and $p = 0.777$, respectively).

Figure 2 shows the adjusted predicted probabilities of the occurrence of a PH according to pretreatment glucose levels and VLCBV volume. In adjusted models, per IQR increase in glucose levels, the predicted probability of PH increased in 75% in patients with VLCBV regions (aOR = 3.07, 95% CI = 1.04–9.10, $p = 0.043$). According to ROC analysis, in the subset of patients with VLCBV regions the cutoff of pretreatment glucose levels with best accuracy for predicting the occurrence of PH was 116 mg/dL (6.4 mmol/L; sensitivity 69%, specificity 65%, positive predictive value 50% and negative predictive value 81%). According to this categorization, a total of 18 patients from 39 of those with VLCBV regions had elevated glucose levels. The observed rate of PH increased steadily from 13% (29 of 219) in patients without VLCBV regions, 19% (4 of 21) in those with VLCBV regions and low glucose levels (≤ 116 mg/dL, ≤ 6.4 mmol/L) and 50% (9 of 18) in patients with VLCBV regions and high glucose levels (> 116 mg/dL, > 6.4 mmol/L) (p for trend < 0.001).

Hemodynamic correlates of PH according to pretreatment glucose levels: CTP-MRI coregistered regions of interest analysis. As shown in Fig. 3A, brain regions that developed PH or infarct at follow-up had lower CBV values in pretreatment CTP compared with mirror regions of the unaffected hemisphere. In addition, CBV values measured at baseline in coregistered brain regions that developed PH or infarct at follow-up were not correlated with pretreatment glucose levels and were similar in patients with levels higher or lower than 116 mg/dL (6.4 mmol/L), as illustrated in Fig. 3B, C. Finally, the quality of reperfusion measured with the mTICI score at the end of MT was not associated with pretreatment glucose levels ($p = 0.952$).

	No PH N = 216	PH N = 42	p
Age (years), median (IQR)	72 (61–80)	67 (59–79)	0.481
Males, n (%)	106 (49)	26 (62)	0.128
Hypertension, n (%)	121 (56)	26 (62)	0.481
Diabetes, n (%)	31 (14)	5 (12)	0.675
Dyslipidemia, n (%)	83 (38)	15 (36)	0.740
Atrial Fibrillation, n (%)	59 (27)	16 (38)	0.159
Previous Antithrombotic treatment, n (%)	84 (39)	20 (48)	0.291
Baseline SBP (mmHg), median (IQR)	140 (125–158)	139 (125–158)	0.793
Glucose (mg/dL), median (IQR)	119 (105–141)	119 (107–143)	0.779
NIHSS at admission, median (IQR)	17 (10–20)	19 (14–21)	0.045
Ischemic core on CTP (mL), median (IQR)	19 (7–34)	18 (11–45)	0.273
Hypoperfused tissue on CTP (mL), median (IQR)	135 (98–186)	144 (99–198)	0.633
VLCBV (mL), median (IQR)	0.03 (0–0.31)	0.34 (0.03–2.07)	0.002
VLCBV regions, n (%)	26 (12)	13 (31)	0.002
Good collaterals, n (%)	158 (73)	27 (64)	0.243
Alteplase + MT, n (%)	116 (54)	25 (60)	0.488
Time to CTP (min), md (IQR)	148 (77–252)	242 (141–339)	0.001
Time to MT onset (min), md (IQR)	231 (161–334)	327 (230–425)	0.001
Recanalization (yes), n (%)	170 (79)	34 (81)	0.743
Time to recanalization (min), median (IQR)	270 (202–375)	359 (303–479)	0.001
Recanalization groups			0.002
Recanalization < 4.5 h, n (%)	86 (40)	6 (14)	
Recanalization > 4.5 h, n (%)	84 (39)	28 (67)	
No rec, n (%)	46 (21)	8 (19)	
Time to MRI (hours), md (IQR)	40 (26–65)	43 (24–69)	0.589
Cardioembolic origin, n (%)	103 (48)	27 (64)	0.049
Location of the occlusion			0.436
Tandem occlusions, n (%)	33 (15)	7 (17)	
ICA-T or M1, n (%)	169 (78)	30 (71)	
M2, n (%)	14 (7)	5 (12)	
Follow-up clinical variables			
Symptomatic ICH, n (%)	1 (1)	7 (17)	<0.001
mRS at 90 days, median (IQR)	2 (1–3)	3 (2–4)	0.019

Table 1. Demographics, baseline and procedure related variables according to the occurrence of parenchymal hematoma. *ASPECTS* Alberta Stroke Program Early CT Score, *CTP* computed tomographic perfusion, *ET* endovascular therapy, *ICA-T* internal carotid artery, *ICH* intracranial hemorrhage, *mRS* modified Rankin Scale, *MT* mechanical thrombectomy, *NIHSS* National Institutes of Health Stroke Scale, *PH* parenchymal hematoma, *SBP* systolic blood pressure, *VLCBV* very low cerebral blood volume.

Glucose, VLCBV and clinical outcome. The association of pretreatment glucose levels, VLCBV regions and their interactions with symptomatic hemorrhagic transformation, mRS at day 90 and mortality are shown in Table 3. Of note, the interaction between pretreatment glucose levels and the presence of VLCBV regions on the prediction of these clinical outcomes was not significant.

Discussion

In this study, we implemented a comprehensive CTP study to evaluate whether elevated glucose levels modified the association between severe hypoperfusion and PH after MT. In this cohort, elevated pretreatment glucose levels were associated with an increased risk of PH after MT in subjects with severe pretreatment hypoperfusion. Moreover, glucose levels were not associated with reduced CBV at pretreatment CTP in coregistered brain regions that developed PH or infarct at follow-up. Overall, these results suggest the existence of synergistic deleterious effects of severe pretreatment hypoperfusion and elevated glucose and give support to their consideration in the evaluation of adjunctive neuroprotective strategies.

In agreement with previous studies, the presence of regions with severe hypoperfusion was significantly associated with an increased risk of PH at follow-up neuroimaging^{9–11,26–29}. Beyond the severity of brain ischemia, a number of additional variables have been also associated with an increased risk of hemorrhagic transformation after MT, including an increased NIHSS score, poor collaterals, antiplatelet use, atrial fibrillation, older age or pretreatment hyperglycemia, among others⁶. As a novel finding of this study, we found that pretreatment glucose

PH at follow-up MRI	OR (95% CI); <i>p</i>	OR (95% CI); <i>p</i>
	Model A	Model B
VLCBV regions	2.816 (1.146–6.918), <i>p</i> = 0.024	1.592 (1.133–2.237), <i>p</i> = 0.007
Pretreatment glucose (per IQR)	1.049 (0.755–1.456), <i>p</i> = 0.777	1.072 (0.771–1.491), <i>p</i> = 0.678
Baseline NIHSS (per IQR)	1.337 (0.948–1.887), <i>p</i> = 0.098	1.260 (0.885–1.795), <i>p</i> = 0.200
Rescue MT (vs primary)	1.395 (0.668–2.916), <i>p</i> = 0.376	1.415 (0.674–2.971), <i>p</i> = 0.359
Recanalization status		
> 4'5 h from stroke onset (vs < 4'5 h)	6.656 (2.444–18.130), <i>p</i> < 0.001	7.552 (2.745–20.779), <i>p</i> < 0.001
No recanalization (vs < 4'5 h)	2.848 (0.867–9.351), <i>p</i> = 0.084	2.810 (0.865–9.132), <i>p</i> = 0.086
Cardioembolic etiology (vs no)	2.584 (1.197–5.577), <i>p</i> = 0.016	2.812 (1.285–6.153), <i>p</i> = 0.010
Sex (females vs males)	0.500 (0.228–1.097), <i>p</i> = 0.084	0.522 (0.237–1.150), <i>p</i> = 0.107
Good collaterals (vs poor)	1.256 (0.550–2.867), <i>p</i> = 0.588	1.369 (0.599–3.129), <i>p</i> = 0.456

Table 2. Predictors of parenchymal hematoma: multivariate analysis. Very low cerebral blood volume (VLCBV) was included as a dichotomic variable (yes vs no) in model A, and as a continuous quantitative variable (estimations per IQR of VLCBV increase) in model B. MT: Mechanical thrombectomy; NIHSS: National Institutes of Health Stroke Scale; PH: parenchymal hematoma. The Hosmer–Lemeshow test showed an adequate goodness-of-fit of the final models (Model A: $X^2 = 4.028$, $p = 0.855$; Model B: $X^2 = 9.329$, $p = 0.315$), and the models classified correctly a total of 84% (Model A) and 85% (Model B) of cases.

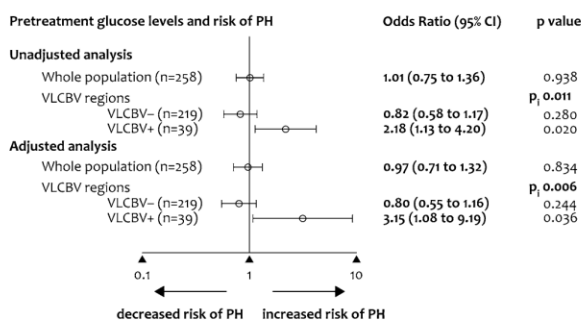


Figure 1. Binary regression models for predicting the occurrence of parenchymal hematoma (PH) in follow-up MRI. *P* is the *p* value for the interaction between pretreatment glucose levels and the presence of very low cerebral blood volume (VLCBV) regions for the prediction of PH. Data are OR and 95% CI per IQR increase in glucose levels obtained by unadjusted models and in models adjusted for pretreatment NIHSS, recanalization and cardioembolic stroke etiology (see Supplemental Table 3 for full models).

levels interacted significantly with severe hypoperfusion on the prediction of PH. Thus, in patients with regions of VLCBV, higher pretreatment glucose levels increased significantly the risk of PH, while this association was not significant in patients without VLCBV regions. Indeed, about 1 in 5 patients with VLCBV regions and low pretreatment glucose levels at baseline developed a PH in follow-up neuroimaging, whereas this rate increased to 1 in 2 patients with concurrent high glucose levels. The consideration of pretreatment glucose in addition to the presence of VLCBV regions resulted in higher positive predictive value for the prediction of PH in comparison with VLCBV alone. From a practical point of view, the combination of these biomarkers could be useful in the evaluation of strategies aimed to protect the blood–brain barrier in this patient population as patients with regions of severe ischemia and elevated pretreatment glucose levels may represent a target population for the early implementation of preventive strategies. These strategies could theoretically include a tighter control of blood pressure, the avoidance of early post-treatment aggressive antithrombotic therapy or the addition of adjunctive neuroprotective or vasculoprotective therapies. Of these potential treatments, the implementation of strategies focused in lowering glucose concentrations and achieving a tight glucose control in the early acute phase have been repeatedly unsuccessful in humans regardless of preventing lactic acidosis^{30–32}. Contrarily, preliminary data from preclinical and clinical studies support that the enhancement of antioxidant exposure in combination with reperfusion therapies could minimize the toxicity of hyperglycemia³³. Importantly, given the strong clinical benefits of MT, the presence of regions of severe reductions of CBV in CTP and concurrent hyperglycemia should not preclude the treatment of patients otherwise eligible for receiving endovascular reperfusion therapies.

In experimental models of brain ischemia, hyperglycemia exacerbates ischemic brain injury by increasing infarct size, brain swelling and blood–brain barrier disruption^{34–37}. Several preclinical studies have shown a direct association between induced hyperglycemia and poorer perfusion metrics during ischemia and after reperfusion

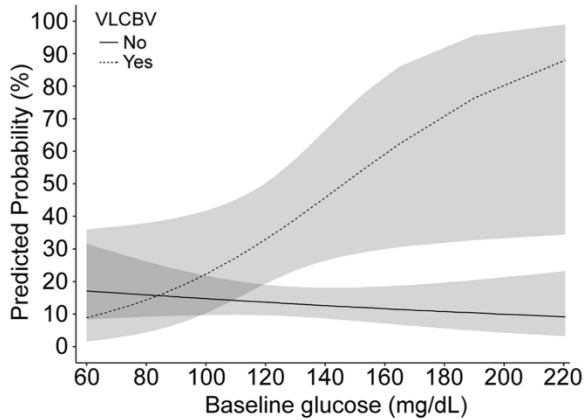


Figure 2. Predicted probability of parenchymal hematoma (PH) at follow-up MRI. Predicted probability of parenchymal hematoma (PH) at follow-up MRI by pretreatment glucose levels according to subgroups defined by the presence or absence of very low cerebral blood volume (VLCBV) regions. Dashed lines show the 95% CI. For graphical purposes, pretreatment glucose was analyzed as a continuous variable. The predicted probabilities were obtained in models adjusted for baseline NIHSS, reperfusion treatment modality, recanalization and stroke etiology.

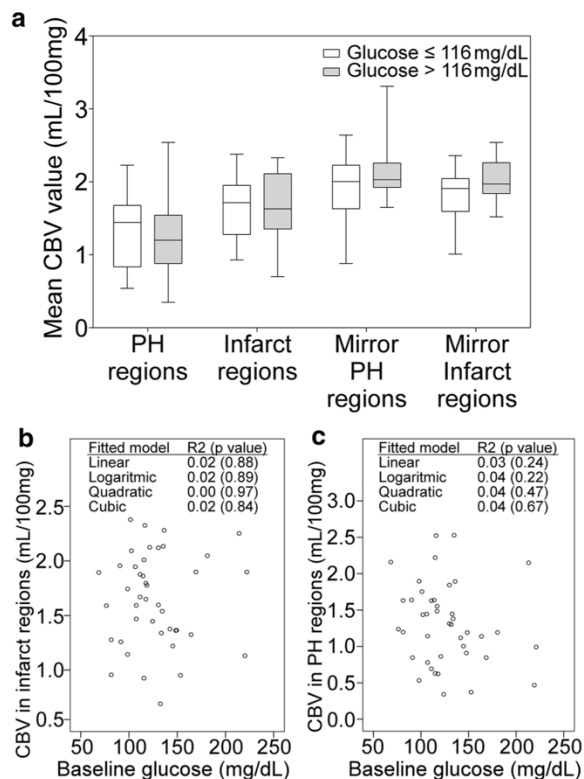


Figure 3. Cerebral blood volume values measured at pretreatment CTP in coregistered brain regions that developed PH or infarct at follow-up. (a) Box-whisker plots of cerebral blood volume (CBV) values extracted from pretreatment computed tomographic perfusion (CTP) in coregistered regions that developed infarct or parenchymal hematoma (PH) at follow-up according to the presence or absence of pretreatment glucose levels higher than 116 mg/dL (6.4 mmol/L). (b, c) Association between baseline glucose levels and CBV values extracted from pretreatment CTP in coregistered regions that developed infarct (b) or PH (c) at follow-up MRI.

	Pretreatment glucose (per IQR increase)	VLCBV regions (yes vs no)	Pi
mRS shift at 90 days	1.310 (1.091–1.587), p=0.006	1.587 (0.887–2.838), p=0.120	0.562
Symptomatic ICH	0.804 (0.424–1.525), p=0.504	0.797 (0.095–6.663), p=0.834	0.998
Mortality at 90 days	0.990 (0.612–1.603), p=0.968	0.932 (0.200–4.338), p=0.929	0.751

Table 3. Association of pretreatment glucose levels and VLCBV with clinical endpoints. Odds ratios, 95% confidence intervals and p values per IQR increase in pretreatment glucose levels (second column) and according to the presence of very low cerebral blood volume (VLCBV) regions (third column) obtained through unadjusted logistic regression analysis. Pi values (fourth column) are the p values for the interaction between pretreatment glucose levels and the presence of VLCBV regions on each of the evaluated clinical outcomes. *ICH* intracranial hemorrhage, *mRS* modified Rankin Scale.

whereas others were not able to identify such relationship^{16–23}. In this study, pretreatment CBV values were not correlated with pretreatment glucose levels and were similar in patients with levels higher or lower than 116 mg/dL (6.4 mmol/L), regardless of the presence of successful recanalization. In addition, the quality of reperfusion obtained at the end of MT was not associated with pretreatment glucose levels, in agreement with findings from a recent meta-analysis that included pooled-data of the pivotal thrombectomy trials¹³. Overall, our results support the relevance of additional pathophysiological mechanisms beyond hyperacute glucose-driven disturbances in cerebral perfusion to explain the association between hyperglycemia and severe hypoperfusion with the risk of PH, such as enhanced thromboinflammatory mechanisms, increased blood–brain barrier disruption and worse cytotoxic injury, among others^{15,36,37}.

The main strength of the study was the use of whole-brain CTP that allowed obtaining perfusion measures of most of the affected brain tissue. Moreover, patients were collected consecutively and managed following a homogeneous therapeutic protocol. The management of hyperglycemia in the acute phase followed the recommendations of contemporary guidelines recommending the administration of insulin in patients with glucose concentrations > 140 mg/dL (7.8 mmol/L). Furthermore, although the sensitivity of MRI to detect hemorrhagic transformation is higher than CT, we do not think this is likely to have significantly affected our result because the imaging modality used for the attribution of the main outcome variable (PH) was identical (gradient-recall echo MRI sequence) in all the study population thus avoiding biases related to the use of different modalities (CT or MRI). Nonetheless, the study has several limitations. First, the assessment of perfusion with dynamic CT in acute stroke is a static evaluation of a multifaceted and time-dependent process. Secondly, perfusion measures may be affected by multiple factors, including acquisition protocols, brain coverage and post-processing platforms, and therefore our results may apply to the protocol of acquisition and analysis that were employed in these series and may not be generalizable to other methodologies. In this study, we used the European Cooperative Acute Stroke Study criteria for qualifying the type of hemorrhagic transformations to allow direct comparisons with previously reported studies on the same matter. Further validation of these results using the new Heidelberg Bleeding Classification specially for assessing the effect of hyperglycemia and severe hypoperfusion on the risk of symptomatic hemorrhagic transformation is warranted³⁸. An additional limitation includes the lack of information on the longitudinal course of glucose at follow up and the undocumented use of blood glucose lowering drugs. Finally, the results were not controlled by type of stroke onset (witnessed versus unwitnessed) or pre-stroke fasting status, as those variables were not registered. Of note, given the retrospective nature of the study no causality assumptions can be inferred from the obtained data.

Conclusions

In summary, this study shows that elevated pretreatment glucose levels were associated with an increased risk of parenchymal hematoma after endovascular reperfusion therapy of acute ischemic stroke in patients with severe pretreatment hypoperfusion. Moreover, the link between pretreatment glucose levels and severe hypoperfusion was not explained by an association of glucose with reduced CBV during ischemia and prior to reperfusion, thus suggesting alternative deleterious mechanisms other than direct glucose-driven hemodynamic impairment. These two factors should be considered in the evaluation of adjunctive neuroprotective strategies aimed to protect the blood–brain barrier in addition to early and complete recanalization.

Data availability

The datasets analyzed during the current study are available from the corresponding author on reasonable request.

Received: 15 November 2019; Accepted: 4 May 2020

Published online: 29 June 2020

References

1. Saver, J. L. *et al.* Time to treatment with endovascular thrombectomy and outcomes from ischemic stroke: A meta-analysis. *JAMA* **316**, 1279 (2016).
2. Goyal, M. *et al.* Endovascular thrombectomy after large-vessel ischaemic stroke: A meta-analysis of individual patient data from five randomised trials. *Lancet* **387**, 1723–1731 (2016).

3. Renú, A. *et al.* Relevance of blood–brain barrier disruption after endovascular treatment of ischemic stroke. *Stroke* **46**, 673–679 (2015).
4. Khatri, P., Wechsler, L. R. & Broderick, J. P. Intracranial hemorrhage associated with revascularization therapies. *Stroke* **38**, 431–440 (2007).
5. Lee, Y. B. *et al.* Predictors and impact of hemorrhagic transformations after endovascular thrombectomy in patients with acute large vessel occlusions. *J. Neurointerv. Surg.* **11**, 469–473 (2019).
6. Hao, Y. *et al.* Predictors for symptomatic intracranial hemorrhage after endovascular treatment of acute ischemic stroke. *Stroke* **48**, 1203–1209 (2017).
7. Raychev, R. *et al.* The impact of general anesthesia, baseline ASPECTS, time to treatment, and IV tPA on intracranial hemorrhage after neurothrombectomy: Pooled analysis of the SWIFT PRIME, SWIFT, and STAR trials. *J. Neurointerv. Surg.* **12**, 2–6 (2020).
8. van Kranendonk, K. R. *et al.* Clinical and imaging markers associated with hemorrhagic transformation in patients with acute ischemic stroke. *Stroke* **50**, 2037–2043 (2019).
9. Rai, A. T., Raghuram, K., Carpenter, J. S., Domico, J. & Hobbs, G. Pre-intervention cerebral blood volume predicts outcomes in patients undergoing endovascular therapy for acute ischemic stroke. *J. Neurointerv. Surg.* **5**, i25–i32. <https://doi.org/10.1136/neurintsurg-2012-010293> (2013).
10. Bhatt, A. *et al.* Lower pretreatment cerebral blood volume affects hemorrhagic risks after intra-arterial revascularization in acute stroke. *Neurosurgery* **63**, 874–879 (2008).
11. Renú, A. *et al.* Brain hemorrhage after endovascular reperfusion therapy of ischemic stroke: a threshold-finding whole-brain perfusion CT study. *J. Cereb. Blood Flow Metab.* **37**, 153–165 (2017).
12. Natarajan, S. K. *et al.* Prediction of adverse outcomes by blood glucose level after endovascular therapy for acute ischemic stroke. *J. Neurosurg.* **114**, 1785–1799 (2011).
13. Chamorro, Á. *et al.* Glucose modifies the effect of endovascular thrombectomy in patients with acute stroke. *Stroke* **50**, 690–696 (2019).
14. Hafez, S., Coucha, M., Bruno, A., Fagan, S. C. & Ergul, A. Hyperglycemia, acute ischemic stroke, and thrombolytic therapy. *Transl. Stroke Res.* **5**, 442–453 (2014).
15. Desilles, J.-P. *et al.* Exacerbation of thromboinflammation by hyperglycemia precipitates cerebral infarct growth and hemorrhagic transformation. *Stroke* **48**, 1932–1940 (2017).
16. Kawai, N., Keep, R. F. & Betz, A. L. Hyperglycemia and the vascular effects of cerebral ischemia. *Stroke* **28**, 149–154 (1997).
17. Nakai, H., Yamamoto, Y. L., Diksic, M., Worsley, K. J. & Takara, E. Triple-tracer autoradiography demonstrates effects of hyperglycemia on cerebral blood flow, pH, and glucose utilization in cerebral ischemia of rats. *Stroke* **19**, 764–772 (1988).
18. Quast, M. J. *et al.* Perfusion deficit parallels exacerbation of cerebral ischemia/reperfusion injury in hyperglycemic rats. *J. Cereb. Blood Flow Metab.* **17**, 553–559 (1997).
19. Duckrow, R. B., Beard, D. C. & Brennan, R. W. Regional cerebral blood flow decreases during chronic and acute hyperglycemia. *Stroke* **18**, 52–58 (1987).
20. Ginsberg, M. D., Welsh, F. A. & Budd, W. W. Deleterious effect of glucose pretreatment on recovery from diffuse cerebral ischemia in the cat. I. Local cerebral blood flow and glucose utilization. *Stroke* **11**, 347–354 (1980).
21. Venables, G. S., Miller, S. A., Gibson, G., Hardy, J. A. & Strong, A. J. The effects of hyperglycaemia on changes during reperfusion following focal cerebral ischaemia in the cat. *J. Neurol. Neurosurg. Psychiatry* **48**, 663–669 (1985).
22. Wagner, K. R., Kleinholz, M., de Courten-Myers, G. M. & Myers, R. E. Hyperglycemic versus normoglycemic stroke: Topography of brain metabolites, intracellular pH, and infarct size. *J. Cereb. Blood Flow Metab.* **12**, 213–222 (1992).
23. Gisselsson, L., Smith, M.-L. & Siesjö, B. K. Hyperglycemia and focal brain ischemia. *J. Cereb. Blood Flow Metab.* **19**, 288–297 (1999).
24. Tan, I. Y. L. *et al.* CT angiography clot burden score and collateral score: correlation with clinical and radiologic outcomes in acute middle cerebral artery infarct. *AJNR. Am. J. Neuroradiol.* **30**, 525–531 (2009).
25. Hacke, W. *et al.* Randomised double-blind placebo-controlled trial of thrombolytic therapy with intravenous alteplase in acute ischaemic stroke (ECASS II). Second European-Australasian Acute Stroke Study Investigators. *Lancet* **352**, 1245–1251 (1998).
26. Campbell, B. C. V. *et al.* Regional very low cerebral blood volume predicts hemorrhagic transformation better than diffusion-weighted imaging volume and thresholded apparent diffusion coefficient in acute ischemic stroke. *Stroke* **41**, 82–88 (2010).
27. Campbell, B. C. V. *et al.* Advanced imaging improves prediction of hemorrhage after stroke thrombolysis. *Ann. Neurol.* **73**, 510–519 (2013).
28. Hermitte, L. *et al.* Very low cerebral blood volume predicts parenchymal hematoma in acute ischemic stroke. *Stroke* **44**, 2318–2320 (2013).
29. Yassi, N. *et al.* Prediction of poststroke hemorrhagic transformation using computed tomography perfusion. *Stroke* **44**, 3039–3043 (2013).
30. Gray, C. S. *et al.* Glucose-potassium-insulin infusions in the management of post-stroke hyperglycaemia: the UK Glucose Insulin in Stroke Trial (GIST-UK). *Lancet. Neurol.* **6**, 397–406 (2007).
31. McCormick, M. *et al.* Randomized, controlled trial of insulin for acute poststroke hyperglycemia. *Ann. Neurol.* **67**, 570–578 (2010).
32. Johnston, K. C. *et al.* Intensive vs standard treatment of hyperglycemia and functional outcome in patients with acute ischemic stroke: The SHINE randomized clinical trial. *JAMA* **322**, 326–335 (2019).
33. Amaro, S. *et al.* Uric acid improves glucose-driven oxidative stress in human ischemic stroke. *Ann. Neurol.* **77**, 775–783 (2015).
34. Martini, S. R. & Kent, T. A. Hyperglycemia in acute ischemic stroke: A vascular perspective. *J. Cereb. Blood Flow Metab.* **27**, 435–451 (2007).
35. Suh, S. W. *et al.* Glucose and NADPH oxidase drive neuronal superoxide formation in stroke. *Ann. Neurol.* **64**, 654–663 (2008).
36. Kamada, H., Yu, F., Nito, C. & Chan, P. H. Influence of hyperglycemia on oxidative stress and matrix metalloproteinase-9 activation after focal cerebral ischemia/reperfusion in rats: Relation to blood–brain barrier dysfunction. *Stroke* **38**, 1044–1049 (2007).
37. Bevers, M. B., Vaishnav, N. H., Pham, L., Battey, T. W. & Kimberly, W. T. Hyperglycemia is associated with more severe cytotoxic injury after stroke. *J. Cereb. Blood Flow Metab.* **37**, 2577–2583 (2017).
38. Neuberger, U. *et al.* Classification of bleeding events. *Stroke* **48**, 1983–1985 (2017).

Acknowledgements

This work was partially developed at the building Centro Esther Koplowitz, Barcelona, CERCA Programme / Generalitat de Catalunya. We thank the support of the Spanish Ministry of Economy and Competitiveness for grant to Dr. Sergio Amaro (PI13/01268 and PI16/00711, funded as part of the Plan Nacional R+D+I and cofinanced by ISCIII-Subdirección General de Evaluación and by the FEDER) and to Angel Chamorro (RETICS-INVICTUS R012/0014, funded by the Spanish Ministry of Economy and Competence). Carlos Laredo receives funding from ISCIII, with a Predoctoral Grant for Health Research (PFIS, FI16/00231).

Author contributions

C.L. obtained the imaging data, implemented the post-processing of the images and performed the statistical analysis. AR, XU, LLI and SR obtained the clinical data. A.R., R.T., A.L.R. and N.G.M. supervised the neuroimage

post-processing and analysis. C.L., A.R., R.T., X.U., L.L.L., S.R., V.O., S.A. and A.C. revised the article critically for intellectual content. SA and AC designed the study, interpreted the data and wrote the final draft of the manuscript.

Competing interests

The authors declare no competing interests.

Additional information

Supplementary information is available for this paper at <https://doi.org/10.1038/s41598-020-67448-x>.

Correspondence and requests for materials should be addressed to S.A. or Á.C.

Reprints and permissions information is available at www.nature.com/reprints.

Publisher's note Springer Nature remains neutral with regard to jurisdictional claims in published maps and institutional affiliations.



Open Access This article is licensed under a Creative Commons Attribution 4.0 International License, which permits use, sharing, adaptation, distribution and reproduction in any medium or format, as long as you give appropriate credit to the original author(s) and the source, provide a link to the Creative Commons license, and indicate if changes were made. The images or other third party material in this article are included in the article's Creative Commons license, unless indicated otherwise in a credit line to the material. If material is not included in the article's Creative Commons license and your intended use is not permitted by statutory regulation or exceeds the permitted use, you will need to obtain permission directly from the copyright holder. To view a copy of this license, visit <http://creativecommons.org/licenses/by/4.0/>.

© The Author(s) 2020

Supplementary Information

Title: Elevated glucose is associated with hemorrhagic transformation after mechanical thrombectomy in patients with severe pretreatment hypoperfusion.

Authors: Carlos Laredo,¹ Arturo Renú,¹ Laura Llull,¹ Raúl Tudela,² Antonio Lopez-Rueda,³ Xabier Urrea,¹ Napoleón G Macías,³ Salvatore Rudilosso,¹ Víctor Obach,¹ Sergio Amaro*,¹ Ángel Chamorro*.¹

Affiliations

¹ Comprehensive Stroke Center, Department of Neuroscience, Hospital Clinic, University of Barcelona and August Pi i Sunyer Biomedical Research Institute (IDIBAPS), Barcelona, Spain.

² CIBER de Bioingeniería, Biomateriales y Nanomedicina (CIBER-BBN), Group of Biomedical Imaging of the University of Barcelona, Barcelona, Spain.

³ Radiology Department, Hospital Clinic, Barcelona, Spain.

Corresponding authors*: Sergio Amaro and Angel Chamorro; Hospital Clinic, Villarroel 170, 08036 Barcelona, Spain. Email: samaro@clinic.cat and achamorro@clinic.cat; Tel.: +34932275414; fax: +34932275783.

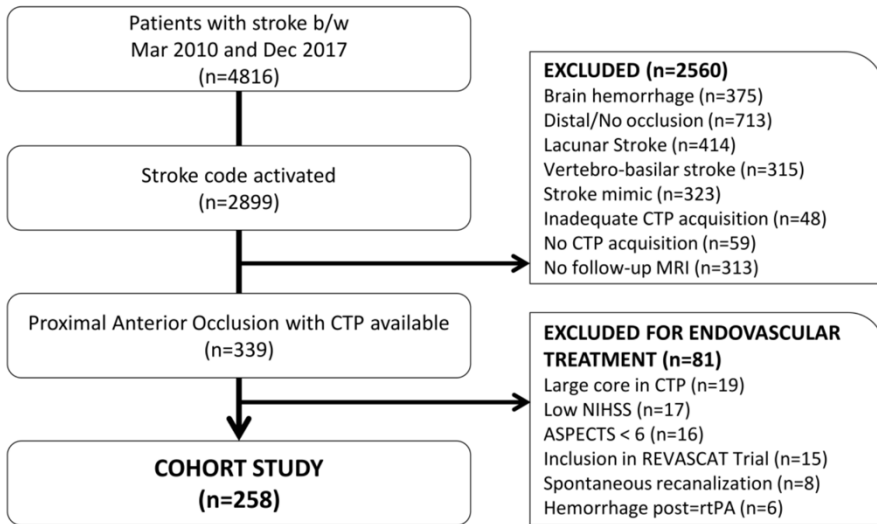
Supplementary methods

CTP imaging and follow-up MRI parameters

Patients were scanned using a SIEMENS Somatom Definition Flash 128-section dual-source multidetector scanner (Siemens Healthcare, Erlangen, Germany), with a 98mm z-coverage and a total acquisition time of 60s (31 time points). The imaging protocol included a baseline multimodal whole-brain CT scan, which included a Non-Contrast CT (NCCT) (140Kv, 127mAs, FoV 225mm, matrix 512x512, slice thickness 5mm), a CT angiography (120Kv, 663mAs, FoV 261mm, matrix 512x512, slice thickness 0,6mm), and a CTP. For CTP acquisition, a total of fifty milliliters of nonionic iodinated contrast was administered intravenously at 5 mL/s by using a power injector, followed by a saline flush of 20ml at an injection rate of 2ml/s. CTP imaging parameters were 80 kV(peak), 250 mAs, 1.5-second rotation, FoV 18mm, matrix 512x512, and 2-mm thickness (49 slices in total). The follow-up MRI included diffusion-weighted images (DWI, parameters: Repetition time (TR)/echo time (TE) 10800/89ms, matrix 192x192, Field of View (FoV) 240mm, slice thickness 3mm, directions x,y,z, b-values: 0 and 1000 mm/s²) and Gradient-Echo T2*-weighted (GRE: TR/TE 764/26 ms; matrix 384x512 ; FoV 240 mm ; slice thickness 5 mm) sequences.

Supplementary Figure S1

Flow chart of the study.



Supplementary Figure S2

Distribution of pretreatment glucose concentration and Very Low CBV regions.

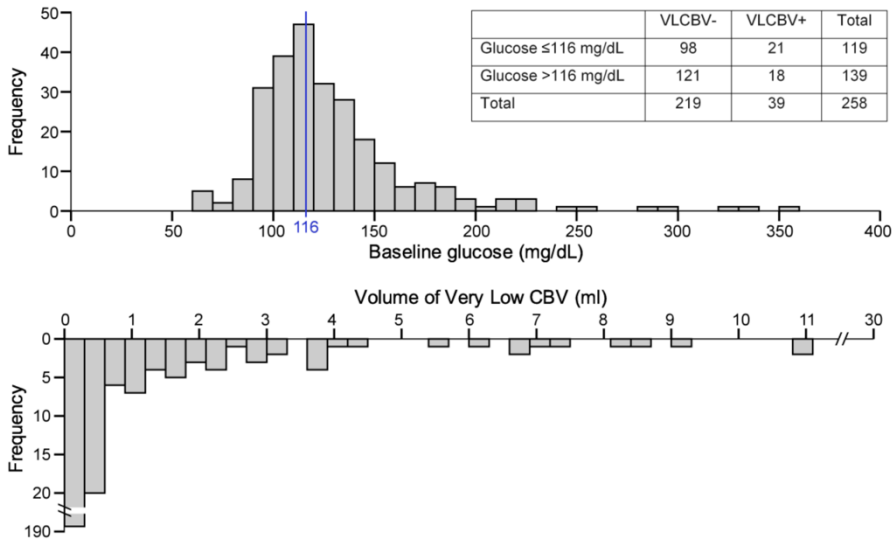


Figure legend: Histograms showing the distribution of pretreatment glucose levels, the volume of regions with very low cerebral blood volume (VLCBV) and the number of patients in categories defined by the presence of VLCBV regions and glucose levels higher or lower than 116 mg/dL.

Supplementary Table 1

Demographics, baseline and procedure related variables according to the presence of Very Low Cerebral Blood Volume regions.

	VLCBV - N=219	VLCBV + N=39	p
Age (years), median (IQR)	72 (61-80)	67 (56-81)	0.216
Males, n (%)	102 (47)	30 (77)	<0.001
Hypertension, n (%)	123 (56)	24 (62)	0.532
Diabetes, n (%)	34 (16)	2 (5)	0.084
Dyslipidemia, n (%)	83 (38)	15 (39)	0.947
Atrial Fibrillation, n (%)	62 (28)	13 (33)	0.524
Previous Antithrombotic treatment, n (%)	85 (39)	19 (49)	0.245
Baseline SBP (mmHg), median (IQR)	142 (125-160)	135 (125-150)	0.178
Glucose (mg/dL), median (IQR)	120 (106-142)	116 (93-134)	0.088
NIHSS at admission, median (IQR)	16 (10-20)	18 (15-21)	0.049
Ischemic core on CTP (mL), median (IQR)	15 (7-27)	54 (43-72)	<0.001
Hypoperfused tissue on CTP (mL), median (IQR)	129 (87-169)	203 (153-234)	<0.001
Good collaterals, n (%)	166 (76)	19 (49)	0.001
Alteplase + MT, n (%)	105 (48)	12 (31)	0.047
Recanalization (yes), n (%)	174 (80)	30 (77)	0.721
Time to recanalization (min), median (IQR)	291 (205-395)	288 (210-405)	0.851
Recanalization groups			0.922
Recanalization <4.5h, n (%)	78 (36)	14 (36)	
Recanalization >4.5h, n (%)	96 (44)	16 (41)	
No rec, n (%)	45 (21)	9 (23)	
Time to MRI (hours), md (IQR)	40 (26-67)	41 (27-70)	0.971
Cardioembolic origin, n (%)	107 (49)	23 (59)	0.244
Location of the occlusion			0.336
Tandem occlusions, n (%)	31 (14)	9 (23)	
ICA-T or M1, n (%)	171 (78)	28 (72)	
M2, n (%)	17 (8)	2 (5)	

ASPECTS: Alberta Stroke Program Early CT Score; CTP: computed tomographic perfusion; ET: endovascular therapy; ICA-T: internal carotid artery; MT: Mechanical Thrombectomy; NIHSS: National Institutes of Health Stroke Scale; SBP: systolic blood pressure; VLCBV: very low cerebral blood volume.

Supplementary Table 2

Demographics, baseline and procedure related variables according to the occurrence of parenchymal hematoma in patients with Very Low Cerebral Blood Volume regions.

	No PH N=26	PH N=13	p
Age (years), median (IQR)	68 (53-81)	63 (57-76)	0.918
Males, n (%)	20 (77)	10 (77)	1.000
Hypertension, n (%)	12 (46)	3 (23)	0.163
Diabetes, n (%)	1 (4)	1 (8)	1.000
Dyslipidemia, n (%)	10 (39)	5 (39)	1.000
Atrial Fibrillation, n (%)	7 (27)	6 (46)	0.290
Previous Antithrombotic treatment, n (%)	10 (39)	9 (69)	0.070
Baseline SBP (mmHg), median (IQR)	135 (125-149)	135 (125-155)	0.965
Glucose (mg/dL), median (IQR)	109 (91-127)	133 (116-150)	0.023
NIHSS at admission, median (IQR)	18 (14-19)	21 (19-23)	0.010
Ischemic core on CTP (mL), median (IQR)	57 (48-72)	53 (32-65)	0.308
Hypoperfused tissue on CTP (mL), median (IQR)	204 (164-229)	198 (143-264)	0.872
VLCBV (mL), median (IQR)	3.8 (2.3-7.3)	3.0 (2.2-7.1)	0.941
Good collaterals, n (%)	14 (54)	5 (39)	0.365
Alteplase + MT, n (%)	19 (73)	8 (62)	0.486
Recanalization (yes), n (%)	20 (77)	10 (77)	1.000
Time to recanalization (min), median (IQR)	270 (216-373)	360 (290-435)	0.087
Recanalization groups			0.117
Recanalization <4.5h, n (%)	12 (46)	2 (15)	
Recanalization >4.5h, n (%)	8 (31)	8 (62)	
No rec, n (%)	6 (23)	3 (23)	
Time to MRI (hours), md (IQR)	41 (28-70)	41 (26-75)	0.987
Cardioembolic origin, n (%)	15 (58)	8 (62)	0.818
Location of the occlusion			0.663
Tandem occlusions, n (%)	7 (27)	2 (15)	
ICA-T or M1, n (%)	18 (69)	10 (77)	
M2, n (%)	1 (4)	1 (8)	

ASPECTS: Alberta Stroke Program Early CT Score; CTP: computed tomographic perfusion; ET: endovascular therapy; ICA-T: internal carotid artery; MT: Mechanical Thrombectomy; NIHSS: National Institutes of Health Stroke Scale; SBP: systolic blood pressure; VLCBV: very low cerebral blood volume.

Supplementary Table 3**Adjusted multivariate models for the prediction of parenchymal hematoma in the whole population and in subgroups defined by the presence of VLCBV regions.**

	Whole population	VLCBV -	VLCBV +
	OR 95%CI p value	OR 95%CI p value	OR 95%CI p value
Pretreatment glucose (per IQR)	0.97 (0.71-1.32) p=0.834	0.80 (0.55-1.16) p=0.244	3.15 (1.08-9.19) p=0.036
Baseline NIHSS (per IQR)	1.42 (1.02-1.96) p=0.037	1.18 (0.81-1.70) p=0.394	2.23 (0.71-7.29) p=0.165
Recanalization >4'5h from stroke onset (vs <4'5h)	5.24 (2.03-13.51) p=0.001	1.18 (0.81-1.70) p=0.394	18.0 (1.28-252.70) p=0.032
No recanalization (vs <4'5h)	2.51 (0.81-7.80) p=0.112	2.38 (0.60-9.47) p=0.220	2.51 (0.16-40.10) p=0.516
Cardioembolic etiology (vs no)	2.12 (1.04-4.32) p=0.039	2.10 (0.90-4.87) p=0.085	0.94 (0.11-7.94) p=0.951

VLCBV: Very low cerebral blood volume; NIHSS: National Institutes of Health Stroke Scale; PH: parenchymal hematoma. The Hosmer–Lemeshow test showed an adequate goodness-of-fit of the three models (p>0.05 for all).

5. DISCUSSION



Ischemic core volume measured on baseline non-contrast CT, MRI-DWI or CTP is now widely used as a selection criterion for the administration of reperfusion therapies and has become a tool to aid decision making in acute stroke treatment mainly in the extended (beyond 6 hours after last known well) time window [32, 33].

There have been shown strong correlations between CTP-derived ischemic core volume estimation with both final infarct volume and clinical outcome [34, 62-65, 69, 73, 74, 77-81, 85, 86, 92, 120]. However, a number of pretreatment and treatment-related variables, including baseline imaging features and acute reperfusion treatment modality, have been extensively proved to modify the performance of CTP for final infarct prediction [60, 65, 69, 70, 71, 73, 74, 87-95]. In this context, the first study of the thesis was focused on delineating the effect of time from onset to recanalization on the accuracy of CTP-predicted infarct core. In that study, we analyzed a cohort of 104 patients achieving complete recanalization after mechanical thrombectomy who had a pretreatment CTP and a 24-h follow-up MRI-DWI. We explored a range of absolute and relative CTP thresholds in perfusion maps at constant increments for ischemic core calculation and we found that time to recanalization modified significantly the association between ischemic core and DWI lesion in a non-linear fashion. The intraclass correlation coefficient values and spatial lesion agreement between CTP-predicted infarct core and DWI lesion were significantly lower in patients with recanalization before 4.5 hours from symptom onset than those with latter recanalization time. We also found that the significance of the associations between CTP-derived infarct core and clinical outcome at 90 days was lost in patients recanalized before 4.5 h. Overall, these results reinforce and expand previous observations supporting the dependency of optimal CTP thresholds on time to recanalization and the notion that CBF thresholds for tissue infarction should be more restrictive in patients with shorter time from stroke onset to reperfusion [69, 78-84]. Beyond the differences in CTP acquisition and post-processing protocols that were used in these previous works, we limited the study to a highly homogeneous stroke population consisting in patients that achieved full reperfusion at the end of MT thus minimizing the risk of evolving infarct growth from the end of MT to follow-up MRI secondary to non-complete recanalization. Moreover, as a novel approach,

we modeled the relationship between time to recanalization and CTP-DWI volumetric differences through curve estimation analyses across different perfusion parameters and thresholds and we also explored their impact on long-term clinical outcome. Indeed, in contraposition with previous published data and according to intraclass correlation coefficient analyses [78-81], in patients with earlier recanalization, the reliability of CTP for the prediction of final infarct volume was only moderate; even using more restrictive perfusion thresholds and ischemic core predicted values tended towards the overestimation of irreversible tissue injury. Furthermore, in the subgroup of patients with earlier and complete recanalization, the significance of the association of CTP-predicted ischemic core values with clinical outcome was lost in multivariate adjusted models regardless of the perfusion parameters and thresholds used for the definition of infarct core.

In the second study of this thesis, we specifically explored the hypothesis that in certain subgroup of patients, the accuracy of CTP-derived infarct core for predicting clinical outcome would be lost due to interactions between several baseline and treatment-related variables with CTP-predicted ischemic core. For that purpose, we analyzed a total of 828 patients with acute proximal arterial occlusions in the carotid territory imaged with a whole-brain CTP within 8 hours from stroke onset and evaluated the potential mediators of the association between CTP-predicted infarct core and clinical outcome in a derivation cohort (n=654) for obtaining a prediction model that was further validated in an independent cohort (n=174). In agreement with previously published data [60, 88-90, 93], in first-order analyses of interaction we found that the strength of the association between CTP-predicted infarct core and clinical outcome was significantly modified by baseline NIHSS, glucose levels and MT. Moreover, by means of an advanced analysis of interaction (AAI) including first and second-order interaction terms, we also identified age and its interaction with the use of MT as additional modifying variables. The AAI model performed better than CTP-derived infarct core alone and showed similar accuracy at derivation and validation cohorts. According to the data presented in the second study of this thesis, the prognostic relevance of CTP-derived infarct core seems compromised in the context of milder stroke syndromes, lower baseline glucose levels and in younger patients, especially when the odds of performing a MT are high.

Overall, the data found in studies 1 and 2 of this thesis agree and support current guidelines arguing against the use of CTP-predicted ischemic core as screening tool to establish the need or lack thereof of reperfusion therapies in the non-extended time window [68, 90]. Furthermore, these observations also discourage the use of CTP-derived infarct core as a selection criterion for MT in patients in whom is anticipated a short delay from stroke onset to complete recanalization (i.e. within the first 4.5h from stroke onset) [68]. Taken together, these data highlight the limited accuracy of CTP for predicting final infarct volume or clinical outcome in AIS patients in the early temporal window, challenges the imaging ischemic core concept and supports the need for an individualized evaluation of perfusion measures.

Early reperfusion is the most effective treatment for AIS patients including rtPA administration and/or MT [121]. However, less than half of the patients who receive treatment obtain a permanent clinical benefit [68]. One of the mechanisms related to the lack of improvement after reperfusion therapies is the early breakdown of the BBB, which in turn is originated, among others, by the severity of brain ischemia. Experimental cerebral ischemia impairs vascular integrity and results in the loss of microvascular structures and erythrocyte extravasation [122, 123], in a process that is dependent on the intensity and duration of the lack of flow [124]. In human stroke, blood flow can be reliably quantified with dynamic contrast-enhanced neuroimaging, such as CTP [59]. In the third study of this doctoral thesis, we aimed to examine the optimal CTP-derived parameters and the impact of the duration of brain ischemia for the prediction of PH after MT in a cohort of 146 patients with anterior circulation occlusions treated with MT. We found that CBV and CBF derived thresholds were more informative of the risk of PH than those extracted from DT maps. The best CBV or CBF thresholds for predicting the development of PH were values lower than 2.5% of mean CBF and CBV values in normal brain [very low CBF (VLCBF) and VLCBV, respectively]. These results contrast with a previous threshold-finding study where the optimal observed CTP derived parameters and thresholds were a $T_{max} > 14$ s, a relative CBF lower than 30% and a relative CBV lower than 35% of normal brain tissue [101]. Beyond the differences in CTP acquisition and post-processing protocols that were

used in these previous works, in our study we included a highly homogeneous stroke population treated with endovascular reperfusion therapy. This selected population contrasts with the former study in which only half of the patients received systemic thrombolysis thus precluding the high rate of early reperfusion encountered in our study. Overall, these data may indicate that the amount of tissue with an extreme reduction of perfusion would be the most relevant hemodynamic parameter for promoting early BBB damage, particularly when multimodal reperfusion therapy is administered to achieve early recanalization.

On the other hand, the reperfusion of a severely ischemic tissue may lead to harmful consequences, which include brain edema, hemorrhagic complications or a combination of them. This deleterious process is called, as mentioned in the Introduction, reperfusion injury and implies a myriad of mechanisms such as oxidative stress, inflammation and activation of proteolytic enzymes that finally involve the disruption of the BBB [125]. In the experimental setting, the duration of ischemia prior to reperfusion is strongly related to the risk of hemorrhagic complications [126]. Post-ischemic reperfusion can impair vascular function and exacerbate ischemic injury after longer durations of ischemia and reperfusion [127]. In experimental models of thromboembolic middle cerebral artery occlusion in rats the duration of brain ischemia prior to reperfusion parallels an increased risk and severity of HT. Thus, after 6 hours of occlusion the risk of PH is significantly increased in comparison with shorter occlusion times (3h) or permanent occlusion [128]. Accordingly, in humans with cardioembolic stroke, recanalization occurring beyond 6 hours is associated in some studies with an increased risk of HT [129]. In agreement with these previous reports, in the third study of this doctoral thesis we found that the risk of PH was increased in patients with delayed recanalization (over 6 hours of stroke onset). Moreover, even in the subgroup of patients achieving early recanalization at the end of ET, we also found a significant association between the time delay to recanalization and the risk of PH. Overall, our results further support that reperfusion may be more deleterious for the integrity of the BBB in patients with longer duration of ischemia. However, given the strong beneficial effects in terms of clinical outcome of endovascular reperfusion therapies recently shown in clinical trials, the presence of regions of VLCBF

or VLCBV in CTP should not preclude the treatment of patients otherwise eligible for receiving endovascular reperfusion therapies. Indeed, the low positive predictive value and high negative predictive value of the best performing thresholds indicate that severe ischemia may be a necessary but not sufficient mediator for PH.

Beyond the severity of brain ischemia, a number of additional variables have been also associated with an increased risk of HT after MT, including an increased NIHSS score, poor collaterals, antiplatelet use, atrial fibrillation, older age or pretreatment hyperglycemia, among others [130].

In the fourth study of this thesis, we aimed to evaluate the existence of synergistic effects between elevated glucose and VLCBF and VLCBV values in the promotion of PH after MT. We analyzed a cohort of 258 patients treated with MT who had a pretreatment CTP and a follow-up MRI and we found that pretreatment glucose levels interacted significantly with severe hypoperfusion on the prediction of PH. Thus, in patients with regions of VLCBV, higher pretreatment glucose levels increased significantly the risk of PH, while this association was not significant in patients without VLCBV regions. Indeed, about 1 in 5 patients with VLCBV regions and low pretreatment glucose levels at baseline developed a PH in follow-up neuroimaging, whereas this rate increased to 1 in 2 patients with concurrent high glucose levels. The consideration of pretreatment glucose in addition to the presence of VLCBV regions resulted in higher positive predictive value for the prediction of PH in comparison with VLCBV alone.

In experimental models of brain ischemia, hyperglycemia exacerbates ischemic brain injury by increasing infarct size, brain swelling and blood-brain barrier disruption [131-134]. Several preclinical studies have shown a direct association between induced hyperglycemia and poorer perfusion metrics during ischemia and after reperfusion whereas others were not able to identify such relationship [112-119]. In the fourth study of this doctoral thesis, pretreatment CBV values were not correlated with pretreatment glucose levels and were similar in patients with levels higher or lower than 116 mg/dL (6.4 mmol/L), regardless of the presence of successful recanalization. In addition, the quality of reperfusion obtained at the end of MT was not associated with pretreatment glucose levels, in

agreement with findings from a recent meta-analysis that included pooled data of the pivotal thrombectomy trials [111]. Overall, our results support the relevance of additional pathophysiological mechanisms beyond hyperacute glucose-driven disturbances in cerebral perfusion to explain the association between hyperglycemia and severe hypoperfusion with the risk of PH, such as enhanced thromboinflammatory mechanisms, increased blood–brain barrier disruption, worse cytotoxic injury or the deleterious effects of glucose-associated oxidative stress [108, 133-135].

As mentioned before, given the strong clinical benefits of MT, the presence of regions of severe reductions of CBV in CTP and concurrent hyperglycemia should not preclude the treatment of patients otherwise eligible for receiving endovascular reperfusion therapies. Even though, from a practical point of view, the combination of these biomarkers could be useful in the evaluation of strategies aimed to protect the BBB as patients with regions of severe ischemia and elevated pretreatment glucose levels may represent a target population for the early implementation of preventive strategies. These strategies could theoretically include a tighter control of blood pressure, the avoidance of early post-treatment aggressive antithrombotic therapy or the addition of adjunctive neuroprotective or vasculoprotective therapies. Of these potential treatments, the implementation of strategies focused in lowering glucose concentrations and achieving a tight glucose control in the early acute phase have been repeatedly unsuccessful in humans regardless of preventing lactic acidosis [136-138]. Contrarily, preliminary data from preclinical and clinical studies support that the enhancement of antioxidant exposure in combination with reperfusion therapies could minimize the toxicity of hyperglycemia [135].

In summary, the results presented in this doctoral thesis provide evidence to reinforce the strengths and limitations of CTP imaging and the need of taking into account baseline and clinical variables (personalized medicine) in the evaluation of tissue viability to predict final infarct volume, clinical outcome and risk of HT in AIS patients.

6. CONCLUSION



- 6.1.1 CTP-derived ischemic core is associated with final infarct DWI volumes in AIS patients who achieve complete recanalization after MT, but this association is significantly modified by time from stroke onset to recanalization in a non-linear fashion. The reliability of CTP-predicted ischemic core is good in patients with complete recanalization after 4.5h from stroke onset, whereas it is only moderate in those who achieve earlier and complete recanalization.
- 6.1.2 CTP-derived ischemic core is associated with poor long-term clinical outcome in AIS patients who achieve complete recanalization after MT, although this association is lost in patients recanalized before 4.5h from symptom onset.
- 6.2 Ischemic core measured in CTP is associated with poor long-term clinical outcome, although this association is significantly modified by baseline stroke severity, pretreatment glucose levels, thrombectomy use and age. Specifically, the prognostic relevance of ischemic core is compromised in the context of milder stroke syndromes, lower baseline glucose levels and in younger patients, especially when the odds of performing of MT are high.
- 6.3 The identification of severe perfusion deficits evaluated with CTP is predictive of the risk of hemorrhagic complications after MT of AIS patients, especially in those with delayed recanalization.
- 6.4 Elevated pretreatment glucose levels are associated with an increased risk of PH after MT in AIS patients with severe pretreatment hypoperfusion.



7. BIBLIOGRAPHY

- [1] Dirnagl U, Iadecola C, Moskowitz MA. *Pathobiology of ischaemic stroke: an integrated view*. Trends Neurosci. 1999 Sep;22(9):391-7. doi:10.1016/S0166-2236(99)01401-0. PMID: 10441299.
- [2] Barber PA, Demchuk AM, Zhang J, Buchan AM. *Validity and reliability of a quantitative computed tomography score in predicting outcome of hyperacute stroke before thrombolytic therapy*. ASPECTS Study Group. Alberta Stroke Programme Early CT Score. Lancet. 2000 May 13;355(9216):1670-4. doi: 10.1016/S0140-6736(00)02237-6. Erratum in: Lancet 2000 Jun 17;355(9221):2170. PMID: 10905241.
- [3] Brott T, Adams HP Jr, Olinger CP, Marler JR, Barsan WG, Biller J, et al. *Measurements of acute cerebral infarction: a clinical examination scale*. Stroke. 1989 Jul;20(7):864-70. doi: 10.1161/01.str.20.7.864. PMID: 2749846.
- [4] Muir KW, Weir CJ, Murray GD, Povey C, Lees KR. *Comparison of neurological scales and scoring systems for acute stroke prognosis*. Stroke. 1996 Oct;27(10):1817-20. doi: 10.1161/01.str.27.10.1817. PMID: 8841337.
- [5] Hernández-Pérez M, Pérez de la Ossa N, Aleu A, Millán M, Gomis M, Dorado L, et al. *Natural history of acute stroke due to occlusion of the middle cerebral artery and intracranial internal carotid artery*. J Neuroimaging. 2014 Jul-Aug;24(4):354-8. doi: 10.1111/jon.12062. Epub 2013 Nov 19. PMID: 24251821.
- [6] Chamorro Á. *Neuroprotectants in the Era of Reperfusion Therapy*. J Stroke. 2018 May;20(2):197-207. doi: 10.5853/jos.2017.02901. Epub 2018 May 31. PMID: 29886725.
- [7] Chamorro Á, Dirnagl U, Urra X, Planas AM. *Neuroprotection in acute stroke: targeting excitotoxicity, oxidative and nitrosative stress, and inflammation*. Lancet Neurol. 2016 Jul;15(8):869-881. doi: 10.1016/S1474-4422(16)00114-9. Epub 2016 May 11. PMID: 27180033.
- [8] Liebeskind DS. *Collateral circulation*. Stroke. 2003 Sep;34(9):2279-84. doi: 10.1161/01.STR.0000086465.41263.06. Epub 2003 Jul 24. PMID: 12881609.

- [9] Moshayedi P, Liebeskind DS. *Hemodynamics in acute stroke: Cerebral and cardiac complications*. *Handb Clin Neurol*. 2021;177:295-317. doi: 10.1016/B978-0-12-819814-8.00015-9. PMID: 33632449.
- [10] Markus HS. *Cerebral perfusion and stroke*. *J Neurol Neurosurg Psychiatry*. 2004 Mar;75(3):353-61. doi: 10.1136/jnnp.2003.025825. PMID: 14966145.
- [11] Astrup J, Siesjö BK, Symon L. *Thresholds in cerebral ischemia - the ischemic penumbra*. *Stroke*. 1981 Nov-Dec;12(6):723-5. doi: 10.1161/01.str.12.6.723. PMID: 6272455.
- [12] Chamorro A. *Role of inflammation in stroke and atherothrombosis*. *Cerebrovasc Dis*. 2004;17 Suppl 3:1-5. doi: 10.1159/000075297. PMID: 14730251.
- [13] Vila N, Castillo J, Dávalos A, Esteve A, Planas AM, Chamorro A. *Levels of anti-inflammatory cytokines and neurological worsening in acute ischemic stroke*. *Stroke*. 2003 Mar;34(3):671-5. doi: 10.1161/01.STR.0000057976.53301.69. Epub 2003 Feb 20. PMID: 12624290.
- [14] Amaro S, Chamorro Á. *Translational stroke research of the combination of thrombolysis and antioxidant therapy*. *Stroke*. 2011 May;42(5):1495-9. doi: 10.1161/STROKEAHA.111.615039. Epub 2011 Apr 7. PMID: 21474803.
- [15] Amaro S, Jiménez-Altayó F, Chamorro Á. *Uric acid therapy for vasculoprotection in acute ischemic stroke*. *Brain Circ*. 2019 Apr-Jun;5(2):55-61. doi: 10.4103/bc.bc_1_19. Epub 2019 Jun 27. PMID: 31334357.
- [16] Lipton P. *Ischemic cell death in brain neurons*. *Physiol Rev*. 1999 Oct;79(4):1431-568. doi: 10.1152/physrev.1999.79.4.1431. PMID: 10508238.
- [17] Kaufmann AM, Firlik AD, Fukui MB, Wechsler LR, Jungries CA, Yonas H. *Ischemic core and penumbra in human stroke*. *Stroke*. 1999 Jan;30(1):93-9. doi: 10.1161/01.str.30.1.93. PMID: 9880395.

- [18] Soares BP, Tong E, Hom J, Cheng SC, Bredno J, Boussel L, et al. *Reperfusion is a more accurate predictor of follow-up infarct volume than recanalization: a proof of concept using CT in acute ischemic stroke patients*. Stroke. 2010 Jan; 41(1):e34-40. doi: 10.1161/STROKEAHA.109.568766. Epub 2009 Nov 12. PMID: 19910542.
- [19] Collen D, Billiau A, Edy J, De Somer P. *Identification of the human plasma protein which inhibits fibrinolysis associated with malignant cells*. Biochim Biophys Acta. 1977 Sep 29;499(2):194-201. doi: 10.1016/0304-4165(77)90002-2. PMID: 198009.
- [20] Matsuo O, Rijken DC, Collen D. *Thrombolysis by human tissue plasminogen activator and urokinase in rabbits with experimental pulmonary embolus*. Nature. 1981 Jun 18;291(5816):590-1. doi: 10.1038/291590a0. PMID: 7195468.
- [21] Lijnen HR, Collen D. *Tissue-type plasminogen activator*. Ann Biol Clin (Paris). 1987;45(2):198-201. PMID: 2956911.
- [22] National Institute of Neurological Disorders and Stroke rt-PA Stroke Study Group. *Tissue plasminogen activator for acute ischemic stroke*. N Engl J Med. 1995 Dec 14;333(24):1581-7. doi: 10.1056/NEJM199512143332401. PMID: 7477192.
- [23] Hacke W, Kaste M, Bluhmki E, Brozman M, Dávalos A, Guidetti D, et al; ECASS Investigators. *Thrombolysis with alteplase 3 to 4.5 hours after acute ischemic stroke*. N Engl J Med. 2008 Sep 25;359(13):1317-29. doi: 10.1056/NEJMoao804656. PMID: 18815396.
- [24] Emberson J, Lees KR, Lyden P, Blackwell L, Albers G, Bluhmki E, et al; Stroke Thrombolysis Trialists' Collaborative Group. *Effect of treatment delay, age, and stroke severity on the effects of intravenous thrombolysis with alteplase for acute ischaemic stroke: a meta-analysis of individual patient data from randomised trials*. Lancet. 2014 Nov 29;384(9958):1929-35. doi: 10.1016/S0140-6736(14)60584-5. Epub 2014 Aug 5. PMID: 25106063.

[25] Lees KR, Emberson J, Blackwell L, Bluhmki E, Davis SM, Donnan GA, et al; Stroke Thrombolysis Trialists' Collaborators Group. *Effects of Alteplase for Acute Stroke on the Distribution of Functional Outcomes: A Pooled Analysis of 9 Trials*. *Stroke*. 2016 Sep;47(9):2373-9. doi: 10.1161/STROKEAHA.116.013644. Epub 2016 Aug 9. PMID: 27507856.

[26] Lees KR, Bluhmki E, von Kummer R, Brodt TG, Toni D, Grotta JC, et al. *Time to treatment with intravenous alteplase and outcome in stroke: an updated pooled analysis of ECASS, ATLANTIS, NINDS, and EPITHET trials*. *Lancet*. 2010 May 15;375(9727):1695-703. doi: 10.1016/S0140-6736(10)60491-6 PMID: 20472172.

[27] Berkhemer OA, Fransen PS, Beumer D, van den Berg LA, Lingsma HF, Yoo AJ, et al; MR CLEAN Investigators. *A randomized trial of intraarterial treatment for acute ischemic stroke*. *N Engl J Med*. 2015 Jan 1;372(1):11-20. doi: 10.1056/NEJMoa1411587. Epub 2014 Dec 17. Erratum in: *N Engl J Med*. 2015 Jan 22;372(4):394. PMID: 25517348.

[28] Saver JL, Goyal M, Bonafe A, Diener HC, Levy EI, Pereira VM, et al; SWIFT PRIME Investigators. *Stent-retriever thrombectomy after intravenous t-PA vs. t-PA alone in stroke*. *N Engl J Med*. 2015 Jun 11;372(24):2285-95. doi: 10.1056/NEJMoa1415061. Epub 2015 Apr 17. PMID: 25882376.

[29] Goyal M, Demchuk AM, Menon BK, Eesa M, Rempel JL, Thornton J, et al; ESCAPE Trial Investigators. *Randomized assessment of rapid endovascular treatment of ischemic stroke*. *N Engl J Med*. 2015 Mar 12;372(11):1019-30. doi: 10.1056/NEJMoa1414905. Epub 2015 Feb 11. PMID: 25671798.

[30] Jovin TG, Chamorro A, Cobo E, de Miquel MA, Molina CA, Rovira A, et al; REVASCAT Trial Investigators. *Thrombectomy within 8 hours after symptom onset in ischemic stroke*. *N Engl J Med*. 2015 Jun 11;372(24):2296-306. doi: 10.1056/NEJMoa1503780. Epub 2015 Apr 17. PMID: 25882510.

[31] Campbell BC, Mitchell PJ, Kleinig TJ, Dewey HM, Churilov L, Yassi N, et al; EXTEND-IA Investigators. *Endovascular therapy for ischemic stroke with*

perfusion-imaging selection. *N Engl J Med.* 2015 Mar 12;372(11):1009-18. doi: 10.1056/NEJMoA1414792. Epub 2015 Feb 11. PMID: 25671797.

[32] Nogueira RG, Jadhav AP, Haussen DC, Bonafe A, Budzik RF, Bhuva P, et al; DAWN Trial Investigators. *Thrombectomy 6 to 24 Hours after Stroke with a Mismatch between Deficit and Infarct.* *N Engl J Med.* 2018 Jan 4;378(1):11-21. doi: 10.1056/NEJMoA1706442. Epub 2017 Nov 11. PMID: 29129157.

[33] Albers GW, Marks MP, Kemp S, Christensen S, Tsai JP, Ortega-Gutierrez S, et al; DEFUSE 3 Investigators. *Thrombectomy for Stroke at 6 to 16 Hours with Selection by Perfusion Imaging.* *N Engl J Med.* 2018 Feb 22;378(8):708-718. doi: 10.1056/NEJMoA1713973. Epub 2018 Jan 24. PMID: 29364767.

[34] Saver JL, Goyal M, van der Lugt A, Menon BK, Majoie CB, Dippel DW, et al; HERMES Collaborators. *Time to Treatment With Endovascular Thrombectomy and Outcomes From Ischemic Stroke: A Meta-analysis.* *JAMA.* 2016 Sep 27;316(12):1279-88. doi: 10.1001/jama.2016.13647. PMID: 27673305.

[35] Badhiwala JH, Nassiri F, Alhazzani W, Selim MH, Farrokhyar F, Spears J, et al. *Endovascular Thrombectomy for Acute Ischemic Stroke: A Meta-analysis.* *JAMA.* 2015 Nov 3;314(17):1832-43. doi: 10.1001/jama.2015.13767. PMID: 26529161.

[36] Goyal M, Menon BK, van Zwam WH, Dippel DW, Mitchell PJ, Demchuk AM, et al; HERMES collaborators. *Endovascular thrombectomy after large-vessel ischaemic stroke: a meta-analysis of individual patient data from five randomised trials.* *Lancet.* 2016 Apr 23;387(10029):1723-31. doi: 10.1016/S0140-6736(16)00163-X. Epub 2016 Feb 18. PMID: 26898852.

[37] Chamorro Á, Blasco J, López A, Amaro S, Román LS, Llull L, et al. *Complete reperfusion is required for maximal benefits of mechanical thrombectomy in stroke patients.* *Sci Rep.* 2017 Sep 14;7(1):11636. doi: 10.1038/s41598-017-11946-y. PMID: 28912596.

[38] Renú A, Blasco J, Millán M, Martí-Fàbregas J, Cardona P, Oleaga L, et al; CHOICE Investigators. *The Chemical Optimization of Cerebral*

Embolectomy trial: Study protocol. Int J Stroke. 2021 Jan;16(1):110-116. doi: 10.1177/1747493019895656. Epub 2019 Dec 18. PMID: 31852410.

[39] Brouns R, De Deyn PP. *The complexity of neurobiological processes in acute ischemic stroke*. Clin Neurol Neurosurg. 2009 Jul;111(6):483-95. doi: 10.1016/j.clineuro.2009.04.001. Epub 2009 May 14. PMID: 19446389.

[40] Khatri R, McKinney AM, Swenson B, Janardhan V. *Blood-brain barrier, reperfusion injury, and hemorrhagic transformation in acute ischemic stroke*. Neurology. 2012 Sep 25;79 (13 Suppl 1): S52-7. doi: 10.1212/WNL.ob013e3182697e70. PMID: 23008413.

[41] Daneman R, Prat A. *The blood-brain barrier*. Cold Spring Harb Perspect Biol. 2015 Jan 5;7(1):a020412. doi: 10.1101/cshperspect.a020412. PMID: 25561720.

[42] Trouillas P, von Kummer R. *Classification and pathogenesis of cerebral hemorrhages after thrombolysis in ischemic stroke*. Stroke. 2006 Feb;37(2):556-61. doi: 10.1161/01.STR.0000196942.84707.71. Epub 2006 Jan 5. PMID: 16397182.

[43] Strbian D, Sairanen T, Meretoja A, Pitkäniemi J, Putaala J, Salonen O, et al; Helsinki Stroke Thrombolysis Registry Group. *Patient outcomes from symptomatic intracerebral hemorrhage after stroke thrombolysis*. Neurology. 2011 Jul 26;77(4):341-8. doi: 10.1212/WNL.ob013e3182267b8c. Epub 2011 Jun 29. PMID: 21715707.

[44] Mokin M, Kan P, Kass-Hout T, Abia AA, Dumont TM, Snyder KV, et al. *Intracerebral hemorrhage secondary to intravenous and endovascular intraarterial revascularization therapies in acute ischemic stroke: an update on risk factors, predictors, and management*. Neurosurg Focus. 2012 Apr;32(4):E2. doi: 10.3171/2012.1.FOCUS11352. PMID: 22463112.

[45] Jordan JD, Powers WJ. *Cerebral autoregulation and acute ischemic stroke*. Am J Hypertens. 2012 Sep;25(9):946-50. doi: 10.1038/ajh.2012.53. Epub 2012 May 10. PMID: 22573015.

- [46] Castro P, Azevedo E, Sorond F. *Cerebral Autoregulation in Stroke*. *Curr Atheroscler Rep*. 2018 May 21;20(8):37. doi: 10.1007/s11883-018-0739-5. PMID: 29785667.
- [47] Shuaib A, Butcher K, Mohammad AA, Saqqur M, Liebeskind DS. *Collateral blood vessels in acute ischaemic stroke: a potential therapeutic target*. *Lancet Neurol*. 2011 Oct;10(10):909-21. doi: 10.1016/S1474-4422(11)70195-8. PMID: 21939900.
- [48] Warach SJ, Luby M, Albers GW, Bammer R, Bivard A, Campbell BC, et al; Stroke Imaging Research (STIR) and VISTA-Imaging Investigators. *Acute Stroke Imaging Research Roadmap III Imaging Selection and Outcomes in Acute Stroke Reperfusion Clinical Trials: Consensus Recommendations and Further Research Priorities*. *Stroke*. 2016 May;47(5):1389-98. doi: 10.1161/STROKEAHA.115.012364. Epub 2016 Apr 12. PMID: 27073243.
- [49] Lev MH. *Perfusion imaging of acute stroke: its role in current and future clinical practice*. *Radiology*. 2013 Jan;266(1):22-7. doi: 10.1148/radiol.12121355. PMID: 23264524.
- [50] Hernández-Pérez M, Puig J, Blasco G, Pérez de la Ossa N, Dorado L, Dávalos A, et al. *Dynamic Magnetic Resonance Angiography Provides Collateral Circulation and Hemodynamic Information in Acute Ischemic Stroke*. *Stroke*. 2016 Feb;47(2):531-4. doi: 10.1161/STROKEAHA.115.010748. Epub 2015 Dec 10. PMID: 26658445.
- [51] Puig J, Shankar J, Liebeskind D, Terceño M, Nael K, Demchuk AM, et al. *From "Time is Brain" to "Imaging is Brain": A Paradigm Shift in the Management of Acute Ischemic Stroke*. *J Neuroimaging*. 2020 Sep;30(5):562-571. doi: 10.1111/jon.12693. Epub 2020 Feb 10. PMID: 32037629.
- [52] Gómez-Choco M, Mengual JJ, Rodríguez-Antigüedad J, Paré-Curell M, Purroy F, Palomeras E, et al. *Pre-Existing Cerebral Small Vessel Disease Limits*

Early Recovery in Patients with Acute Lacunar Infarct. J Stroke Cerebrovasc Dis. 2019 Nov;28(11):104312. doi: 10.1016/j.jstrokecerebrovasdis.2019.104312. Epub 2019 Aug 5. PMID: 31395422.

[53] Fung SH, Roccatagliata L, Gonzalez RG, Schaefer PW. *MR diffusion imaging in ischemic stroke.* Neuroimaging Clin N Am. 2011 May;21(2):345-77, xi. doi: 10.1016/j.nic.2011.03.001. PMID: 21640304.

[54] Axel L. *Cerebral blood flow determination by rapid-sequence computed tomography: theoretical analysis.* Radiology. 1980 Dec;137(3):679-86. doi: 10.1148/radiology.137.3.7003648. PMID: 7003648.

[55] Axel L. *A method of calculating brain blood flow with a CT dynamic scanner.* Adv Neurol. 1981;30:67-71. PMID: 7304311.

[56] Kudo K, Sasaki M, Østergaard L, Christensen S, Uwano I, Suzuki M, et al. *Susceptibility of Tmax to tracer delay on perfusion analysis: quantitative evaluation of various deconvolution algorithms using digital phantoms.* J Cereb Blood Flow Metab. 2011 Mar;31(3):908-12. doi: 10.1038/jcbfm.2010.169. Epub 2010 Sep 22. PMID: 20859294.

[57] Ostergaard L, Weisskoff RM, Chesler DA, Gyldensted C, Rosen BR. *High resolution measurement of cerebral blood flow using intravascular tracer bolus passages. Part I: Mathematical approach and statistical analysis.* Magn Reson Med. 1996 Nov;36(5):715-25. doi: 10.1002/mrm.1910360510. PMID: 8916022.

[58] Vagal A, Wintermark M, Nael K, Bivard A, Parsons M, Grossman AW, et al. *Automated CT perfusion imaging for acute ischemic stroke: Pearls and pitfalls for real-world use.* Neurology. 2019 Nov 12;93(20):888-898. doi: 10.1212/WNL.0000000000008481. Epub 2019 Oct 21. PMID: 31636160.

[59] Bivard A, Levi C, Spratt N, Parsons M. *Perfusion CT in acute stroke: a comprehensive analysis of infarct and penumbra.* Radiology. 2013 May;267(2):543-50. doi: 10.1148/radiol.12120971. Epub 2012 Dec 21. PMID: 23264345.

[60] Wintermark M, Albers GW, Broderick JP, Demchuk AM, Fiebach JB, Fiehler J, et al. *Acute Stroke Imaging Research Roadmap II*. *Stroke*. 2013;44:2628-39. doi: 10.1161/STROKEAHA.113.002015. PMID: 23860298

[61] Schellinger PD, Bryan RN, Caplan LR, Detre JA, Edelman RR, Jaigobin C, et al; Therapeutics and Technology Assessment Subcommittee of the American Academy of Neurology. *Evidence-based guideline: The role of diffusion and perfusion MRI for the diagnosis of acute ischemic stroke: report of the Therapeutics and Technology Assessment Subcommittee of the American Academy of Neurology*. *Neurology*. 2010 Jul 13;75(2):177-85. doi: 10.1212/WNL.0b013e3181e7c9dd. Erratum in: *Neurology*. 2010 Sep 7;75(10):938. PMID: 20625171.

[62] Campbell BC, Christensen S, Levi CR, Desmond PM, Donnan GA, Davis SM, et al. *Cerebral blood flow is the optimal CT perfusion parameter for assessing infarct core*. *Stroke*. 2011 Dec;42(12):3435-40. doi: 10.1161/STROKEAHA.111.618355. Epub 2011 Oct 6. PMID: 21980202.

[63] Campbell BC, Christensen S, Levi CR, Desmond PM, Donnan GA, Davis SM, et al. *Comparison of computed tomography perfusion and magnetic resonance imaging perfusion-diffusion mismatch in ischemic stroke*. *Stroke*. 2012 Oct;43(10):2648-53. doi: 10.1161/STROKEAHA.112.660548. Epub 2012 Aug 2. PMID: 22858726.

[64] Lin L, Bivard A, Krishnamurthy V, Levi CR, Parsons MW. *Whole-Brain CT Perfusion to Quantify Acute Ischemic Penumbra and Core*. *Radiology*. 2016 Jun;279(3):876-87. doi: 10.1148/radiol.2015150319. Epub 2016 Jan 18. PMID: 26785041.

[65] Cereda CW, Christensen S, Campbell BCV, Mishra NK, Mlynash M, Levi C, et al. *A benchmarking tool to evaluate computer tomography perfusion infarct core predictions against a DWI standard*. *J Cereb Blood Flow Metab*. 2016 Oct;36(10):1780-1789. doi: 10.1177/0271678X15610586. Epub 2015 Oct 19. PMID: 26661203.

[66] Donahue J, Wintermark M. *Perfusion CT and acute stroke imaging: foundations, applications, and literature review*. *J Neuroradiol*. 2015

Feb;42(1):21-9. doi: 10.1016/j.neurad.2014.11.003. Epub 2015 Jan 27. PMID: 25636991.

[67] Dani KA, Thomas RG, Chappell FM, Shuler K, MacLeod MJ, Muir KW, et al; Translational Medicine Research Collaboration Multicentre Acute Stroke Imaging Study. *Computed tomography and magnetic resonance perfusion imaging in ischemic stroke: definitions and thresholds*. *Ann Neurol*. 2011 Sep;70(3):384-401. doi: 10.1002/ana.22500. Epub 2011 Jul 27. PMID: 21796665.

[68] Powers WJ, Rabinstein AA, Ackerson T, Adeoye OM, Bambakidis NC, Becker K, et al. *Guidelines for the Early Management of Patients With Acute Ischemic Stroke: 2019 Update to the 2018 Guidelines for the Early Management of Acute Ischemic Stroke: A Guideline for Healthcare Professionals From the American Heart Association/American Stroke Association*. *Stroke*. 2019 Dec;50(12):e344-e418. doi: 10.1161/STR.0000000000000211. Epub 2019 Oct 30. Erratum in: *Stroke*. 2019 Dec;50(12):e440-e441. PMID: 31662037.

[69] d'Esterre CD, Boesen ME, Ahn SH, Pordeli P, Najm M, Minhas P, et al. *Time-Dependent Computed Tomographic Perfusion Thresholds for Patients With Acute Ischemic Stroke*. *Stroke*. 2015 Dec;46(12):3390-7. doi: 10.1161/STROKEAHA.115.009250. Epub 2015 Oct 29. PMID: 26514186.

[70] Schaefer PW, Souza L, Kamalian S, Hirsch JA, Yoo AJ, Kamalian S, et al. *Limited reliability of computed tomographic perfusion acute infarct volume measurements compared with diffusion-weighted imaging in anterior circulation stroke*. *Stroke*. 2015 Feb;46(2):419-24. doi: 10.1161/STROKEAHA.114.007117. Epub 2014 Dec 30. PMID: 25550366.

[71] Christensen S, Lansberg MG. *CT perfusion in acute stroke: Practical guidance for implementation in clinical practice*. *J Cereb Blood Flow Metab*. 2019 Sep;39(9):1664-1668. doi: 10.1177/0271678X18805590. Epub 2018 Oct 22. PMID: 30346227.

[72] Boers AMM, Jansen IGH, Beenen LFM, Devlin TG, San Roman L, Heo JH, et al. *Association of follow-up infarct volume with functional outcome in*

acute ischemic stroke: a pooled analysis of seven randomized trials. *J Neurointerv Surg*. 2018 Dec;10(12):1137-1142. doi: 10.1136/neurintsurg-2017-013724. Epub 2018 Apr 7. PMID: 29627794.

[73] Kamalian S, Kamalian S, Maas MB, Goldmacher GV, Payabvash S, Akbar A, et al. *CT cerebral blood flow maps optimally correlate with admission diffusion-weighted imaging in acute stroke but thresholds vary by postprocessing platform*. *Stroke*. 2011 Jul;42(7):1923-8. doi: 10.1161/STROKEAHA.110.610618. Epub 2011 May 5. PMID: 21546490.

[74] Chen C, Bivard A, Lin L, Levi CR, Spratt NJ, Parsons MW. *Thresholds for infarction vary between gray matter and white matter in acute ischemic stroke: A CT perfusion study*. *J Cereb Blood Flow Metab*. 2019 Mar;39(3):536-546. doi: 10.1177/0271678X17744453. Epub 2017 Nov 27. PMID: 29172990.

[75] Haranhalli N, Mbabuike N, Grewal SS, Hasan TF, Heckman MG, Freeman WD, et al. *Topographic correlation of infarct area on CT perfusion with functional outcome in acute ischemic stroke*. *J Neurosurg*. 2019 Jan 11;132(1):33-41. doi: 10.3171/2018.8.JNS181095. PMID: 30641833.

[76] Tian H, Parsons MW, Levi CR, Lin L, Aviv RI, Spratt NJ, et al. *Influence of occlusion site and baseline ischemic core on outcome in patients with ischemic stroke*. *Neurology*. 2019 Jun 4;92(23):e2626-e2643. doi: 10.1212/WNL.0000000000007553. Epub 2019 May 1. PMID: 31043475.

[77] Bivard A, Spratt N, Miteff F, Levi C, Parsons MW. *Tissue Is More Important than Time in Stroke Patients Being Assessed for Thrombolysis*. *Front Neurol*. 2018 Feb 5;9:41. doi: 10.3389/fneur.2018.00041. PMID: 29467716.

[78] Qiao Y, Zhu G, Patrie J, Xin W, Michel P, Eskandari A, et al. *Optimal perfusion computed tomographic thresholds for ischemic core and penumbra are not time dependent in the clinically relevant time window*. *Stroke*. 2014 May;45(5):1355-62. doi: 10.1161/STROKEAHA.113.003362. Epub 2014 Mar 13. PMID: 24627117.

[79] Mui K, Yoo AJ, Verduzco L, Copen WA, Hirsch JA, González RG, et al. *Cerebral blood flow thresholds for tissue infarction in patients with acute ischemic stroke treated with intra-arterial revascularization therapy depend on timing of reperfusion.* AJNR Am J Neuroradiol. 2011 May;32(5):846-51. doi: 10.3174/ajnr.A2415. Epub 2011 Apr 7. PMID: 21474633.

[80] Copen WA, Yoo AJ, Rost NS, Morais LT, Schaefer PW, González RG, et al. *In patients with suspected acute stroke, CT perfusion-based cerebral blood flow maps cannot substitute for DWI in measuring the ischemic core.* PLoS One. 2017 Nov 30;12(11):e0188891. doi: 10.1371/journal.pone.0188891. PMID: 29190675.

[81] Bivard A, Kleinig T, Miteff F, Butcher K, Lin L, Levi C, et al. *Ischemic core thresholds change with time to reperfusion: A case control study.* Ann Neurol. 2017 Dec;82(6):995-1003. doi: 10.1002/ana.25109. PMID: 29205466.

[82] Martins N, Aires A, Mendez B, Boned S, Rubiera M, Tomasello A, et al. *Ghost Infarct Core and Admission Computed Tomography Perfusion: Redefining the Role of Neuroimaging in Acute Ischemic Stroke.* Interv Neurol. 2018 Oct;7(6):513-521. doi: 10.1159/000490117. Epub 2018 Aug 31. PMID: 30410531.

[83] Hoving JW, Marquering HA, Majoie CBLM, Yassi N, Sharma G, Liebeskind DS, et al. *Volumetric and Spatial Accuracy of Computed Tomography Perfusion Estimated Ischemic Core Volume in Patients With Acute Ischemic Stroke.* Stroke. 2018 Oct;49(10):2368-2375. doi: 10.1161/STROKEAHA.118.020846. PMID: 30355095.

[84] Najm M, Al-Ajlan FS, Boesen ME, Hur L, Kim CK, Fainardi E, et al. *Defining CT Perfusion Thresholds for Infarction in the Golden Hour and With Ultra-Early Reperfusion.* Can J Neurol Sci. 2018 May;45(3):339-342. doi: 10.1017/cjn.2017.287. Epub 2018 Feb 19. PMID: 29455683.

[85] Parsons MW, Pepper EM, Chan V, Siddique S, Rajaratnam S, Bateman GA, et al. *Perfusion computed tomography: prediction of final infarct extent and stroke outcome.* Ann Neurol. 2005 Nov;58(5):672-9. doi: 10.1002/ana.20638. PMID: 16240339.

- [86] Xie Y, Oppenheim C, Guillemin F, Gautheron V, Gory B, Raoult H, et al; THRACE investigators. *Pretreatment lesional volume impacts clinical outcome and thrombectomy efficacy*. *Ann Neurol*. 2018 Jan;83(1):178-185. doi: 10.1002/ana.25133. PMID: 29314208.
- [87] Ribo M, Flores A, Mansilla E, Rubiera M, Tomasello A, Coscojuela P, et al. *Age-adjusted infarct volume threshold for good outcome after endovascular treatment*. *J Neurointerv Surg*. 2014;6:418-22. doi: 10.1136/neurintsurg-2013-010786. PMID: 23832414.
- [88] Goyal M, Ospel JM, Menon B, Almekhlafi M, Jayaraman M, Fiehler J, et al. *Challenging the Ischemic Core Concept in Acute Ischemic Stroke Imaging*. *Stroke*. 2020;51:3147-3155. doi: 10.1161/STROKEAHA.120.030620. PMID: 32933417.
- [89] Qiu W, Kuang H, Lee TY, Boers AM, Brown S, Muir K, et al. *Confirmatory Study of Time-Dependent Computed Tomographic Perfusion Thresholds for Use in Acute Ischemic Stroke*. *Stroke*. 2019;50:3269-3273. doi: 10.1161/STROKEAHA.119.026281. PMID: 31480968.
- [90] Albers GW, Goyal M, Jahan R, Bonafe A, Diener HC, Levy EI, et al. *Ischemic core and hypoperfusion volumes predict infarct size in SWIFT PRIME*. *Ann Neurol*. 2016;79:76-89. doi: 10.1002/ana.24543. PMID: 26476022.
- [91] Vagal A, Menon BK, Foster LD, Livorine A, Yeatts SD, Qazi E, et al. *Association Between CT Angiogram Collaterals and CT Perfusion in the Interventional Management of Stroke III Trial*. *Stroke*. 2016 Feb;47(2):535-8. doi: 10.1161/STROKEAHA.115.011461. Epub 2015 Dec 10. PMID: 26658448.
- [92] Haussen DC, Dehkharghani S, Rangaraju S, Rebello LC, Bouslama M, Grossberg JA, et al. *Automated CT Perfusion Ischemic Core Volume and Noncontrast CT ASPECTS (Alberta Stroke Program Early CT Score): Correlation and Clinical Outcome Prediction in Large Vessel Stroke*. *Stroke*. 2016 Sep;47(9):2318-22. doi: 10.1161/STROKEAHA.116.014117. Epub 2016 Aug 9. PMID: 27507858.

[93] Luitse MJ, van Seeters T, Horsch AD, Kool HA, Velthuis BK, Kappelle LJ, et al. Admission hyperglycaemia and cerebral perfusion deficits in acute ischaemic stroke. *Cerebrovasc Dis.* 2013;35:163-7. doi: 10.1159/000346588. PMID: 23429063.

[94] Rudilosso S, Laredo C, Vivancos C, Urra X, Llull L, Renú A, et al. Leukoaraiosis May Confound the Interpretation of CT Perfusion in Patients Treated with Mechanical Thrombectomy for Acute Ischemic Stroke. *AJNR Am J Neuroradiol.* 2019;40:1323-1329. doi: 10.3174/ajnr.A6139. PMID: 31345941.

[95] Ay H, Arsava EM, Rosand J, Furie KL, Singhal AB, Schaefer PW, et al. Severity of leukoaraiosis and susceptibility to infarct growth in acute stroke. *Stroke.* 2008;39:1409-1413. doi: 10.1161/STROKEAHA.107.501932. PMID: 18340093.

[96] Campbell BC, Christensen S, Butcher KS, Gordon I, Parsons MW, Desmond PM, et al; EPITHET Investigators. Regional very low cerebral blood volume predicts hemorrhagic transformation better than diffusion-weighted imaging volume and thresholded apparent diffusion coefficient in acute ischemic stroke. *Stroke.* 2010 Jan;41(1):82-8. doi: 10.1161/STROKEAHA.109.562116. Epub 2009 Dec 3. PMID: 19959537.

[97] Campbell BC, Christensen S, Parsons MW, Churilov L, Desmond PM, Barber PA, et al; EPITHET and DEFUSE Investigators. Advanced imaging improves prediction of hemorrhage after stroke thrombolysis. *Ann Neurol.* 2013 Apr;73(4):510-9. doi: 10.1002/ana.23837. Epub 2013 Feb 26. PMID: 23444008.

[98] Hermitte L, Cho TH, Ozenne B, Nighoghossian N, Mikkelsen IK, Ribe L, et al. Very low cerebral blood volume predicts parenchymal hematoma in acute ischemic stroke. *Stroke.* 2013 Aug;44(8):2318-20. doi: 10.1161/STROKEAHA.113.001751. Epub 2013 May 30. PMID: 23723309.

[99] Jain AR, Jain M, Kanthala AR, Damania D, Stead LG, Wang HZ, et al. Association of CT perfusion parameters with hemorrhagic transformation in acute ischemic stroke. *AJNR Am J Neuroradiol.* 2013 Oct;34(10):1895-900. doi: 10.3174/ajnr.A3502. Epub 2013 Apr 18. PMID: 23598828.

[100] Souza LC, Payabvash S, Wang Y, Kamalian S, Schaefer P, Gonzalez RG, et al. *Admission CT perfusion is an independent predictor of hemorrhagic transformation in acute stroke with similar accuracy to DWI*. *Cerebrovasc Dis*. 2012;33(1):8-15. doi: 10.1159/000331914. Epub 2011 Nov 30. PMID: 22143195.

[101] Yassi N, Parsons MW, Christensen S, Sharma G, Bivard A, Donnan GA, et al. *Prediction of poststroke hemorrhagic transformation using computed tomography perfusion*. *Stroke*. 2013 Nov;44(11):3039-43. doi: 10.1161/STROKEAHA.113.002396. Epub 2013 Sep 3. PMID: 24003043.

[102] Puig J, Blasco G, Daunis-I-Estadella P, van Eendenburg C, Carrillo-García M, Aboud C, et al. *High-permeability region size on perfusion CT predicts hemorrhagic transformation after intravenous thrombolysis in stroke*. *PLoS One*. 2017 Nov 28;12(11):e0188238. doi: 10.1371/journal.pone.0188238. PMID: 29182658; PMCID: PMC5705117.

[103] Shinoyama M, Nakagawara J, Yoneda H, Suzuki M, Ono H, Kunitsugu I, et al. *Initial 'TTP Map-Defect' of Computed Tomography Perfusion as a Predictor of Hemorrhagic Transformation of Acute Ischemic Stroke*. *Cerebrovasc Dis Extra*. 2013 Feb 13;3(1):14-25. doi: 10.1159/000346113. PMID: 23637697.

[104] Rai AT, Raghuram K, Carpenter JS, Domico J, Hobbs G. *Pre-intervention cerebral blood volume predicts outcomes in patients undergoing endovascular therapy for acute ischemic stroke*. *J Neurointerv Surg*. 2013 May;5 Suppl 1:i25-32. doi: 10.1136/neurintsurg-2012-010293. Epub 2012 Mar 20. PMID: 22434904.

[105] Bhatt A, Vora NA, Thomas AJ, Majid A, Kassab M, Hammer MD, et al. *Lower pretreatment cerebral blood volume affects hemorrhagic risks after intra-arterial revascularization in acute stroke*. *Neurosurgery*. 2008 Nov;63(5):874-8; discussion 878-9. doi: 10.1227/01.NEU.0000333259.11739.AD. PMID: 19005377.

[106] Gupta R, Yonas H, Gebel J, Goldstein S, Horowitz M, Grahovac SZ, et al. *Reduced pretreatment ipsilateral middle cerebral artery cerebral blood flow is predictive of symptomatic hemorrhage post-intra-arterial thrombolysis in patients with middle cerebral artery occlusion.* Stroke. 2006 Oct;37(10):2526-30. doi: 10.1161/01.STR.0000240687.14265.b4. Epub 2006 Sep 7. PMID: 16960093.

[107] Hafez S, Coucha M, Bruno A, Fagan SC, Ergul A. *Hyperglycemia, acute ischemic stroke, and thrombolytic therapy.* Transl Stroke Res. 2014 Aug;5(4):442-453. doi: 10.1007/s12975-014-0336-z. Epub 2014 Mar 13. PMID: 24619488

[108] Desilles JP, Syvannarath V, Ollivier V, Journé C, Delbosc S, Ducroux C, et al. *Exacerbation of Thromboinflammation by Hyperglycemia Precipitates Cerebral Infarct Growth and Hemorrhagic Transformation.* Stroke. 2017 Jul;48(7):1932-1940. doi: 10.1161/STROKEAHA.117.017080. Epub 2017 May 19. PMID: 28526762.

[109] Khatri P, Wechsler LR, Broderick JP. *Intracranial hemorrhage associated with revascularization therapies.* Stroke. 2007 Feb;38(2):431-40. doi: 10.1161/01.STR.0000254524.23708.c9. Epub 2007 Jan 18. PMID: 17234988.

[110] Natarajan SK, Dandona P, Karmon Y, Yoo AJ, Kalia JS, Hao Q, et al. *Prediction of adverse outcomes by blood glucose level after endovascular therapy for acute ischemic stroke.* J Neurosurg. 2011 Jun;114(6):1785-99. doi: 10.3171/2011.1.JNS10884. Epub 2011 Feb 25. PMID: 21351835.

[111] Chamorro Á, Brown S, Amaro S, Hill MD, Muir KW, Dippel DWJ, et al; HERMES Collaborators. *Glucose Modifies the Effect of Endovascular Thrombectomy in Patients With Acute Stroke.* Stroke. 2019 Mar;50(3):690-696. doi: 10.1161/STROKEAHA.118.023769. PMID: 30777000.

[112] Kawai N, Keep RF, Betz AL. *Hyperglycemia and the vascular effects of cerebral ischemia.* Stroke. 1997 Jan;28(1):149-54. doi: 10.1161/01.str.28.1.149. PMID: 8996504.

- [113] Nakai H, Yamamoto YL, Diksic M, Worsley KJ, Takara E. *Triple-tracer autoradiography demonstrates effects of hyperglycemia on cerebral blood flow, pH, and glucose utilization in cerebral ischemia of rats.* *Stroke.* 1988 Jun;19(6):764-72. doi: 10.1161/01.str.19.6.764. PMID: 3376169.
- [114] Quast MJ, Wei J, Huang NC, Brunder DG, Sell SL, Gonzalez JM, et al. *Perfusion deficit parallels exacerbation of cerebral ischemia/reperfusion injury in hyperglycemic rats.* *J Cereb Blood Flow Metab.* 1997 May;17(5):553-9. doi: 10.1097/00004647-199705000-00009. PMID: 9183293.
- [115] Duckrow RB, Beard DC, Brennan RW. *Regional cerebral blood flow decreases during chronic and acute hyperglycemia.* *Stroke.* 1987 Jan-Feb;18(1):52-8. doi: 10.1161/01.str.18.1.52. PMID: 2949400.
- [116] Ginsberg MD, Welsh FA, Budd WW. *Deleterious effect of glucose pretreatment on recovery from diffuse cerebral ischemia in the cat. I. Local cerebral blood flow and glucose utilization.* *Stroke.* 1980 Jul-Aug;11(4):347-54. doi: 10.1161/01.str.11.4.347. PMID: 7414662.
- [117] Venables GS, Miller SA, Gibson G, Hardy JA, Strong AJ. *The effects of hyperglycaemia on changes during reperfusion following focal cerebral ischaemia in the cat.* *J Neurol Neurosurg Psychiatry.* 1985 Jul;48(7):663-9. doi: 10.1136/jnnp.48.7.663. PMID: 4031911.
- [118] Wagner KR, Kleinholz M, de Courten-Myers GM, Myers RE. *Hyperglycemic versus normoglycemic stroke: topography of brain metabolites, intracellular pH, and infarct size.* *J Cereb Blood Flow Metab.* 1992 Mar;12(2):213-22. doi: 10.1038/jcbfm.1992.31. PMID: 1548294.
- [119] Gisselsson L, Smith ML, Siesjö BK. *Hyperglycemia and focal brain ischemia.* *J Cereb Blood Flow Metab.* 1999 Mar;19(3):288-97. doi: 10.1097/00004647-199903000-00007. PMID: 10078881.
- [120] Bivard A, Levi C, Krishnamurthy V, McElduff P, Miteff F, Spratt NJ, et al. *Perfusion computed tomography to assist decision making for stroke thrombolysis.* *Brain.* 2015 Jul;138(Pt 7):1919-31. doi: 10.1093/brain/awv071. Epub 2015 Mar 25. PMID: 25808369.

[121] Rha JH, Saver JL. *The impact of recanalization on ischemic stroke outcome: a meta-analysis*. Stroke. 2007 Mar;38(3):967-73. doi: 10.1161/01.STR.0000258112.14918.24. Epub 2007 Feb 1. PMID: 17272772.

[122] Hamann GF, Okada Y, del Zoppo GJ. *Hemorrhagic transformation and microvascular integrity during focal cerebral ischemia/reperfusion*. J Cereb Blood Flow Metab. 1996 Nov;16(6):1373-8. doi: 10.1097/00004647-199611000-00036. PMID: 8898714.

[123] Hamann GF, Liebetrau M, Martens H, Burggraf D, Kloss CU, Bültmeier G, et al. *Microvascular basal lamina injury after experimental focal cerebral ischemia and reperfusion in the rat*. J Cereb Blood Flow Metab. 2002 May;22(5):526-33. doi: 10.1097/00004647-200205000-00004. Erratum in: J Cereb Blood Flow Metab 2002 Dec;22(12):1452. PMID: 11973425.

[124] del Zoppo GJ, von Kummer R, Hamann GF. *Ischaemic damage of brain microvessels: inherent risks for thrombolytic treatment in stroke*. J Neurol Neurosurg Psychiatry. 1998 Jul;65(1):1-9. doi: 10.1136/jnnp.65.1.1. PMID: 9667553.

[125] Maier CM, Hsieh L, Crandall T, Narasimhan P, Chan PH. *Evaluating therapeutic targets for reperfusion-related brain hemorrhage*. Ann Neurol. 2006 Jun;59(6):929-38. doi: 10.1002/ana.20850. PMID: 16673393.

[126] Jickling GC, Liu D, Stamova B, Ander BP, Zhan X, Lu A, et al. *Hemorrhagic transformation after ischemic stroke in animals and humans*. J Cereb Blood Flow Metab. 2014 Feb;34(2):185-99. doi: 10.1038/jcbfm.2013.203. Epub 2013 Nov 27. PMID: 24281743.

[127] Palomares SM, Cipolla MJ. *Vascular Protection Following Cerebral Ischemia and Reperfusion*. J Neurol Neurophysiol. 2011 Sep 20;2011:S1- 004. doi: 10.4172/2155-9562.s1-004. PMID: 22102980.

[128] Copin JC, Gasche Y. *Effect of the duration of middle cerebral artery occlusion on the risk of hemorrhagic transformation after tissue plasminogen activator injection in rats*. Brain Res. 2008 Dec 3;1243:161-6. doi: 10.1016/j.brainres.2008.09.025. Epub 2008 Sep 19. PMID: 18835259.

- [129] Molina CA, Montaner J, Abilleira S, Ibarra B, Romero F, Arenillas JF, et al. *Timing of spontaneous recanalization and risk of hemorrhagic transformation in acute cardioembolic stroke*. *Stroke*. 2001 May;32(5):1079-84. doi: 10.1161/01.str.32.5.1079. PMID: 11340213.
- [130] Hao Y, Yang D, Wang H, Zi W, Zhang M, Geng Y, et al; ACTUAL Investigators (Endovascular Treatment for Acute Anterior Circulation Ischemic Stroke Registry). *Predictors for Symptomatic Intracranial Hemorrhage After Endovascular Treatment of Acute Ischemic Stroke*. *Stroke*. 2017 May;48(5):1203-1209. doi: 10.1161/STROKEAHA.116.016368. Epub 2017 Apr 3. PMID: 28373302.
- [131] Martini SR, Kent TA. *Hyperglycemia in acute ischemic stroke: a vascular perspective*. *J Cereb Blood Flow Metab*. 2007 Mar;27(3):435-51. doi: 10.1038/sj.jcbfm.9600355. Epub 2006 Jun 28. PMID: 16804552.
- [132] Suh SW, Shin BS, Ma H, Van Hoecke M, Brennan AM, Yenari MA, et al. *Glucose and NADPH oxidase drive neuronal superoxide formation in stroke*. *Ann Neurol*. 2008 Dec;64(6):654-63. doi: 10.1002/ana.21511. PMID: 19107988.
- [133] Kamada H, Yu F, Nito C, Chan PH. *Influence of hyperglycemia on oxidative stress and matrix metalloproteinase-9 activation after focal cerebral ischemia/reperfusion in rats: relation to blood-brain barrier dysfunction*. *Stroke*. 2007 Mar;38(3):1044-9. doi: 10.1161/01.STR.0000258041.75739.cb. Epub 2007 Feb 1. PMID: 17272778.
- [134] Bevers MB, Vaishnav NH, Pham L, Battey TW, Kimberly WT. *Hyperglycemia is associated with more severe cytotoxic injury after stroke*. *J Cereb Blood Flow Metab*. 2017 Jul;37(7):2577-2583. doi: 10.1177/0271678X16671730. Epub 2016 Jan 1. PMID: 27671250.
- [135] Amaro S, Llull L, Renú A, Laredo C, Perez B, Vila E, et al. *Uric acid improves glucose-driven oxidative stress in human ischemic stroke*. *Ann Neurol*. 2015 May;77(5):775-83. doi: 10.1002/ana.24378. Epub 2015 Mar 13. PMID: 25627874.

[136] Gray CS, Hildreth AJ, Sandercock PA, O'Connell JE, Johnston DE, Cartlidge NE, et al; GIST Trialists Collaboration. *Glucose-potassium-insulin infusions in the management of post-stroke hyperglycaemia: the UK Glucose Insulin in Stroke Trial (GIST-UK)*. *Lancet Neurol*. 2007 May;6(5):397-406. doi: 10.1016/S1474-4422(07)70080-7. PMID: 17434094.

[137] McCormick M, Hadley D, McLean JR, Macfarlane JA, Condon B, Muir KW. *Randomized, controlled trial of insulin for acute poststroke hyperglycemia*. *Ann Neurol*. 2010 May;67(5):570-8. doi: 10.1002/ana.21983. PMID: 20437554.

[138] Johnston KC, Bruno A, Pauls Q, Hall CE, Barrett KM, Barsan W, et al; Neurological Emergencies Treatment Trials Network and the SHINE Trial Investigators. *Intensive vs Standard Treatment of Hyperglycemia and Functional Outcome in Patients With Acute Ischemic Stroke: The SHINE Randomized Clinical Trial*. *JAMA*. 2019 Jul 23;322(4):326-335. doi: 10.1001/jama.2019.9346. Erratum in: *JAMA*. 2019 Nov 5;322(17):1718. PMID: 31334795.

